SINGLE-PHASE AC-DC CASCADED BOOST-CûK (CBC) CONVERTER FOR HIGH STEP-UP APPLICATIONS USING COMMON PART SHARING METHOD (CPSM)

A THESIS SUBMITTED TO THE ACADEMIC FACULTY IN PARTIAL FULFILLMENT OF THE REQUIREMENT FOR THE DEGREE OF BACHELOR OF SCIENCE IN TECHNICAL EDUCATION IN ELECTRICAL AND ELECTRONIC ENGINEERING

Islamic University of Technology (IUT)

Organization of Islamic Cooperation (OIC)

SUBMITTED BY

MD. NASIF FUAD PARASH (STUDENT NO: 142433)

MONSUR HABIB (STUDENT NO: 142435)

ANAGH MEHRAN (STUDENT NO: 142434)

ASHIKUR RAHMAN (STUDENT NO: 142436)

UNDER THE SUPERVISION OF

DR. GOLAM SAROWAR

ASSISTANT PROFESSOR

DEPARTMENT OF ELECTRICAL AND ELECTRONIC ENGINEERING

ISLAMIC UNIVERSITY OF TECHNOLOGY (IUT)

SINGLE-PHASE AC-DC CASCADED BOOST-CûK (CBC) CONVERTER FOR HIGH STEP-UP APPLICATIONS USING COMMON PART SHARING METHOD (CPSM)

by

Md. Nasif Fuad Parash (142433)
Monsur Habib (142435)
Anagh Mehran (142434)
Md. Ashikur Rahman (142436)

A Thesis Submitted to the Academic Faculty in Partial Fulfillment of the Requirements for the Degree of

BACHELOR OF SCIENCE IN ELECTRICAL AND ELECTRONIC ENGINEERING

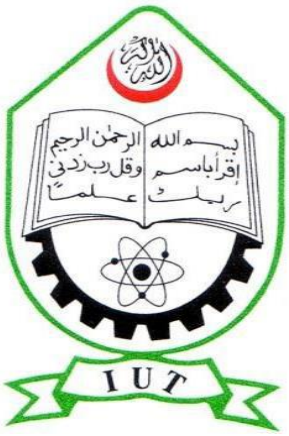

Department of Electrical and Electronic Engineering
Islamic University of Technology (IUT)
Gazipur, Bangladesh

SINGLE-PHASE AC-DC CASCADED BOOST-CûK (CBC) CONVERTER FOR HIGH STEP-UP APPLICATIONS USING COMMON PART SHARING METHOD (CPSM)

We hereby declare that this thesis has been prepared in partial fulfillment of the requirement for the degree of Bachelor of Science in Electrical and Electronic engineering at the Islamic University of Technology (IUT), Board Bazar, Gazipur-1704 and has not been submitted anywhere else for any other degree.

| --- | --- | --- | --- |
| Md. Nasif Fuad Parash
142433 | Monsur Habib
142435 | Anagh Mehran
142434 | Md. Ashikur Rahman
142436 |

Approved by:

Dr. Golam Sarowar

Supervisor and Assistant Professor,
Department of Electrical and Electronic Engineering
Islamic University of Technology (IUT)
Board Bazar, Gazipur-1704
Bangladesh.

Dr. Golam Sarowar

Supervisor and Assistant Professor,
Department of Electrical and Electronic Engineering
Islamic University of Technology (IUT)
Board Bazar, Gazipur-1704
Bangladesh.

Date: _

Table of Contents

LIST OF FIGURES

LIST OF TABLE

Acknowledgements

All the praises are for Allah for blessing us with the knowledge and ability to do the present study. Our indebt gratitude must be to the most benevolent and merciful for everything we have from Him.

We wish to express our deepest gratitude to our academic and research advisor **Dr. Golam Sarowar**, Assistant professor, Department of EEE, IUT for his continuous guidance, supervision and invaluable suggestions during the entire thesis work.

We also wish to acknowledge and express our appreciation to friends and others who directly or indirectly helped with, worth suggestions and information in completing the thesis.

Finally, we thank the Electrical and Electronic Engineering Department for their invaluable assistance during these eight semesters of study.

Abstract

Due to the rising need of renewable energy the importance of the development of more efficient circuits that transform energy has also risen. The multi-pulse AC-DC converters used in wind turbines often prove to be insufficient in the elimination of harmonics. This leads to additional active power filters, which operate at high switching frequencies, being used and the cost of the system being increased.

The chief advantage of Boost converter topology is the continuity of the input current, which is very important for renewable energy applications since most renewable energy sources have a better performance when their electrical current is continuous.

The reason for using bridgeless Boost converters is the reduced current input current ripple, but they also should provide an output voltage higher than the peak input voltage. The current that passes through power converter devices from the main supply results in high Total Harmonic Distortion (THD) and reduced Power Factor (PF). Thus power factor correction helps greatly in the reduction of input power loss which may emanate from input current harmonics.

Even though a bridgeless power factor correction converter suffers from the difficulty of implementing control because of two switches, conduction losses can be reduced by a bridgeless topology from rectifying bridges; thus, increasing overall system efficiency. Additionally, a bridgeless topology has the advantage of reduction in the total harmonic distortion resulting from input diode reduction.

This letter details the design and function of a novel topology of Cascaded Boost-Cûk(CBC) converter which combines the Boost converter with an isolated Cûk converter as a series output module in order to obtain high step-up ratio and to overcome the drawbacks faced when using conventional circuits. The demand for high voltage, efficient and lossless converters has increased in the 21st century. In order to facilitate the demand cascaded converters has been proposed which not only provides high performance in terms of efficiency, reduction in Total Harmonic Distortion (THD) of the input current and improved input power factor (PF) but also proper voltage regulation at all duty cycles. The proposed CBC converter has been simulated and verified using PSIM environment and is appropriate for high voltage and high performance applications. Similar works has been done in cascading Boost-SEPIC converters using common parts sharing method.

Chapter 1

Introduction

1.1 Fundamentals of Power Electronics

This chapter gives a description and overview of power electronic technologies including a description of the fundamental systems that are used as building blocks in power electronic systems. Technologies that are described include: power semiconductor switching devices, converter circuits that process energy from one DC level to another DC level, converters that produce variable frequency from DC sources, principles of rectifying AC input voltage in uncontrolled DC output voltage and their extension to controlled rectifiers, converters that convert to AC from DC (inverters) or from AC with fixed or variable output frequency (AC controllers, DC–DC–AC converters, matrix converters, or cyclo- converters). The chapter also covers control of power converters with focus on pulse width modulation (PWM) control techniques.

1.1.1 Definition, History, Applications and Trends of Power Electronics

Power electronics (PE) experienced tremendous growth after the introduction of the first solid-state power switch, the silicon controlled rectifier (SCR) in 1957. Today, almost all of the technologies that require control of power control utilize PE technology. This chapter will give the reader an overview on the field of PE including:

• A description of the fundamentals of the power semiconductor switching devices.

• Converter circuits that process energy from one DC level to another DC level.

• Converters that produce variable frequency from DC sources.

• Principles of rectifying AC input voltage in uncontrolled DC output voltage and their extension to controlled rectifiers.

• Converters that convert to AC from DC (inverters) or from AC with fixed or variable output frequency.

• AC controllers.

• DC–DC–AC converters.

• Matrix converters or cyclo-converters.

• Detailed description of pulse width modulations control techniques.

Power electronic circuits are used to control the power conversion from one or more AC or DC sources to one or more AC or DC loads, and sometimes with bidirectional capabilities. In most power electronics systems, this conversion is accomplished with two functional modules called the control stage and the power stage. Figure 1.1 shows the topology for a single source and single load converter application that includes a power processor (the power stage) and a controller (the control stage). The converter, handles the power transfer from the input to output, or vice versa, and is constituted of power semiconductor devices acting as switches, plus passive devices (inductor

and capacitor). The controller is responsible for operating the switches according to specific algorithms monitoring physical quantities (usually voltages and currents) measured at the system input and or output.

The modern PE era began in 1957. It was during that year the first commercial thyristor, or Silicon Controlled Rectifier (SCR), was introduced by General Electric Company. The SCR, started replacing the mercury arc rectifiers, invented in 1902, and the later developed thyratron (invented in 1923) and ignitron (invented in 1931), allowed the commercialization of several industrial circuits conceived during the 1920s and 1940s (like the cyclo-converter, the chopper, and the parallel inverter) as well as the Graetz bridge conceived in 1897.

The SCR was the only available power device for more than 25 years after its invention (and still is very useful for extremely high power applications). Since it is very difficult to impose turn-off conditions for SCR's, faster devices, with higher voltage and current capabilities, with better controllability were developed, including the bipolar junction transistor (BJT) invented in 1970. The BJT was used in applications from low to medium power and frequency and now is considered obsolete. The metal oxide semiconductor field effect transistor (MOSFET) was invented in 1978 and is used for power electronic switching applications of low power and high frequencies. The gate turn-off thyristor (GTO), is used in applications from medium to high power and from low to medium frequencies. The insulated gate bipolar transistor (IGBT) developed in 1983 is used in applications from low to medium power and frequency. The integrated gate commutated thyristor (IGCT) invented in 1997 is used in applications from medium to high power and from low to medium frequencies.

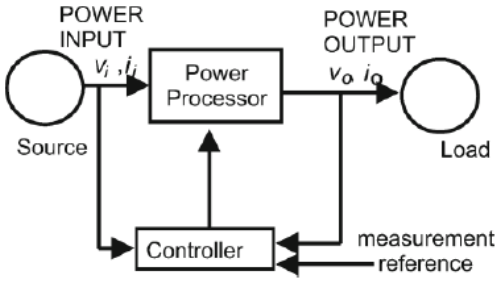

Fig. 1.1 A general power electronic system

Through the use of this switching technology power electronics systems can operate in the range from few watts up to GW, with frequency range from some 100 Hz up to some 100 kHz, depending on the power handled [1]. The advent of microelectronics and computer control made it possible to apply modern control theory to PE and at same the time made possible very complex circuit functions. Therefore, the area of PE, became interdisciplinary, as indicated in Fig. 1.2. At the high power level, PE deals with static and rotating equipment for generation, transmission, and distribution handling large amount of power. For consumer electronic applications power converters and circuits are important for information processing, employing analog and digital circuits, or microprocessors including microcontrollers, digital signal processors (DSP), and field programmable gate arrays (FPGA). In the area of control, PE deals with stability and response characteristics in systems with feedback loops, based on classical or modern control. With the development of very large system integration (VLSI), ultra large system integration (ULSI), and other sophisticated computer-assisted designs; advanced control systems could be used to develop new power electronic topologies.

Through the use of this switching technology power electronics systems can operate in the range from few watts up to GW, with frequency range from some 100 Hz up to some 100 kHz, depending on the power handled[14]. The advent of microelectronics and computer control made it possible to apply modern control theory to PE and at same the time made possible very complex circuit functions. Therefore, the area of PE, became interdisciplinary, as indicated in Fig. 1.2. At the high power level, PE deals with static and rotating equipment for generation, transmission, and distribution handling large amount of power. For consumer electronic applications power converters and circuits are important for information processing, employing analog and digital circuits, or microprocessors including microcontrollers, digital signal processors (DSP), and field programmable gate arrays (FPGA). In the area of control, PE deals with stability and response characteristics in systems with feedback loops, based on classical or modern control. With the development of very large system integration (VLSI), ultra large

system integration (ULSI), and other sophisticated computer-assisted designs; advanced control systems could be used to develop new power electronic topologies.
The development of devices and equipment able to individually or in combination convert efficiently electric energy from AC to DC, DC to DC, DC to AC, and AC to AC together with the changes that occurred in electrical power engineering has resulted in wide spread of PE in a large spectrum of applications.

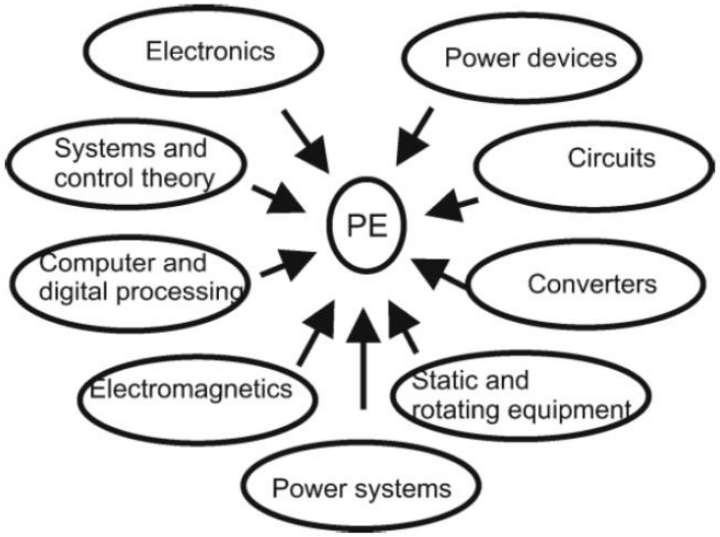

Fig. 1.2 Power electronics and related topics

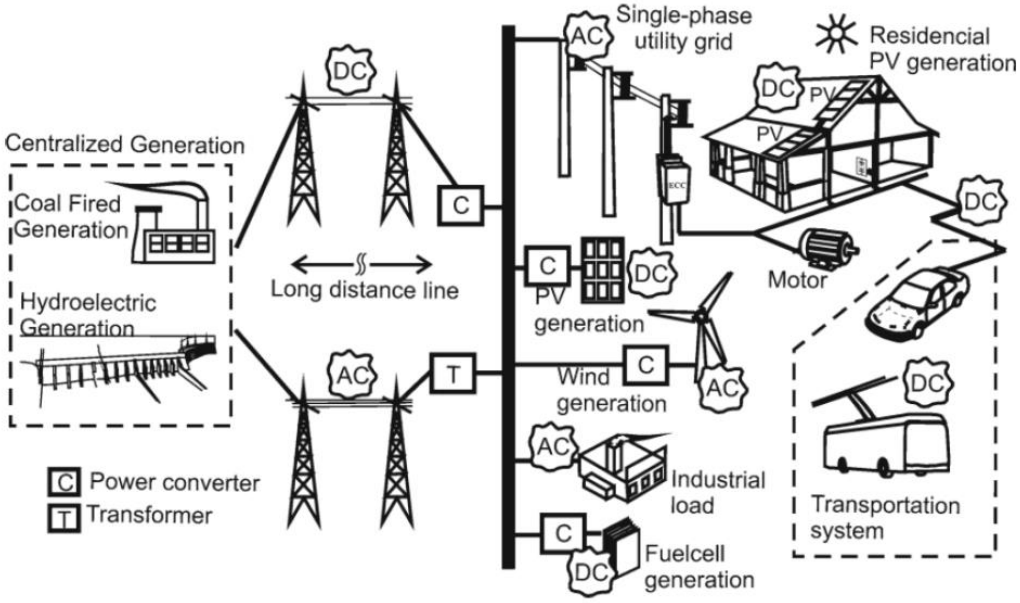

Fig. 1.3 Power electronics and electrical energy generation transmission, storage, and distribution

Figure 1.3 shows how electrical energy generation is distributed for the end-user, showing transmission, distribution, storage, renewable energy sources and users. In fact, nowadays PE is a key technology for all those sub-systems, and has spread in many applications, examples including:

• Residential: heaters, home appliances, electronic lighting, equipment sources;

• Commercial: heaters, fans, elevators Uninterruptible Power Supply (UPS), AC and DC breakers, battery chargers;

• Industrial: pumps, blowers, robots, inductive heaters, welding, machine drive, portable sources;

• Transportation: electrical and hybrid vehicles, battery chargers, railroad electric system;

• Utility systems: high voltage direct current, generators, reactive compensators, interface for photovoltaic, wind, fuel cells systems, Flexible AC Transmission System (FACTS) equipment;

• Aerospace: sources for spacecrafts, satellites, planes;

• Communication: sources, RF amplifiers, audio-amplifiers.

Power electronics will continue to be an enabling technology to address our future electricity needs. It is expected that new power devices for higher power, higher frequency, and lower losses will continue to be invented. Global energy concerns will provoke a large interest in the increase of the conversion efficiency and more application of PE in power quality, distributed generation, energy conservation, and smart grids. The integration of power and control circuitry into functional modules will result in systems solutions that are highly integrated into packaged products that will be both more reliable and affordable.

1.1.2 Power Semiconductor Devices

Electronic switches capable of handling high voltage and current operations at high frequency (HF) are the most important devices needed in the design of energy conversion systems that use PE. For the purposes of this discussion we will define the concept of an ideal switch. An ideal power electronic switch can be represented as a three terminals device as shown in Fig. 1.4. The input, the output, and a control terminal that imposes ON/OFF conditions on the switch. A switch is considered ‘‘ideal’’ when it is open, it has zero-current through it and can handle infinite voltage. When the switch is closed it has zero-voltage across it and can carry infinite current. Also, an ideal switch changes condition instantly, which means that it takes zero-time to switch from ON-to-OFF or OFF-to-ON. Additional characteristics of an ideal switch include that it exhibits zero-power dissipation, carries bidirectional current, and can support bidirectional voltage. If we plot the switch current (*i*) with respect to its voltage (*v*) we define four quadrants that are often referred to as the *v-i* plane and are shown in Fig. 1.5. By definition, an ideal switch can operate in all four quadrants.

Practical or real switches do have their limitations in all of the characteristics explained in an ideal switch. For example, when a switch is on, it has some voltage across it, known as the on-voltage and it carries a finite current. During the off stage, it may carry a small current known as the leakage current while supporting a finite voltage. The switching from ON-to-OFF and vice versa does not happen instantaneously. Of course, all actual switching devices take times to switch and we define these characteristics as the delay, rise, storage, and fall times. As a consequence of the above two non-ideal cases, there is voltage and current across the switch at all times, which will result in two types of losses. The first loss occurs during the on and off-states and is defined as the ‘‘conduction loss’’. The second loss is defined as the ‘‘switching loss’’ which occurs just as the switch changes state as either opening or closing. The switch losses result in raising the overall switch temperature. Further, the ON/OFF-state of the power switch must be controlled though an external signal.

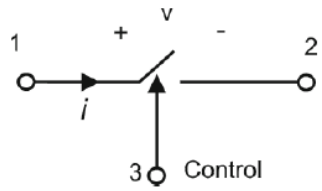

Fig. 1.4 Ideal switch

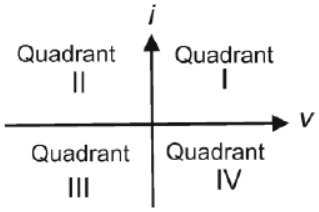

Fig. 1.5 *4-quadrant* switch
v-i characteristics

1.1.3 Classifications of Power Switches

The concept of the ideal switch is important when evaluating circuit topologies. Assumptions of zero-voltage drop, zero-leakage current, and instantaneous transitions make it easier to simulate and model the behavior of various electrical designs. Using the characteristics of an ideal switch, there are three classes of power switches:
1. *Uncontrolled switch*: The switch has no control terminal. The state of the switch is determined by the external voltage or current conditions of the circuit in which the switch is connected. A diode is an example of such switch.

2. *Semi-controlled switch*: In this case the circuit designer has limited control over the switch. For example, the switch can be turned-on from the control terminal. However, once ON, it cannot be turned-off from the control signal. The switch can be switched off by the operation of the circuit or by an auxiliary circuit that is added to force the switch to turn-off. A thyristor or a SCR is an example of this switch type.

3. *Fully controlled switch*: The switch can be turned-on and off via the control terminal. Examples of this switch are the BJT, the MOSFET, the IGBT, the GTO thyristor, and the MOS-controlled thyristor (MCT).

1.1.4 Uncontrolled Switches

A diode, also known as rectifier, is an *uncontrolled switch*. It is a two terminal device with a symbol depicted in Fig. 1.6a. The terminals are known as Anode (*A*) and cathode (*K*). In the ideal case, the diode current (*id*) is unidirectional and current can only flow from the anode to the cathode. The diode voltage (*vd*) is measured as being positive from the anode to the cathode.
The *v-i* characteristics for a real (non-ideal) diode are shown in Fig. 1.6b. In quadrant I, the diode is in the ON-state, and is known as the forward-biased region. When it is ON the diode carries a positive current while supporting a small voltage. The diode current varies exponentially with the diode voltage. The diode is reversed-biased in quadrant III, which is the OFF-state. When it is OFF, the diode supports a negative voltage and carries a negligible current (leakage current). When the negative voltage exceeds a certain limit, known as the breakdown voltage, the leakage current increases rapidly while the voltage remains at the breaking value, which potentially damages the device. Therefore, operation that exceeds the breakdown voltage must be avoided.
The ideal diode characteristics are shown in Fig. 1.6c. During the ON-state, the diode has zero-voltage across it and carries a positive current. During the OFF- state, the diode carries zero-current and supports a negative voltage.

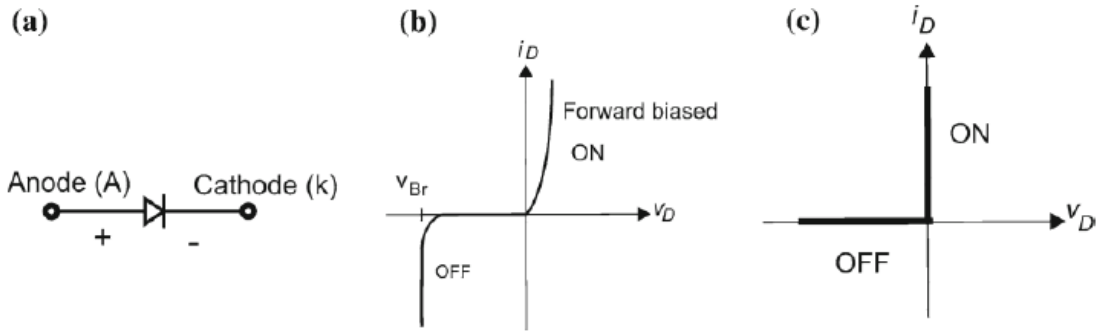

Fig. 1.6 Diode: a) symbol, b) *i-v* characteristics, and c) idealized characteristics

1.1.5 Semi-controlled Switches

The thyristor or SCR is a power semiconductor switch whose turn-on can be activated from the control terminal Gate but once it turns ON, the control terminal becomes ineffective and the thyristor behaves similar to a diode. Therefore, the thyristor is considered a *semi-controlled switch*. The name, controlled rectifier, is an indication that a thyristor is a device that can be considered as a diode whose turn-on can be commanded externally. Figure 1.7a

shows the circuit symbol for a thyristor. Although there are similarities between the diode and the thyristor circuit symbols, their operation is very different. The thyristor current, *IA*, flows from the anode (*A*) to the cathode (*K*) and the voltage *VAk*, across the thyristor is positive when the anode is at higher voltage than the cathode. Figure 1.7b shows the *v-i* characteristics of a real or non-ideal thyristor. In quadrant I, in the absence of a gate current, the device is OFF in the forward blocking region and supports a positive voltage. If a gate current is applied, the device switches to the on-state region and the device has a *v-i* characteristic similar to that of a diode. In quadrant III, the device is OFF, and the region is known as the reverse blocking region. Again, the characteristics are similar to those of a diode. Comparing the switching characteristics of a diode and a thyristor, it appears that when the thyristor is OFF, it can block large positive or negative voltage, which is a fundamental feature that is important in circuit applications, such as AC/AC converters. This can be clearly seen in the ideal characteristics of the thyristor as shown in Fig. 1.7c. In the ON- state, the thyristor has zero-voltage across it and carries a positive current. In the OFF-state, the thyristor can support a positive voltage in the forward blocking region or a negative voltage, similar to a diode, in the reverse blocking region. Therefore, the thyristor can be considered to carry a unidirectional current and supports a bidirectional voltage.

The triac, shown in Fig. 1.8a, is also a semi-controlled switch. A triac can be modeled as two thyristors connected back-to-back as shown in Fig. 1.8b. Triacs are considered as bidirectional voltage and bidirectional current devices, as shown by the *v-i* characteristics in Fig. 1.8c. The ideal characteristics are in Fig. 1.8d. As a low-cost bidirectional switch, the triac is the primary switch that is used for low power electronic commercial circuits such as light dimmers and control circuits for single-phase motors used in home appliances.

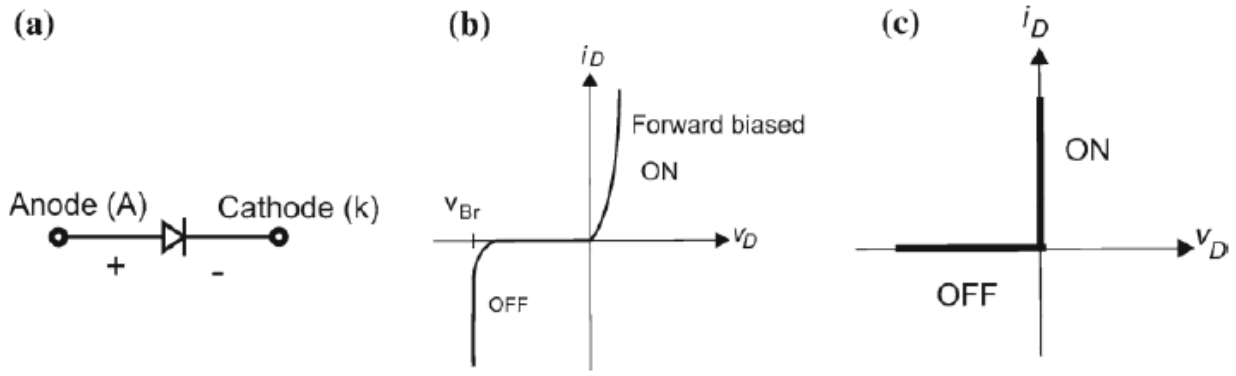

Fig. 2.6 Diode: a) symbol, b) *i-v* characteristics, and c) idealized characteristics

1.1.5 Semi-controlled Switches

The thyristor or SCR is a power semiconductor switch whose turn-on can be activated from the control terminal Gate but once it turns ON, the control terminal becomes ineffective and the thyristor behaves similar to a diode. Therefore, the thyristor is considered a *semi-controlled switch*. The name, controlled rectifier, is an indication that a thyristor is a device that can be considered as a diode whose turn-on can be commanded externally. Figure 1.7a shows the circuit symbol for a thyristor. Although there are similarities between the diode and the thyristor circuit symbols, their operation is very different. The thyristor current, *IA*, flows from the anode (*A*) to the cathode (*K*) and the voltage *VAk*, across the thyristor is positive when the anode is at higher voltage than the cathode. Figure 1.7b shows the *v-i* characteristics of a real or non-ideal thyristor. In quadrant I, in the absence of a gate current, the device is OFF in the forward blocking region and supports a positive voltage. If a gate current is applied, the device switches to the on-state region and the device has a *v-i* characteristic similar to that of a diode. In quadrant III, the device is OFF, and the region is known as the reverse blocking region. Again, the characteristics are similar to those of a diode. Comparing the switching characteristics of a diode and a thyristor, it appears that when the thyristor is OFF, it can block large positive or negative voltage, which is a fundamental feature that is important in circuit applications, such as AC/AC converters. This can be clearly seen in the ideal characteristics of the thyristor as shown in Fig. 1.7c. In the ON- state, the thyristor has zero-voltage across it and carries a positive current. In the

OFF-state, the thyristor can support a positive voltage in the forward blocking region or a negative voltage, similar to a diode, in the reverse blocking region. Therefore, the thyristor can be considered to carry a unidirectional current and supports a bidirectional voltage.

The triac, shown in Fig. 1.8a, is also a semi-controlled switch. A triac can be modeled as two thyristors connected back-to-back as shown in Fig. 1.8b. Triacs are considered as bidirectional voltage and bidirectional current devices, as shown by the *v-i* characteristics in Fig. 1.8c. The ideal characteristics are in Fig. 1.8d. As a low-cost bidirectional switch, the triac is the primary switch that is used for low power electronic commercial circuits such as light dimmers and control circuits for single-phase motors used in home appliances.

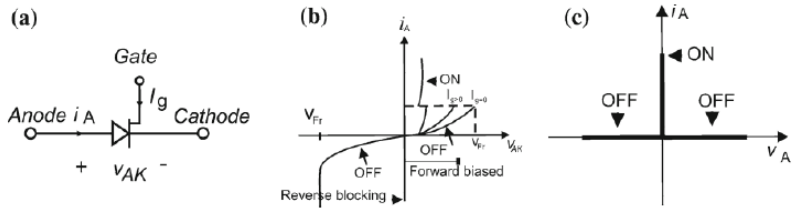

Fig. 1.7 Thyristor: a) symbol, b) *i-v* characteristics, and c) idealized characteristics

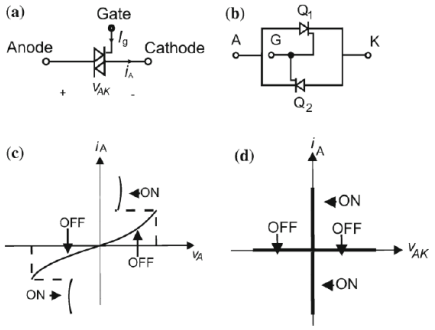

Fig. 1.8 The triac: a) symbol, b) two-thyristor-representation, c) *i-v* characteristics, and d) idealized characteristics

1.1.5.1 Fully Controlled Switches

In a *fully controlled switch,* the ON- and OFF-states can be activated externally through a control terminal. A number of power switches fall into the category of controlled switches; some of them are transistor-based devices and others are thyristor-based devices. A brief description of each device is given in the following sections:

1.1.5.1.1 The Bipolar Junction Transistor

Figure 1.9a shows the circuit symbol for an npn-type BJT. The base (*B*) is the control terminal, where the power terminals are the collector (*C*) and the emitter (*E*). The *v-i* characteristics of the device are shown in Fig. 1.9b. The device operates in quadrant I and is characterized by the plot of the collector current versus the collector to emitter voltage. The device has three regions two of them where the device operates as a switch and the third is where the device operates as a linear amplifier. The device is OFF in the region below *iB* 0 and is ON in the region where *vCE* is less than *vCE*(Sat). Neglecting the middle region, the idealized device characteristics as a switch are shown in Fig. 1.9c.

During the ON- state the device carries a collector current IC > 0 with VCE = 0. In the OFF-state, the device supports positive VCE >0 with IC = 0. Therefore, the BJT is unidirectional current and voltage device. The BJT has historical importance, but today most of its function are covered by devices like the IGBT.

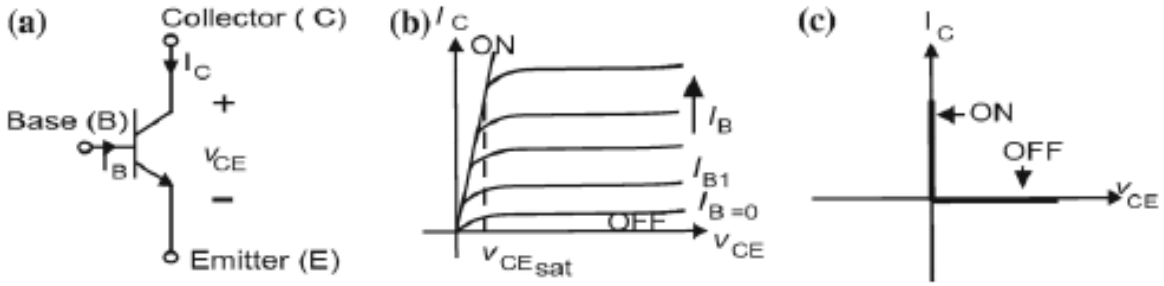

Fig. 2.9 The BJT: a) symbol, b) i-v characteristics, and c) idealized characteristics

1.1.5.1.2 The Metal Oxide Semiconductor Field Effect Transistor

Figure 1.10a shows the circuit symbol for an n-channel, enhancement mode MOSFET. Similar to the BJT, it has a control terminal known as the gate (G) and the power terminals are the drain (D) and source (S). The device is controlled by sup- plying a voltage (vGS) between the gate and the source. This makes it a voltage- controlled device compared to the BJT, which is a current-controlled device. The real v-i characteristics of device are shown in Fig. 1.10b. Similar to the BJT, the MOSFET operates within three operating regions. Two of the regions are used when the device is operated as a switch, and the third is when the device is used as an amplifier. To maintain the MOSFET in the off-state, vGS must be less than a threshold voltage known as vT, which is the region below the line marked OFF. And when the device is ON it act as resistance determined by the slope of the line marked ON. The idealized characteristics of a MOSFET switch are shown in Fig. 1.10c. When the device is ON, it has zero vDS and carriers a current ID>0 and when the device is OFF it supports a positive vDS and has zero drain current (ID = 0).

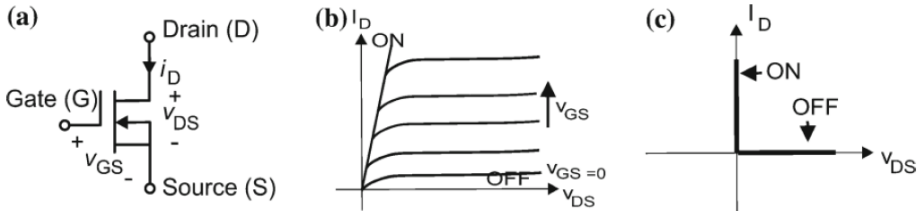

Fig. 1.10 The MOSFET: a) symbol, b) *i-v* characteristics, and c) idealized characteristics

Three other MOSFET configurations include: n-channel depletion mode and p-channel enhancement and depletion modes.

1.1.5.1.3 The Insulated Gate Bipolar Transistor (IGBT)

The IGBT is a hybrid or also known as double mechanism device. Its control port resembles a MOSFET and its output or power port resembles a BJT. Therefore, an IGBT combines the fast switching of a MOSFET and the low power conduction loss of a BJT. Figure 2.11a shows a circuit symbol that is used for an IGBT, which is slightly different from the MOSFET with similar terminal labels. The control terminal is labeled as gate (*G*) and the power terminals are labeled as collector (*C*) and emitter (*E*). The *i-v* characteristics of a real IGBT are shown in Fig. 2.11b, which shows that the device operates in quadrants I and III. The ideal characteristics of the device are shown in Fig. 2.11c. The device can block bidirectional voltage and conduct unidirectional current. An IGBT can change to the ON-state very fast but is slower than a MOSFET device. Discharging the gate capacitance completes control of the IGBT to the OFF-state. IGBT's are typically used for high power switching applications such as motor controls and for medium power PV and wind PE.

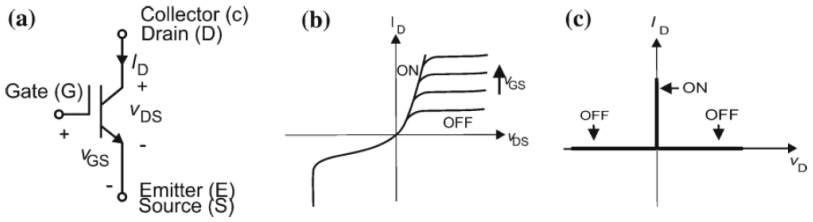

Fig. 2.11 The IGBT: a) symbol, b) i-v characteristics, and c) idealized characteristics

1.1.5.1.4 The Gate Turn-Off Thyristor

The GTO thyristor is a device that operates similar to a normal thyristor except the device physics, design and manufacturing features allow it to be turned-off by a negative gate current which is accomplished through the use of a bipolar transistor. The circuit symbol for a GTO is shown in Fig. 1.12a. The *v-i* characteristics and the ideal switch characteristics are shown in Fig. 1.12 b, c. Although the device has been in existence since the late 1960s, and it has been successfully used in high power drives, IGBTs have reached price and rating party and are expected to replace GTO's in new power electronic designs.

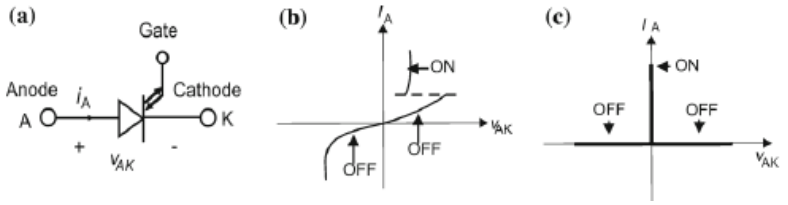

Fig. 1.12 The GTO: a) symbol, b) i-v characteristics, and c) idealized characteristics

1.1.5.1.5 The MOS-Controlled Thyristor

Similar to the IGBT, the MCT is a hybrid or double mechanism device that was designed to have a control port of a MOSFET and a power port of a thyristor. The circuit symbol for the device is shown in Fig. 2.13a. The real device characteristics and the idealized characteristics are shown in Fig. 2.13b, c. The characteristics are similar to the GTO, except that the gate drive circuitry for the MCT is less complicated than the design for a GTO as the control circuit of the MCT uses a MOSFET instead of a transistor. As a result, the MCT was supposed to have higher switching frequency. Although the MCT was invented at the same time period of the IGBT it never became fully commercially available and at the time of writing this book it is unknown the future market plans.

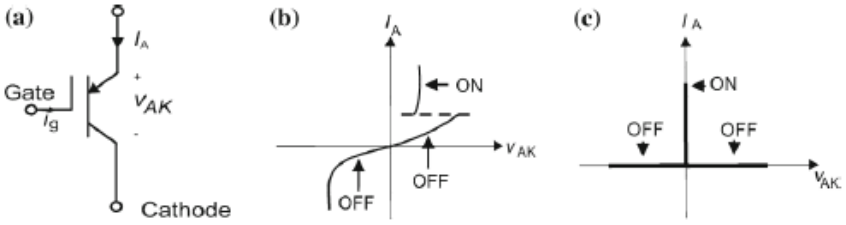

Fig. 1.13 The MCT: a symbol, b i-v characteristics, and c idealized characteristics

1.1.6 Power Electronic Converter Topologies

Power electronic converters are switch-mode circuits that process power between two electrical systems using power semiconductor switches. The electrical systems can be either DC or AC. Therefore, there are four possible types of converters; namely DC/DC, DC/AC, AC/DC, and AC/AC. The four converter types are described below:

1. *DC/DC Converter*: is also known as ‘‘Switching Regulator’’. The circuit will change the level voltage available from a DC source such as a battery, solar cell, or a fuel cell to another DC level, either to supply a DC load or to be used as an intermediate voltage for an adjacent power electronic conversion such as a DC/AC converter. DC/DC converters coupled together with AC/DC converters enable the use of high voltage DC (HVDC) transmission which has been adopted in transmission lines throughout the world.

2. *DC/AC Converter*: Also described as ‘‘Inverter’’ is a circuit that converts a DC source into a sinusoidal AC voltage to supply AC loads, control AC motors, or even connect DC devices that are connected to the grid. Similar to a DC/DC converter, the input to an inverter can be a stiff source such as battery, solar cell, or fuel cell or can be from an intermediate DC link that can be supplied from an AC source.

3. *AC/DC Converter*: This type of converter is also known as ‘‘Rectifier’’. Usually the AC input to the circuit is a sinusoidal voltage source that operates at 120 V, 60 Hz or a 230 V, 50 Hz, which are used for power distribution applications. The AC voltage is rectified into a unidirectional DC voltage, which can be used directly to supply power to a DC resistive load or control a DC motor. In some applications the DC voltage is subjected to further conversion using a DC/DC or DC/AC converter. A rectifier is typically used as a front-end circuit in many power system applications. If not applied correctly, rectifiers can cause harmonics and low power factor when they are connected to the power grid.

4. *AC/AC Converter*: This circuit is more complicated than the previous converters because AC conversion requires change of voltage, frequency, and bipolar voltage blocking capabilities, which usually requires complex device topologies. Converters that have the same fundamental input and output frequencies are called ‘‘AC controllers’’. The conversion is from a fixed voltage fixed frequency (FVFF) to a variable voltage fixed frequency (VVFF). Applications include: light dimmers and control of single-phase AC motors that are typically used in home appliances. When both voltage and frequency are changed, the circuits are called ‘‘Cyclo-converters’’, which convert a FVFF to variable voltage variable frequency (VVVF) and when fully controlled switches are used, this class of circuit is called ‘‘Matrix Converter’’. Another way of achieving AC/AC conversion is by using AC/DC and DC/AC through an intermediate DC link. This type of combined converter approach can be complex as the correct control approach must be implemented including simultaneous regulation of the DC link, injection of power with a prescribed power factor and bidirectional control of energy flow.

1.1.6.1 DC/DC Converters

A generalized circuit for a DC/DC converter is depicted in Fig. 1.14 where all possible switches connecting the input to the output are represented. If one P-switch and one N-switch are used, the resulting circuit is shown in Fig. 1.15a. The switches are controlled ON and OFF within a specified period *T*.

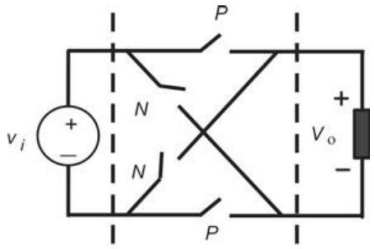

Fig. 1.14 Generalized circuit for DC/DC converter circuits

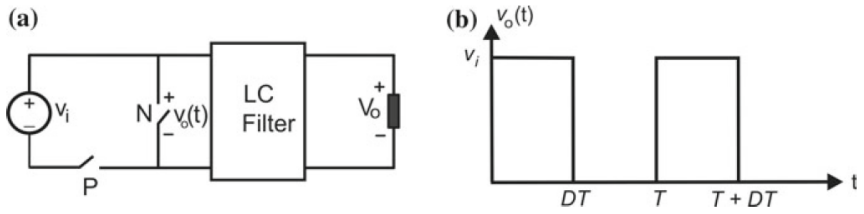

Fig. 1.15 Non-isolated down (buck) DC/DC converter: a) circuit and b) waveforms

The output voltage is equal to the input voltage when the P-switch is ON, and is equal to zero when the N-switch is ON. The ratio of the ON-time of switch P switch to the period T is defined as the duty ratio or duty-cycle (D). The waveform of the output voltage $v_0(t)$ is shown in Fig. 1.15b. Since $v_o(t)$ is a pulsating waveform, an LC circuit is used to filter the voltage to a DC. In this case the average V_o or DC component of the output voltage is given by Eq. (1.1),

$$V_{\text{avg}} = \frac{1}{T}\int_0^{DT} V_i = DV_i \tag{1.1}$$

Since $D < 1$, the DC output voltage of this converter is always less than the input voltage.
When all the generalized converter switches are used, the resulting circuit is shown in Fig. 1.16. When the P-switches are ON, the output voltage is equal to the input voltage and when the N-switches are ON, the output voltage is equal to the negative of the input voltage. The resulting waveform is shown in Fig. 1.16b. The DC component or the average of the output voltage is given by:

$$V_{\text{avg}} = \frac{1}{T}\left[\int_0^{DT} V_i dt + \int_{DT}^{T} -V_i dt\right] = (2D-1)V_i \tag{1.2}$$

Equation (1.2) indicates that the output voltage is less than the input voltage with a changed polarity. For duty-cycle $D>0.5$ the output has a positive value and for duty-cycle $D<0.5$ the output has a negative value. The LC circuit in

the design is used to filter the harmonic components of the output voltage so that the load receives a DC voltage with negligible ripple. Both voltages given by Eqn. (1.1) and (1.2) indicate that output has a lower DC value than the input voltage. Therefore, the converters are referred to as step down or buck converters.

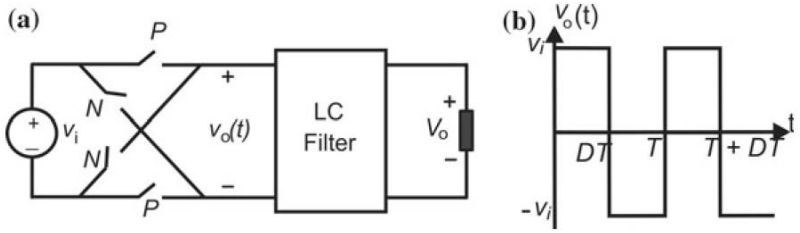

Fig. 1.16 Full-bridge non-isolated down (buck) DC/DC converter: a circuit, and b waveforms

Two other basic DC/DC converters include the boost and buck/boost converters. A boost converter can be defined as when the DC output voltage is higher than the input voltage. This design is also referred to as a step-up converter and a typical design is shown in Fig. 1.17. In this circuit, the switches are inserted between the inductor and the capacitor. If the converter is lossless, the ratio of the output DC voltage to the input DC voltage is given by Eq. (1.3). Since D is less than one, the output voltage is always higher than the input voltage.

$$V_{\text{avg}} = \frac{V_i}{D} \tag{1.3}$$

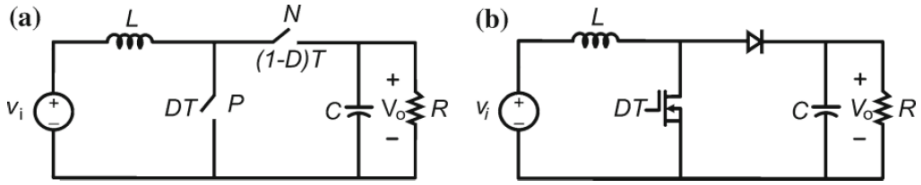

Fig. 2.17 Non-isolated boost (*up*) DC/DC converter: a circuit, and b switch implementation

A buck/boost or step-up/down converter is shown in Fig. 1.18. This converter is capable of providing a DC output voltage that can be lower or higher than the input DC voltage. The input/output conversion ratio is given by Eq. (1.4).

$$\frac{V_o}{V_i} = \frac{D}{1-D} \tag{1.4}$$

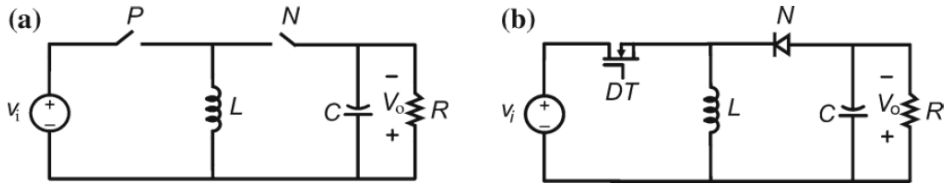

Fig. 1.18 The buck-boost (up/down) non-isolated DC/DC converter: a circuit, and b switch implementation

When the D, is less than 0.5 the converter operates as a buck or step-down converter and when D>0.5 the converter operates as step-up or boost converter. For all basic DC/DC converters discussed so far. The switch is implemented by a controlled switch (transistor) and an uncontrolled switch (diode). When the transistor and the diode are alternately switched, the mode of operation is referred to as continuous conduction mode (CCM). In this mode, the inductor current never reaches zero and the output voltage-to-input voltage conversion ratio becomes only a function of the duty ratio. If the inductor current is zero for a portion of the cycle, the mode of operation is known as the discontinuous conduction mode (DCM). The converter will operate at DCM when circuit parameters such as

inductance is decreased or when the switching frequency is decreased or when the load resistance is increased. Therefore, the output-input conversion ratio is a function of the duty ratio and several of those parameters.

The three basic DC/DC converters discussed so far are referred to as non- isolated converter topologies. Another class of converter is called isolated converters whose utilize a transformer that is placed directly between the input and output and usually have more switches and more filter components than non- isolated converters. Isolated DC/DC converters can be designed to provide multiple output DC voltages. There are some non-isolated converters that use higher order filter such as the Cuk converter, the SEPIC converter and the ZETA converter.

1.1.6.2 DC/AC Converters (Inverters)

Inverters are power electronic circuits that transform DC voltage from sources such as batteries, solar cells or fuel cells (or the output of a rectifier) into AC, for powering motor drives, providing stand-alone AC output, or interconnecting to the AC grid. Inverters can be usually classified according to their AC output as single- phase or three-phase and also as half- and full-bridge converters.

1.1.6.2.1 Single-Phase Inverters

Figure 1.19a represents a generalized DC/AC single-phase inverter. Figure 2.19b shows the resulting AC waveform when the P- and N-switches operate at a $D = 0.5$. The graph shows that the AC waveform is a square wave $D = 0.5$. Further, the voltage has no DC component which can also be shown by substituting $D = 0.5$ in Eq. (1.2). A half-bridge converter can be obtained using two DC sources of equal voltages, one P-Switch and one N-switch as shown in Fig. 2.20. The output is a square wave with a period T, which corresponds to an AC fundamental frequency as:

$$f = \frac{1}{T} \text{ Hz} \quad \text{or} \quad \omega = 2\pi f = \frac{2\pi}{T} \text{ rad/s} \tag{1.5}$$

The amplitude of the nth sinusoidal voltage can be evaluated by Fourier series of the square wave v_o(t) as

$$v_{on} = \frac{2}{T}\int_0^T v_o(t)\sin n\omega_a t dt = \frac{4V_i}{n\pi} \quad \rightarrow n = 1, 3, 5, \ldots \text{odd} \tag{1.6}$$

A filter such as a resonant LC-type circuit can be designed to filter most of the harmonics present in the square wave and prevent them from appearing across load. The fundamental voltage available from the square voltage has a fixed amplitude (as obtained by substituting $n = 1$ in Eq. (1.6). Half-bridge converters have fixed amplitude, but the full-bridge ones (as shown in Fig. 1.21) do not have this limitation.

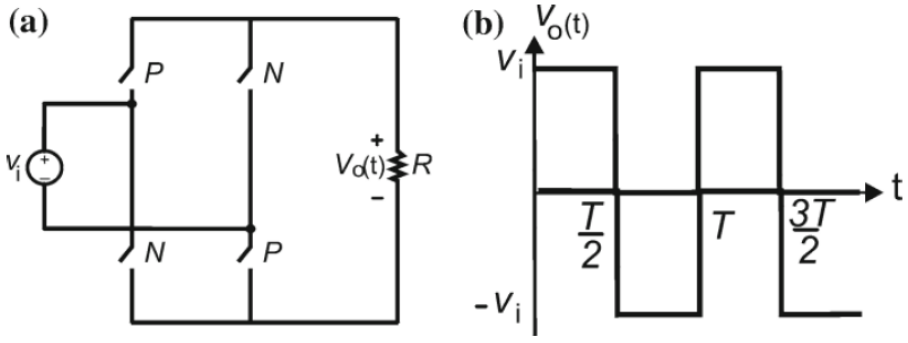

Fig. 1.19 Full bridge (*FB*) DC/AC converter: a circuit, and b waveforms

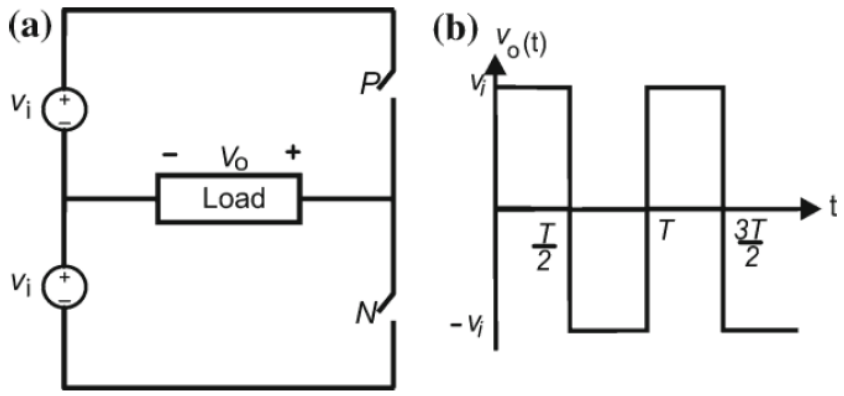

Fig. 1.20 Half-bridge (HB) DC/AC converter (inverter): a circuit, and b waveforms

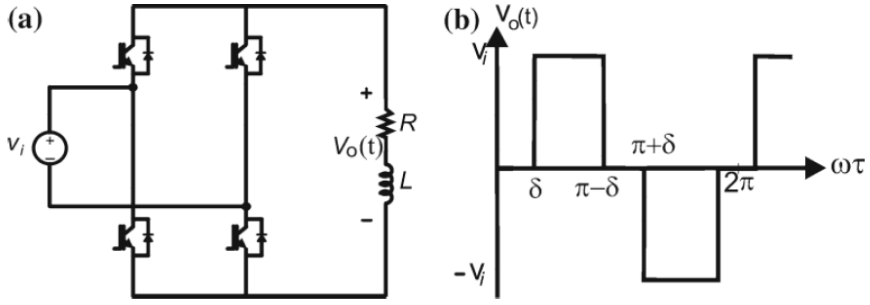

Fig. 1.21 Full-bridge (FB) DC/AC converter with variable AC voltage: a circuit, and b waveforms

Rather than having the voltage v_o to have only two levels V_{dc} or $-V_{dc}$, a third level can be used where the voltage v_o is zero and is called a three-level inverter. The resultant voltage waveform is shown in Fig. 1.21b. The angle d is a phase- shift between the two transistor legs and is used to control the amplitude of the sinusoidal nth voltage, as demonstrated by Fourier series of v_o.

$$v_{on} = \frac{4}{T}\int_0^T v_o(t)\sin n\omega_a t \;\; \mathrm{d}(\omega t) = \frac{4V_i}{n\pi}\cos n\delta \quad \rightarrow n = 1,\ 3,\ 5,\ldots\text{odd} \tag{1.7}$$

It can be seen that by varying δ from zero to π, the voltage can be varied from a fixed voltage a δ = 0 to zero-voltage at δ = π. This δ-control introduces a variable AC and also can eliminate one harmonic voltage as long a Eq.(1.8) is observed.

$$\cos n\delta = 0, \text{ which means } n\delta = \frac{\pi}{2} \tag{1.8}$$

For example, if the third harmonic voltage is chosen to be eliminated then d = p/6. This method of harmonic elimination is known as active filtering contrasted to passive filtering that requires actual filter components. Another method of active filtering is known as harmonic cancellation where harmonics are eliminated by processing waveforms. Figure 1.22shows two converters where both converters are switched at a steady square wave voltage.

The output waveforms $v_{o1}(t)$ and $v_{o2}(t)$ of the two converters are shown in Fig. 1.22b. It can be seen that each of the two converters produces a fixed two-level square wave voltage. By shifting the control of one converter by angle d, and adding the two voltage the resulting output voltage $v_o(t)$ is a variable three-level inverter, similar to the one shown in Fig. 1.21. Each of the inverters' output contains a third harmonic. However, by adding the two inverters output, the resulting voltage will not have third harmonic voltage if d is chosen to be 30°. Numerous control methods for harmonic elimination and harmonic cancellation have been proposed in the literature. These methods have resulted in two major breakthroughs in active-wave shaping or active filters; namely the method of pulse-width modulation (PWM) and the method of multilevel inverters, which will briefly be discussed later.

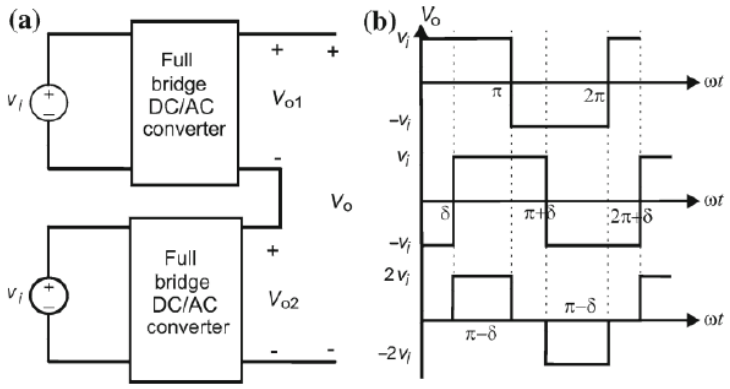

Fig. 2.22 Active filtering using harmonic elimination: a circuit, and b waveforms

The *d*-control method imposes a zero-voltage on the output voltage and if more of the zero-voltage segments are introduced, the harmonic content of the AC voltage can be reduced. For example, if two segments are introduced as shown in Fig. 1.23a, with $d = 30^\circ$ and $c = 12°$, then it can be shown that both the third and fifth harmonic voltages can be eliminated[14]. Also, if these zero-voltage regions can be introduced at high frequency (HF) with a variable width that is sinusoidally distributed at the fundamental frequency of the AC voltage, the resulting AC voltage will contain only the fundamental AC component and components at the HF of the *d*-control.

Figure 1.23b shows a converter similar to the full-bridge topology where the switches are controlled at either HF or a low frequency (LF). The HF switches operate at a frequency known as the carrier frequency, which is much higher than the fundamental AC frequency. The LF switches are operated at the fundamental frequency, referred to as the modulating frequency. During the positive half cycle of the LF switches, the HF switches are alternating at the constant carrier frequency with different on-times, i.e., a variable duty ratio. The duty ratio can be obtained by comparing a triangular wave signal at the carrier frequency with a sine wave signal at the modulating frequency, as shown in Fig. 1.23c. The resulting output waveform has a constant frequency with a modulated pulse width, so this technique is called PWM. Although no specific harmonic elimination (or cancellation) is introduced, the unwanted frequencies are pushed to higher frequency decades above the fundamental AC frequency and, as a result, the amount of passive filtering that is required can be minimized.

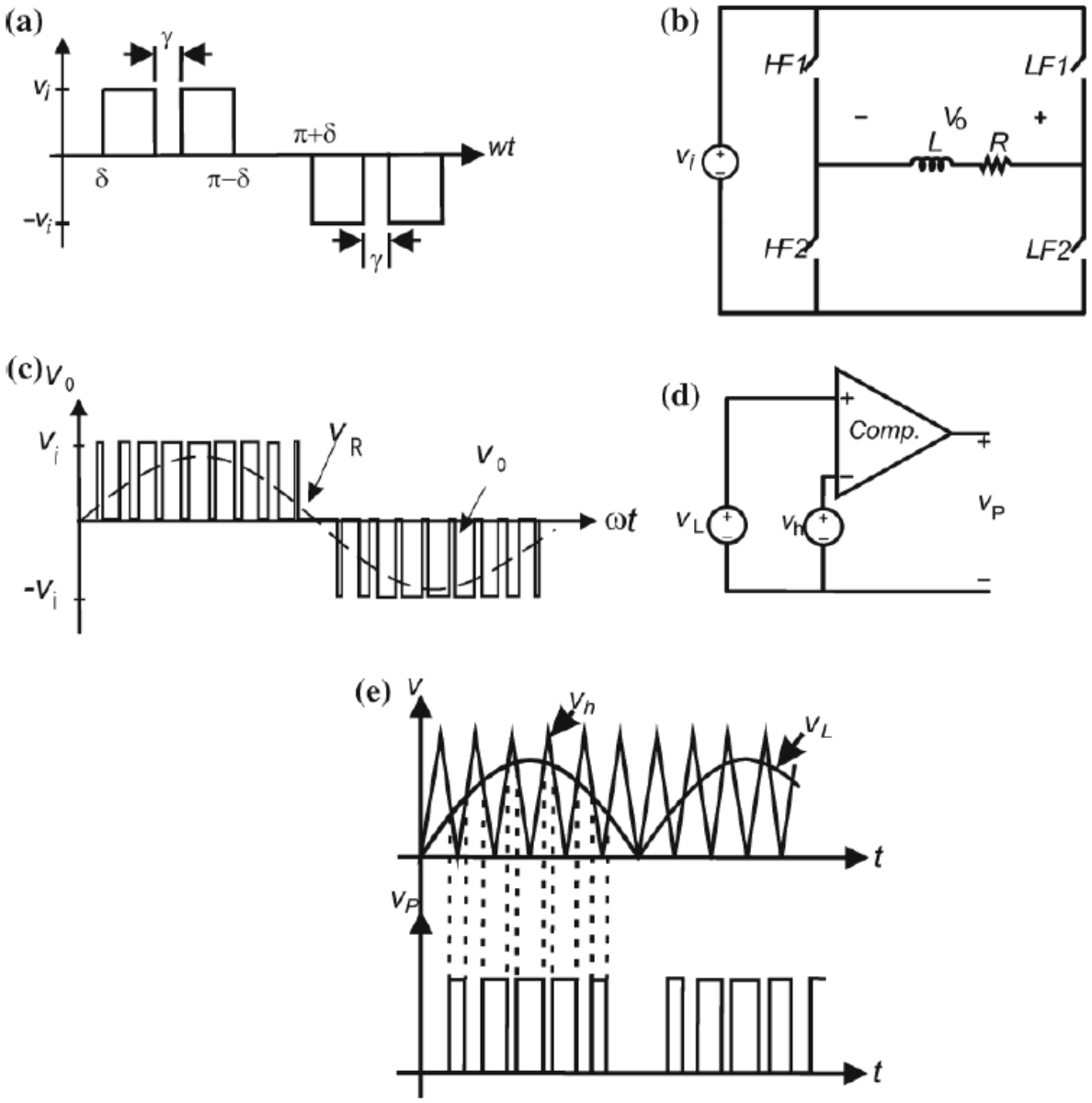

Fig. 1.23 Pulse-width modulation (PWM) switching technique: a multiple harmonic elimination, b PWM circuit, c PWM AC output, d PWM generation, and e PWM signal

1.1.6.3 Three-Phase Inverters

Three-phase DC/AC converters can be constructed using single-phase DC/AC converters (one leg branch). Three single-phase inverters can be connected to a common DC source, as shown in Fig. 1.24a. Their switch controls are shifted by 120°, with resulting output voltages shown in Fig. 1.24b. The three outputs can be connected in *Y* or D as shown in Fig.1.24c. It can be shown that the number of switches for the three independent single-phase bridge converters can be reduced to six switches rather than twelve and this design is shown in Fig. 1.25a and b. This converter design is the standard circuit topology that is used for conversion of DC to three-phase AC. The AC output depends on the control of the six switches. For example, if the switches are controlled with a phase-shift command of 60°, the resulting waveforms are shown in Fig. 1.25c.
When a DC voltage is the input to a converter, the design is defined as voltage- fed inverter (VFI) or voltage source inverter (VSI). When a DC current is the input to a converter it is defined as either a current-fed inverter (CFI) or current source inverter (CSI) as depicted in Fig. 1.26. The CSI operation constraints are: (1) there must always exist a current path for the current source; (2) the output phases cannot be short-circuited. The DC current is unidirectional, and only two switches conduct at same time providing the path for current circulation. The switch types for this design must be fully controlled in current and bidirectional in voltage. Switches that meet this requirement include: SCR, GTO, and the recently introduced IGBT.

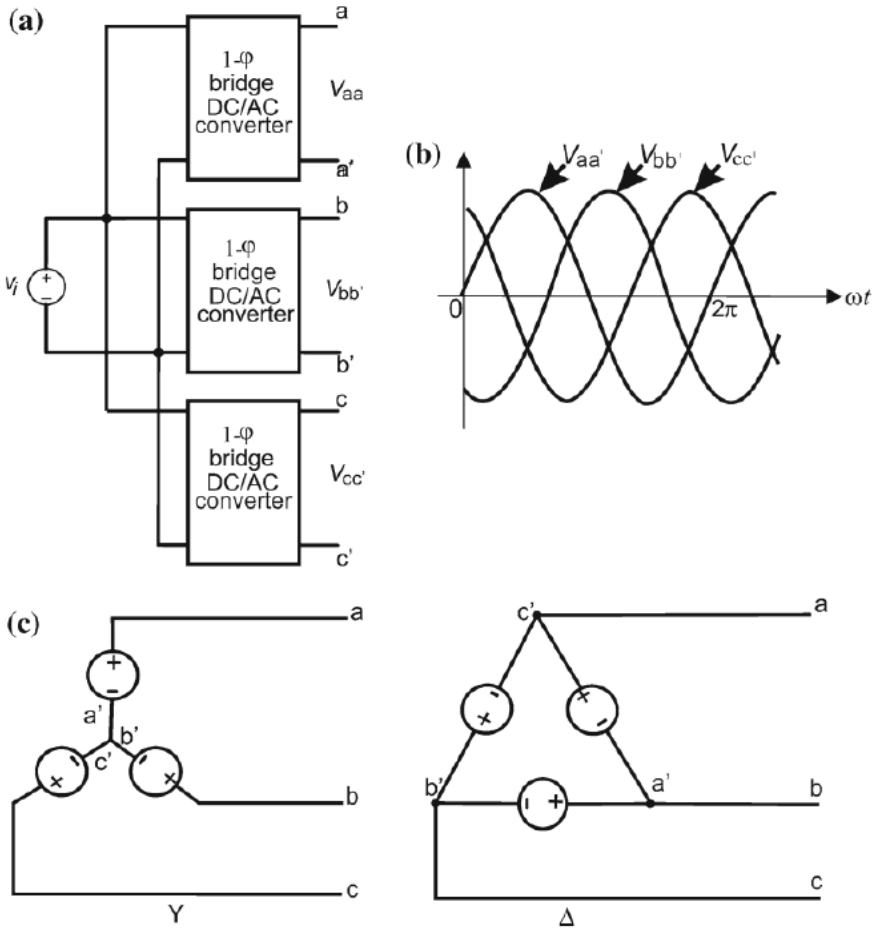

Fig. 1.24 Three-phase AC/DC converter: a circuit, b waveforms, and c connections

1.1.6.3.1 AC/DC Converters (Rectifiers)

AC/DC converters are called rectifiers circuits, which can be broadly classified based on the type of AC source and the type of semiconductor switch is used as shown in Fig. 1.27. Rectifiers are usually used in either single-phase or three-phase applications, but multi-phase topologies are possible for high power applications. Switches that are used in rectifier's designs can be either uncontrolled (diode) or controlled devices (thyristor). Single-phase rectifiers can be classified as either half-wave or full-wave circuits. Three-phase rectifiers are classified based on the number of pulses of the rectified output voltage, i.e., 3-pulse rectifiers, 6-pulse, 12- pulse, or more generally 3 9 2^n-pulse (where $n = 0, 1, 2, 3\ldots$). The number of pulses is the ratio of the fundamental frequency of the rectifier output to the frequency of the AC input.

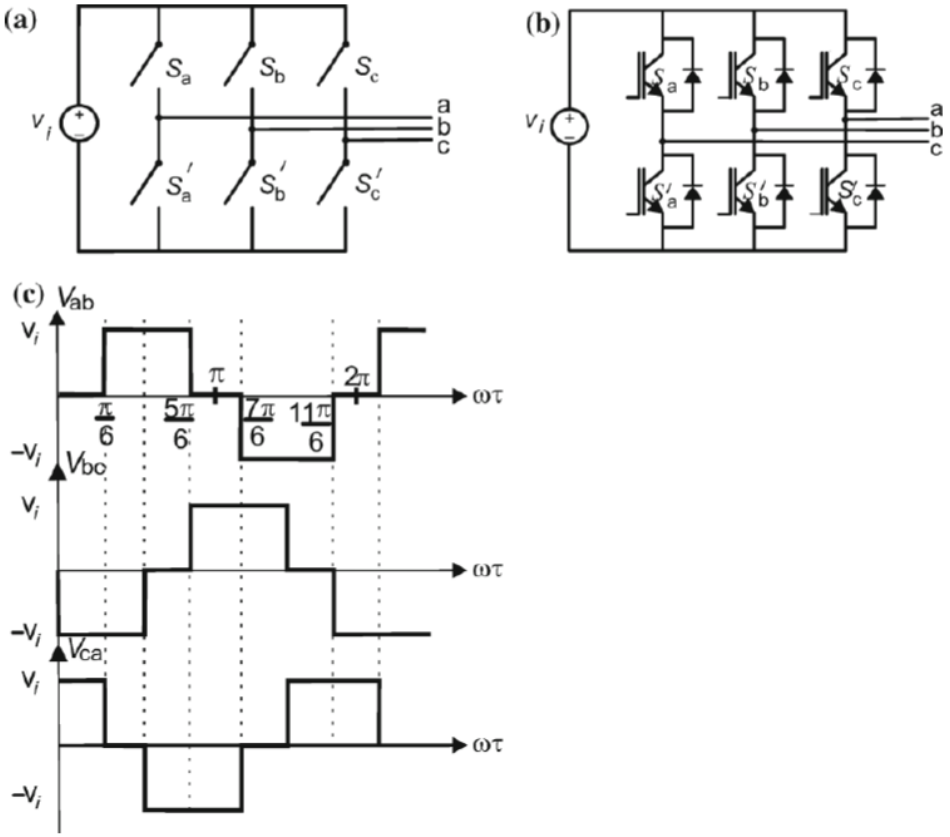

Fig. 1.25 Six-step inverter and waveforms: a circuit, b switch implementation, and c waveforms

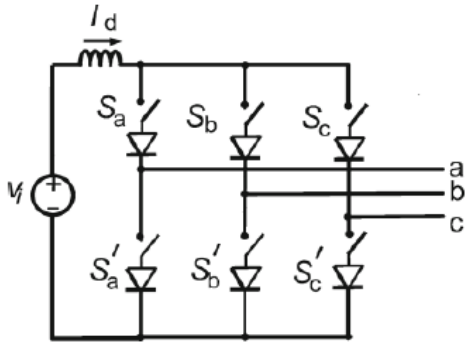

Fig. 2.26 Current source inverter (CSI)

1.1.6.3.1 Single-Phase Rectifiers

A general circuit for a single-phase rectifier is illustrated in Fig. 1.28. Note that this design is the same as the generalized DC/DC converter shown in Fig. 1.14 except that a sinusoidal voltage replaces the input DC source. The basic single- phase rectifier circuits are completed by setting the P- and N-switches to be either permanently closed or open. For example, if all the N-switches are permanently open and the bottom P-switch is permanently closed, the resulting circuit is a half- wave rectifier circuit. If the remaining P-switch is a thyristor, then the resulting circuit is a controlled half-wave rectifier. A depiction of this topology is shown in Fig. 1.28b and resulting waveforms are shown in Fig. 1.28c. In such case, the angle *a* is the thyristor turn-on delay angle, which is measured starting at the zero- crossings of the input voltage source.

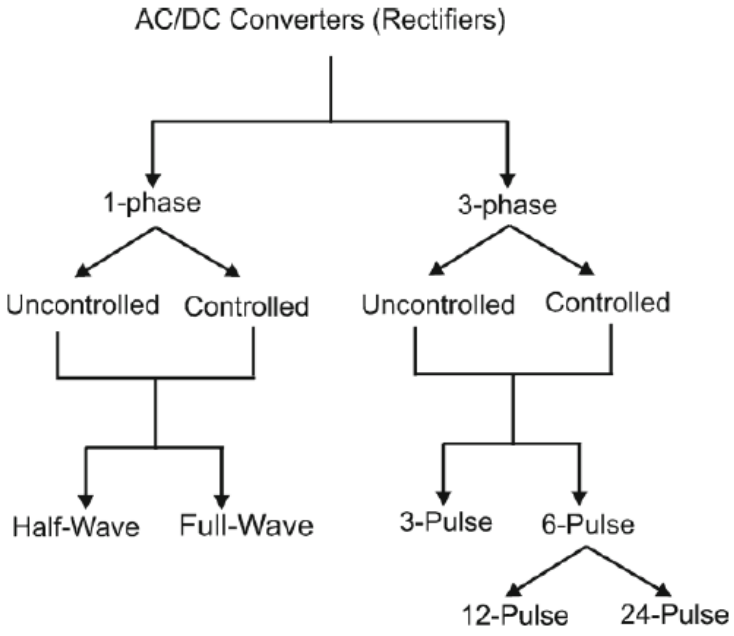

Fig. 1.27 Classifications of rectifier circuits

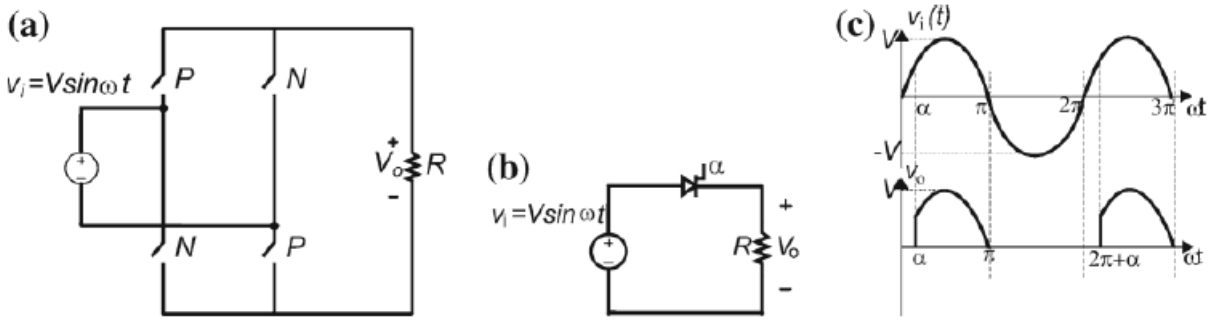

Fig.1.28 a General 1-phase rectifier circuit, b 1-phase controlled rectifier, and c Input and output voltage waveforms

The output waveform has an average value (the required DC component), which can be calculated using Eq. (1.9) as,

$$V_{\text{avg}} = \frac{1}{T}\int_0^T v(t)\,\mathrm{d}t = \frac{1}{2\pi}\int_\alpha^\pi V\sin\omega t\,\mathrm{d}(\omega t) = \frac{V}{2\pi}(1+\cos\alpha) \tag{1.9}$$

Equation (1.9) shows that the value of the DC voltage can be varied as *a* is changed. A half-wave uncontrolled rectifier is possible when the remaining P- switch is implemented through the use of a diode; this circuit is the same as in Fig. 2.28b except the thyristor is replaced by a diode. Since the diode is an uncontrolled switch, a is set to zero and the diode will turn-on at the zero-crossings of the supply voltage. When a = 0 is substituted into Eq. (1.9) then average voltage is given as:

$$V_{\text{avg}} = \frac{1}{2\pi}\int_{0}^{\pi} V \sin \omega t \, \mathrm{d}(\omega t) = \frac{V}{\pi} \tag{1.10}$$

Equation (1.10) shows that the DC voltage is fixed and cannot be changed and as a result this type of rectifier is defined as uncontrolled.

If all the switches of Fig. 1.28a are used, then the resulting circuit is a full-wave rectifier as shown in Fig. 1.29a. When all the switches are diodes, the resulting waveform is illustrated in Fig. 1.29b. The DC voltage in a full-wave rectifier design will be double the one from the half-wave rectifier.

There are circuit topologies, such as one-quadrant, two-quadrant, and four- quadrant, for half- or full-wave types. Some of them are uncontrolled, and others are fully controlled depending on the combination of diodes and thyristors, which are usually classified as semi-controlled or hybrid rectifiers. Some rectifiers use transformers for isolation for further rectification capability.

1.1.6.3.4 Three-Phase (3-U) Rectifiers

As mentioned in the classification of three-phase rectifiers, the output is defined in terms of the number of pulses per one cycle of the input voltage. The 3-pulse rectifier is a basic three-phase rectifier circuit (connected to a three-phase system), and can be used as building block for most of other three-phase rectifiers. Each of the three-phase input voltages can be determined using Eq. (1.11). The operation of a three-phase 3-pulse rectifier is shown in Fig. 1.30a, b.

$$\begin{aligned} v_a &= V \sin \omega t \ \text{V} \\ v_b &= V \sin(\omega t - 120°) \ \text{V} \\ v_b &= V \sin(\omega t + 120°) \ \text{V} \end{aligned} \tag{1.11}$$

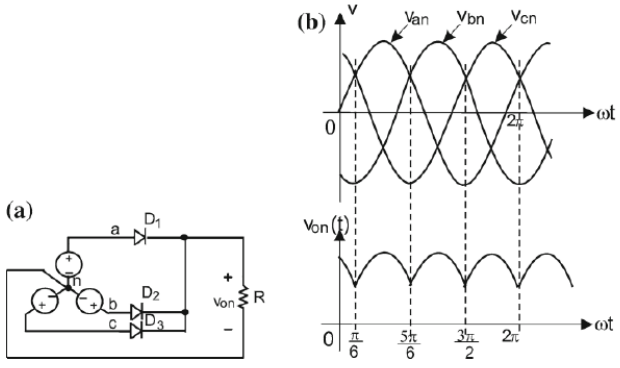

Fig. 1.30 three-phase, 3-pulse rectifier circuit: a circuit and b waveforms

In this case the switches are implemented with diodes (uncontrolled rectifier). A diode will turn-on when its voltage is higher than the other two diodes, i.e., the diode connected to the highest of the three voltages will conduct. The resulting output is shown in Fig. 1.30b; notice that the diode conduction starts and ends when two of the three voltages are equal. Also, each diode conducts for an angle of 120°, and the output voltage has 3 pulses, during one cycle of the input. Therefore, the fundamental frequency of the output voltage is three times the frequency of the input voltage. The DC component of the output of each of them can be calculated by the average over its period as:

$$V_{avg} = \frac{1}{(2\pi/3)} \int_{\frac{\pi}{6}}^{\frac{5\pi}{6}} V \sin \omega t \, d(\omega t) = \frac{3\sqrt{3}V}{2\pi} \tag{1.12}$$

The DC voltage, given by Eq. (1.12), is higher than the output voltage of a single-phase full-wave rectifier. Of course, the drawback is the need of a three- phase source, which is most common for industrial applications.

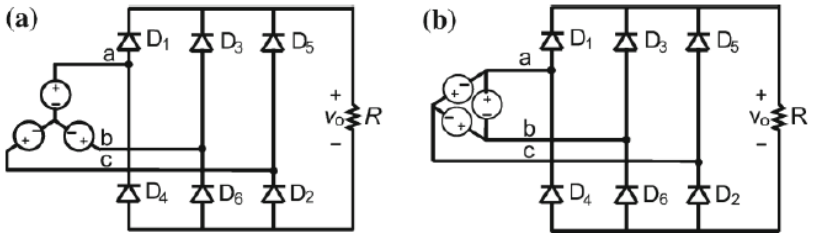

Fig. 1.31 6-pulse rectifier circuits: a Y-connected source, and b D-connected source

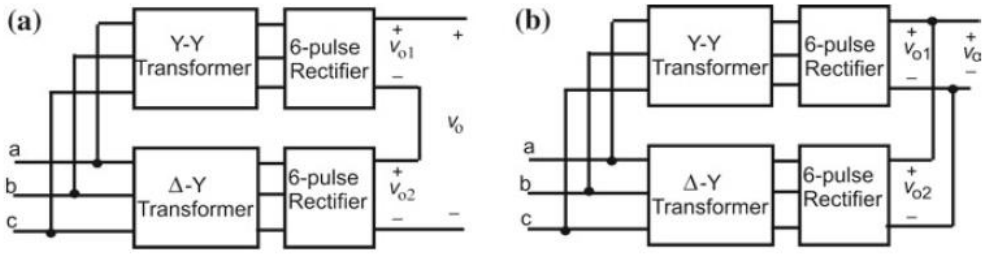

Fig. 1.32 12-pulse rectifier circuits: a high voltage 12-pulse rectifier, and b high current 12- pulse rectifier

If two 3-pulse rectifiers are connected the resulting topology is shown in Fig. 1.31. This circuit is known as a 6-pulse rectifier, and it is the building block for all high power multiple-pulse rectifier circuits.

Two 6-pulse rectifier circuits can be connected through the use of Y-Y and D-Y transformers for building 12-pulse rectifiers. If the two rectifiers are connected in series, the resulting circuit is shown in Fig. 1.32a and is suitable for high voltage, whereas the converter is connected in parallel as shown in Fig. 1.32b, the circuit is suitable for high current.

1.1.6.3.5 Controlled Rectifiers

When diodes are replaced by thyristors, the three-phase rectifier circuit becomes a controlled one, and the delay angle *a* (measured relative to the time where the diodes start to conduct) will control the output voltage. Similar to single-phase rectifiers, there are combinations of switches and transformers that result in higher pulse three-phase rectifiers.

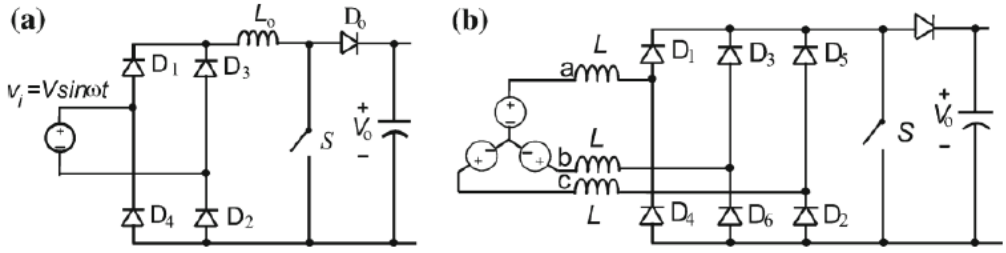

Fig. 1.33 PWM rectifier: a single-phase, and b three-phase

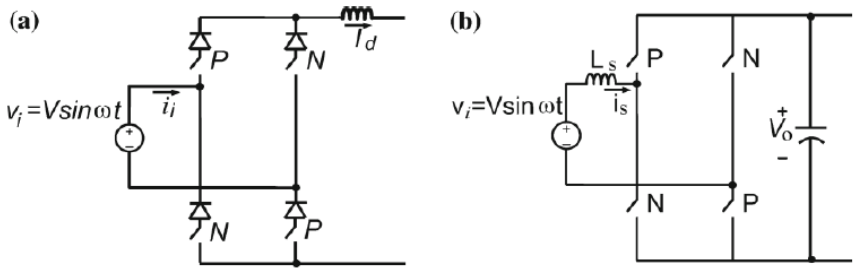

Fig. 1.34 Single-phase PWM rectifiers

1.1.6.3.6 PWM Rectifiers

PWM rectifiers can be implemented as unidirectional or bidirectional as regarding their power flow capabilities. A basic unidirectional boost version consists of an uncontrolled diode bridge followed by a boost converter as shown in Fig. 1.33a. When the switch is ON the inductor current increases proportionally to the input voltage (which is sinusoidal). When the switch is OFF, the inductor current decreases, and its energy is transferred to the capacitor, repeating such cycle with variable input voltage. The boost converter regulates the capacitor voltage, and also impresses a sinusoidal input current profile, which improves the input power factor. Since this converter can operate in either Continuous Conduction Mode (CCM) or in Discontinuous Conduction Mode (DCM), its control should be designed to be stable and work in both conditions. A three-phase version of the unidirectional boost rectifier is shown in Fig. 1.33b, but the inductors are connected at the AC side.

In order to implement a bidirectional converter fully controlled switches replace the diodes, as shown in Fig. 1.34a. This topology is called a current source rectifier (CSR). In this design, the output voltage, *V*0, is smaller than the amplitude of the input voltage, *V*, as indicated in Eq. (1.13). Therefore, the CSR is also defined as a Buck Rectifier, where the objective is to provide a constant current *I*d at the output.

$$V_0 < \frac{\sqrt{3}}{2} V \tag{1.13}$$

The boost function is possible by connecting the boost converter inductor on the AC side, as shown in Fig. 1.34b. When the AC voltage is positive and the switch T2 is ON, the inductor current increases proportionally to the AC voltage and when T2 turns-off the inductor energy is pumped to the capacitor via diodes D1 and D4. Similarly, when the AC voltage is negative T4 is turned-on. When it turns-off the energy flows via diodes D2 and D3. This topology is known as the voltage source rectifier (VSR). In VSR the output voltage, V0 is greater than the amplitude of the input voltage, V, as indicated in Eq. (1.14).

$$V_0 > V \tag{1.14}$$

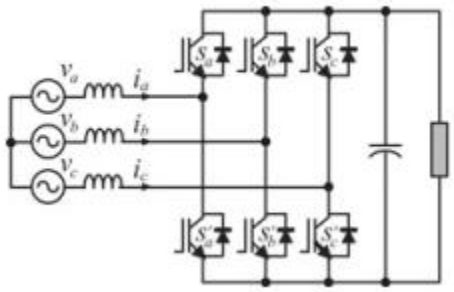

Fig. 1.35 Implementation of the three-phase VSR

The VSR is also known as Boost Rectifier with objective to provide a constant voltage V0 at the output. The CSR and the VSR are dual from each other. Figure 2.35 shows the implementation of a three-phase version of the PWM

VSR (with IGBTs). The VSR requires a large capacitor across the output, it is inherently bidirectional and can be applied in several applications where the line side converter must be able to deliver energy back to the source, such as in locomotives, cranes, and renewable energy sources connected to the DC link side.

1.1.6.4 AC/AC Converters

AC/AC converters are used to interconnect AC sources, for example from single- phase or a three-phase source to single-phase or a three-phase source. In applications that require variable AC such as light dimmers and AC motor drives, energy is converted from a FVFF to a single-phase or three-phase VVFF or VVVF. A very simple AC/AC converter circuit, to regulate the AC power for a resistive load is shown in Fig. 1.36a and the waveform shown in Fig. 1.36b. This circuit is known as AC controller, which converts from single-phase AC FVFF to VVFF single-phase AC. The fundamental frequency of the input and output is the same. By varying the switch turn-on delay angle, *a*, the amplitude of the fundamental voltage is varied. Typical applications of this circuit are light dimmers and single-phase motor drives used in home appliances. The switch implementation is usually a

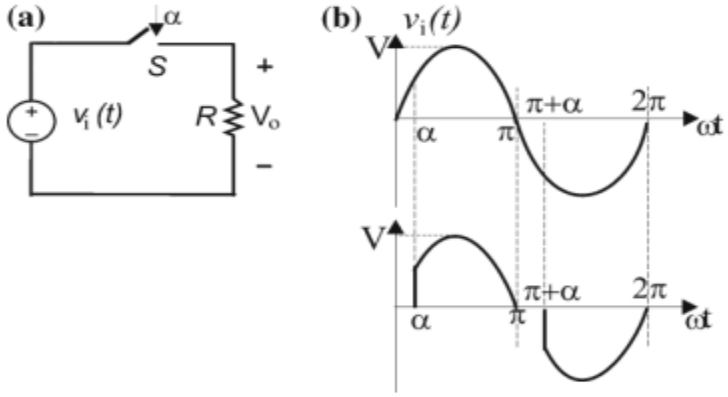

Fig. 1.36 Variable voltage fixed frequency (*VVFF*) AC/ AC converter

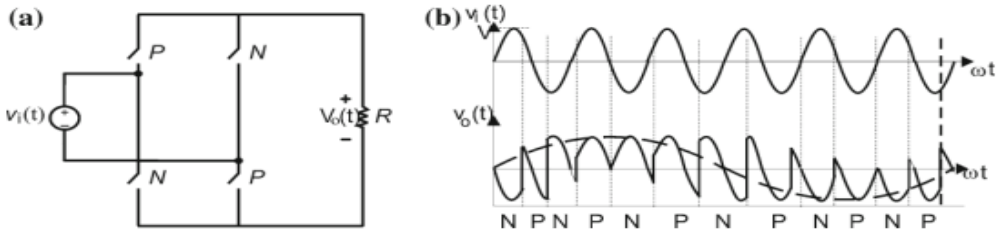

Fig. 1.37 Cyclo-converter as VVVF AC/AC converters

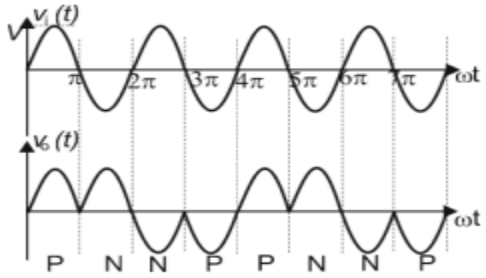

Fig. 1.38 Integral-cycle control for (VVVF) AC/AC converter

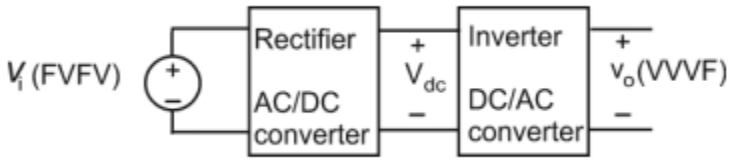

Fig. 1.39 FVFF to VVVF AC/AC converter through a DC link

triac (combination of two SCR's in anti-parallel) controlling the positive half cycle of the AC source with one thyristor and the negative half cycle with the other one. The circuit shown in Fig. 1.37a is a general AC/AC converter, referred to as a cyclo-converter. The switches can be controlled to produce an output voltage with variable amplitude and variable frequency. This is referred to as VVVF output as shown in Fig. 1.37b[14]. The P- and the N-switch are controlled to achieve an output voltage at a frequency lower than the input frequency. Another possible approach for controlling AC/AC converter is known as integral-cycle control, as shown by the waveforms in Fig. 1.38, exemplifying a case where the fundamental frequency of the output is twice the input[15].

AC/AC conversion can also be obtained by cascading an AC/DC converter with a DC/AC converter, as shown in Fig.1.39; the approach is known as ''DC link conversion'' approach. The implementation of this converter with IGBTs is shown in Fig. 1.40. This design allows two-way energy flow and four-quadrant operation and is usually applied to motor drives, electric power generation using asynchronous machines, energy storage systems (such as batteries, UPS, and flywheel energy systems), and the connection of two independent grids. Because a CSR can be modeled as a controllable DC current source, the natural load is a CSI that supports a FVFF to VVVF AC/AC converter through an inductive DC link

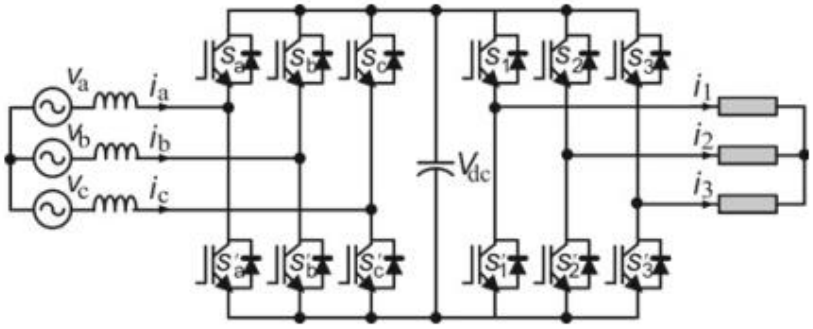

Fig. 1.40 Implementation of a FVFF to VVVF AC/AC converter through a DC link

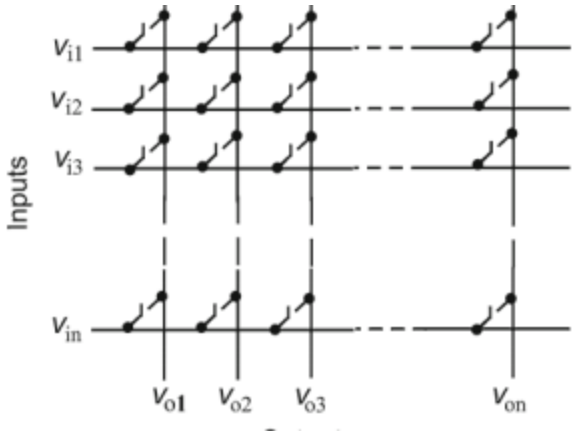

Fig. 1.41 Generalized matrix converters

1.1.7 Advanced Converter Topologies

Several advanced circuits have been developed and the field of PE is still an emerging and rapidly growing field with new converters. Some of those topologies are application-specific and will be discussed in the next sections.

1.1.7.1 The Matrix Converter

A matrix converter consists of a multi-input multi-output switching matrix that can represent all the switching converters. It can be considered as a fully controlled four-quadrant bidirectional switch, which allows HF operation. Figure 1.41 has an example of a matrix converter with n-inputs and m-outputs. Figure 1.42a shows a specific case where $n = m = 3$, i.e., a three-phase to three-phase AC/AC

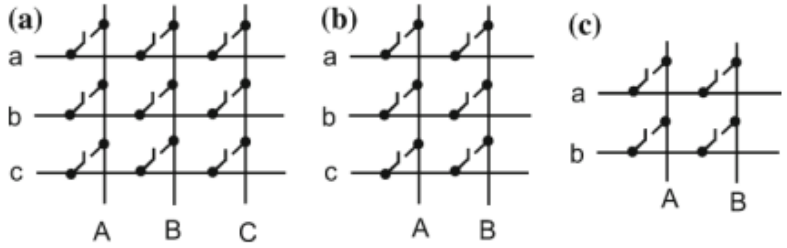

Fig. 1.42 Examples of converters derived from the matrix converter: a AC/AC, b AC/DC, and c AC/DC and DC/DC

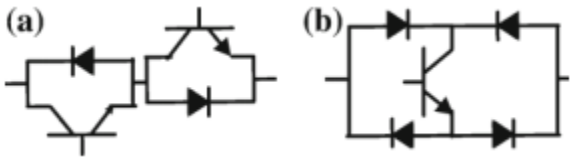

Fig. 1.43 Implementation of a fully bidirectional switch

converter, while Fig. 1.42b shows the case for $n = 3$ and $m = 1$, which can be either a three-phase AC/DC converter or a DC to three-phase AC converter. Figure 1.42c shows the converter for $n = m = 1$ (i.e., any DC/DC converter, single-phase AC/DC converter, or DC to single-phase AC converter).

The bidirectional voltage and current switch can be made of diodes and con- trolled switches as indicated in Figs. 1.43a, b. A three-phase AC to AC converter is shown in Fig. 1.44. Although the matrix converter topology has been

around for quite some time, it has gained attention in many applications because of the recent availability of switching power electronic devices and controllers.

1.1.7.2 Multilevel Inverters

Multilevel inverters are AC/DC converters where a series connection of power electronic devices and split capacitors allow high voltage applications. These inverters are modulated in a way such that the output voltage resembles a staircase

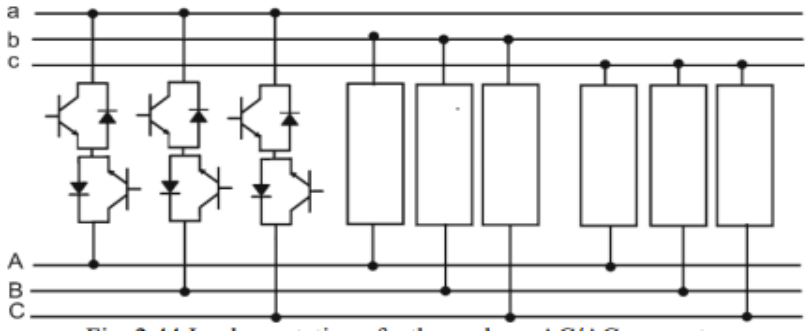

Fig. 1.44 Implementation of a three-phase AC/AC converter

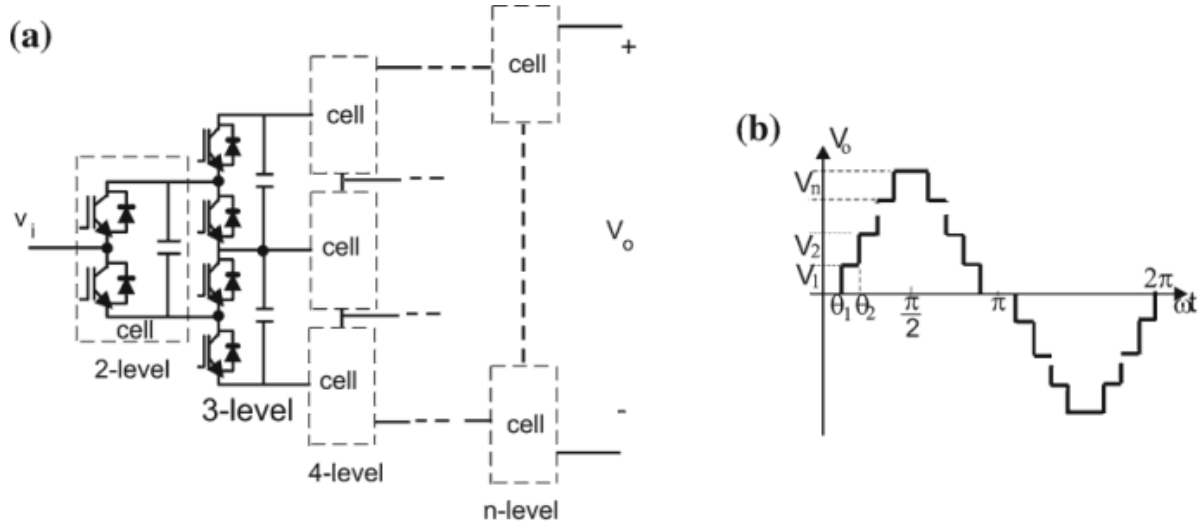

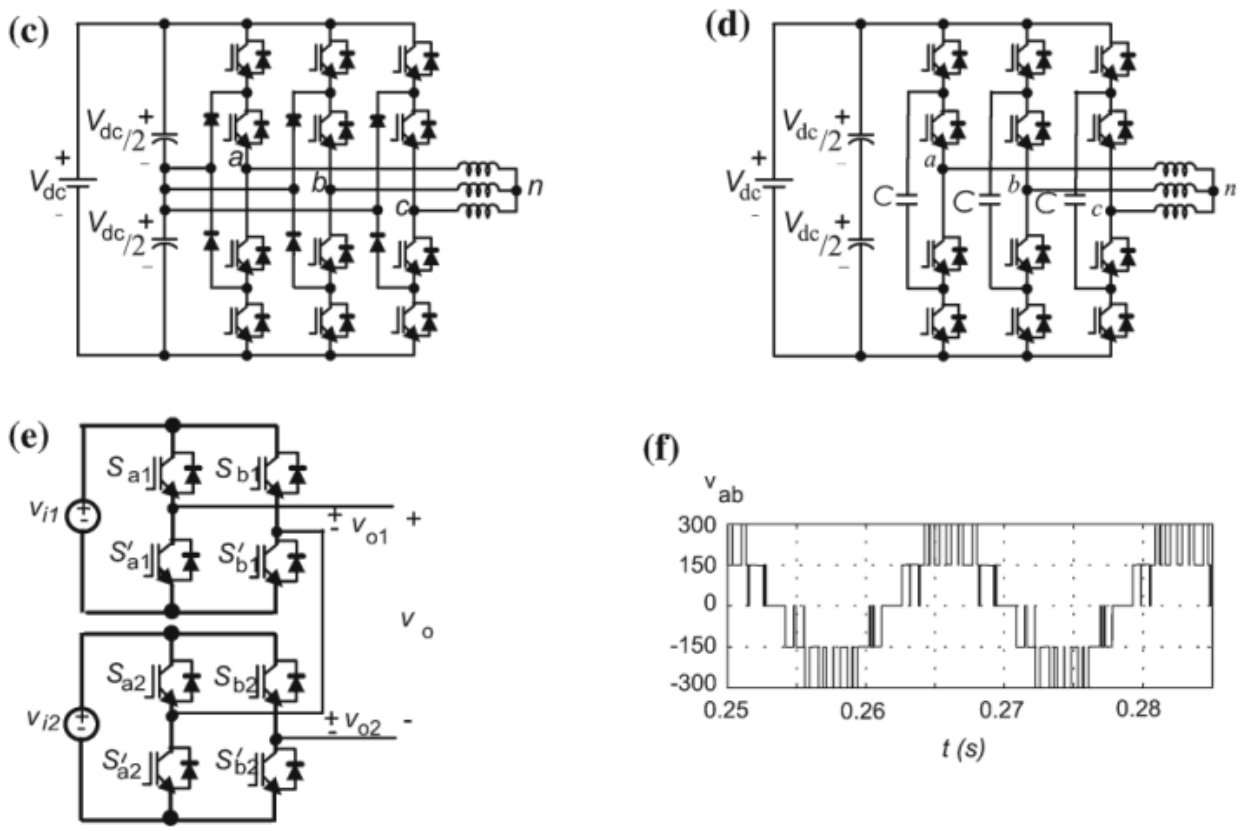

Fig. 1.45 Multilevel inverter: a generalized multi-level converter, b generalized waveforms, c NPC inverter, d flying capacitor inverter, e Hbridge cascaded inverter, and f NPC line voltage waveform

as shown by the generalized multilevel inverter in Fig. 1.45a. A three-level converter consists of series capacitor with a center tap as the neutral where each phase leg of the converter has two pairs of switching devices in series. As the number of levels increase, the synthesized output waveform adds more steps, producing a more refined staircase wave with minimum harmonic distortion, as shown in Fig. 1.45b. Of course, a zero-harmonic distortion of the output wave can be obtained by an infinite number of levels. More levels also mean that series device can provide higher output voltages without any device voltage-sharing problems. Such multiple switches and circuits usually make multilevel inverters more expensive than twolevel inverters and are cost-effective only for very specific utility and transmission or distribution power system applications. Different multilevel inverter topologies can be developed from the basic circuit of Fig. 1.45, for example the Diode Clamped (or Neutral-Point Clamped, NPC), and of the Capacitor Clamped or flying capacitor (FC) inverters, as shown in Fig. 1.45c, d, respectively, for three-level inverters. Another popular configuration is the Cascaded H-Bridge, with separate DC sources that is evolved from the two-level inverter, shown in Fig. 1.45e for five-level inverter. All these inverters can also be controlled by PWM techniques , of which one example is shown in Fig. 1.45f for the three-level NPC inverter.

1.1.8 Control of Power Converters

There are several objectives in the applications of the power converters, such as control of grid voltage, control of current, control of DC link voltage or current, as load or DC connection, control of AC load voltage or current, control of harmonics, control of speed, and so on. The control strategy applied to these cases often deal with the regulation of two variables with different dynamics, one is probably slow and another fast. Examples are: (1) for a rectifier: capacitor voltage (slow) and grid current (fast), (2) for a motor drive: motor speed (slow) and motor current (fast), (3) grid connected inverter: output current (slow) and input voltage (fast)

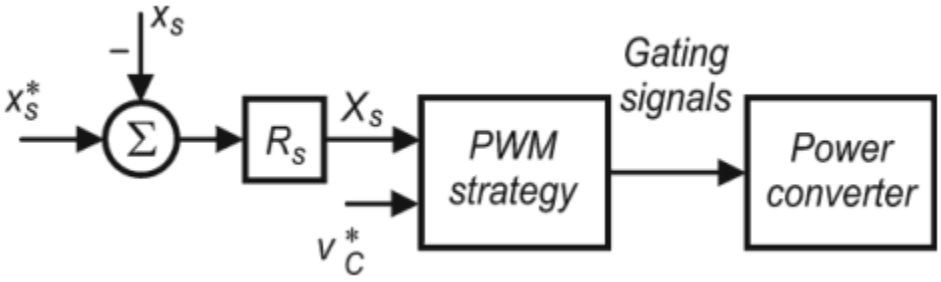

Fig. 1.46 Slow variable controller

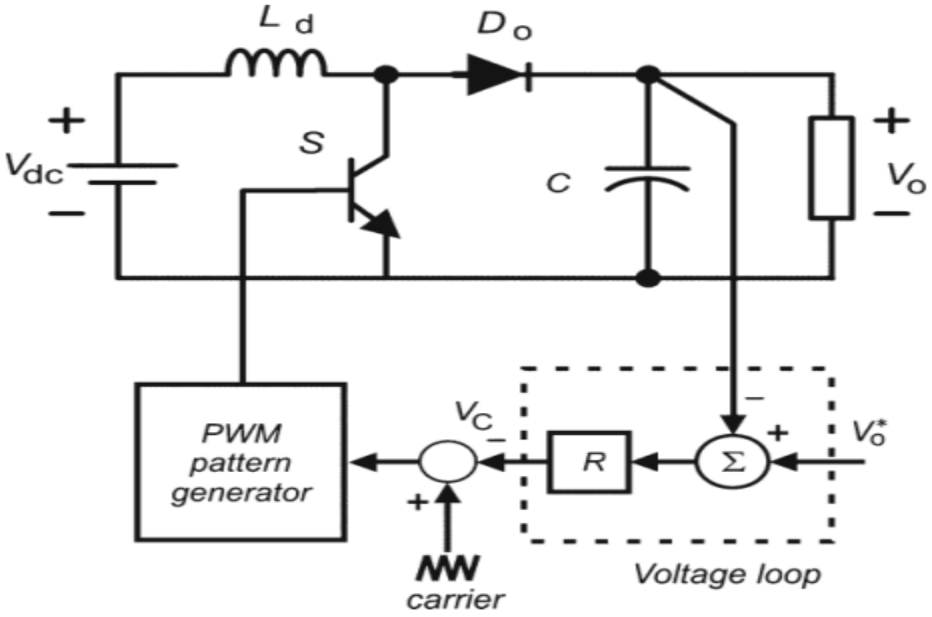

Fig. 1.47 Voltage control of a boost converter

This section will only consider the control of voltages and currents. Figure 1.46 shows a typical PWM control for a slow variable, defined as X_s is compared with its reference X_{sm}. The resulting error is regulated by the slow variable regulator, R_s: This regulator has a dynamic performance such as D is directly adjusted so that the slow variable remains regulated. This scheme can be directly applied to DC/DC converters. An example is for a boost DC/DC converter shown in Fig. 1.47, where the objective is to regulate the output voltage, V_o: For this, the error between the reference and the actual output voltage typically feeds a proportional-integrative (PI) regulator, R. The output of the regulator, the voltage control X_s v_c is compared to the carrier signal to produce a direct duty ratio PWM control. This type of control can also be employed when only one variable is controlled, such as the voltage in the PWM VSI, and the current in the PWM CSI.

The control scheme can be generalized by using a cascaded strategy, in which any external (slow variable) control defines the reference for an internal (fast variable) control. This kind of control is most often stable since both loops have different dynamics. In order to ensure a desired fast variable profile, the output of regulator R_s is synchronized with a template signal to define the internal control reference, x_{mf}: As an example, for obtaining near unity power factor operation, the PWM input line current pattern is synchronized with the grid voltage. This can be achieved in two ways: (1) the grid voltage, after filtering, can be used directly as a template for current, or (2) the zero crossing of the grid or the capacitor voltage can be used as a synchronization signal.

Two schemes for internal control will be now considered: the first one is shown in Fig. 1.48, where x_f is compared with the internal loop reference, x_{mf}; in order to generate the gating pulses. Considering only CCM operation, this comparator can:

(1) employ hysteresis (bang–bang) techniques, in which the regulated variable is maintained inside a tolerance band; (2) compare directly x_{mf} and x_f, and (3) compare the integral of x_s with x_{mf}: These three principles are indicated in Fig. 1.49 when the controlled variable is the current and the template is a sinusoidal waveform. In the hysteresis technique shown in Fig. 1.49a the measured current is compared with a tolerance band around the reference. The corresponding switch is turned on when the current reaches the lower limit of the band, Imm in; and is turned-off when the actual current reaches the upper limit of the band, Imm ax. The switching frequency varies along the current waveform. Different from the previous technique, case (2),

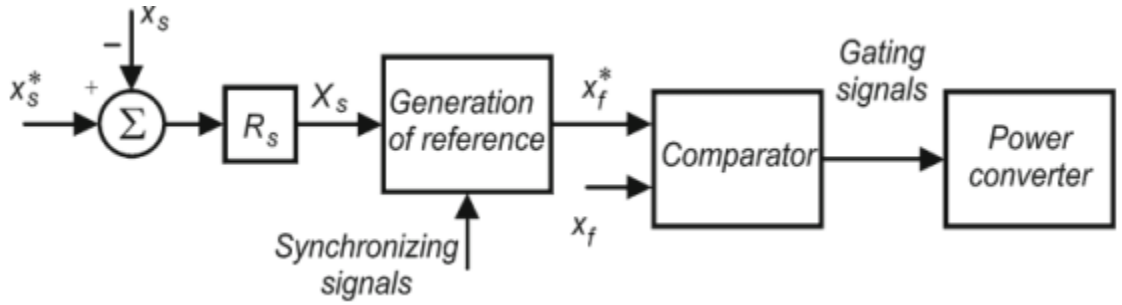

Fig. 1.48 Block scheme for both slow and fast variable control

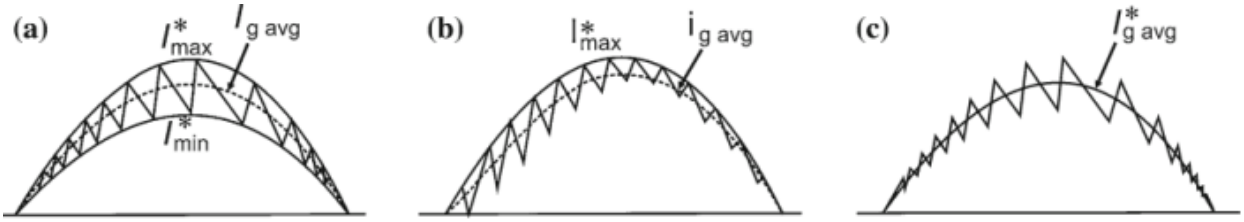

Fig. 1.49 CCM: a hysteresis control, b current peak control, and c average current control

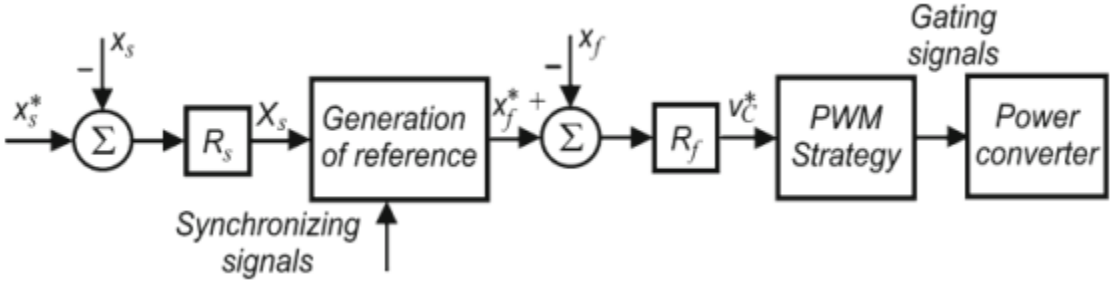

Fig. 1.50 Generalized control strategy applied to power converters

Fig. 1.49b, operates with constant switching frequency: the corresponding switch is turned-on by a clock at the beginning of each switching interval and is turned-off when the actual current tries to go beyond the reference. This technique is known as current peak control. In Fig. 1.49c the measured current is integrated so that its average value can be compared with the current reference. For this reason, this approach is known as average current control. For more information on these and other current control schemes the reader is referred to.

A possible scheme is given in Fig. 1.50 where the control error is regulated by the regulator R_f, whose output furnishes the modulating signal to be applied to the chosen PWM strategy

Consider, as an example, the control of the PWM VSR circuit, as shown in Fig. 1.51. In this case, the output voltage and the grid current are the main objectives of the converter control. In the scheme of Fig. 1.51, x_s is the capacitor voltage and x_f is the grid current.

The scheme in Fig. 1.51 includes a fast current controller, a slow DC voltage controller, such as PI, P, Fuzzy or other, and a PWM generator. Since, for power factor control, the input current reference, i_m; must be sinusoidal, and the voltage controller output is multiplied by a sinusoidal signal (template signal) with the same frequency and the same phase-shift angle of the mains supply. This template is used to produce the PWM pattern that forces the input currents to follow the desired current template I_m: This voltage source current controlled PWM rectifier is simpler and more stable than the voltage source voltage controlled PWM rectifier method. Its stability can be ensured by adequate choice of the controller gains .

Other control strategies such as the space vector scheme are also used (Fig. 1.52). In this case the voltage controller provides the value of the reference of the *d* component current, X_{dm}; while the reference of the *q* component current, X_{qm}; is fixed to zero in order to obtain unitary power factor. These references are compared with the input currents that are represented in *d-q* coordinates.

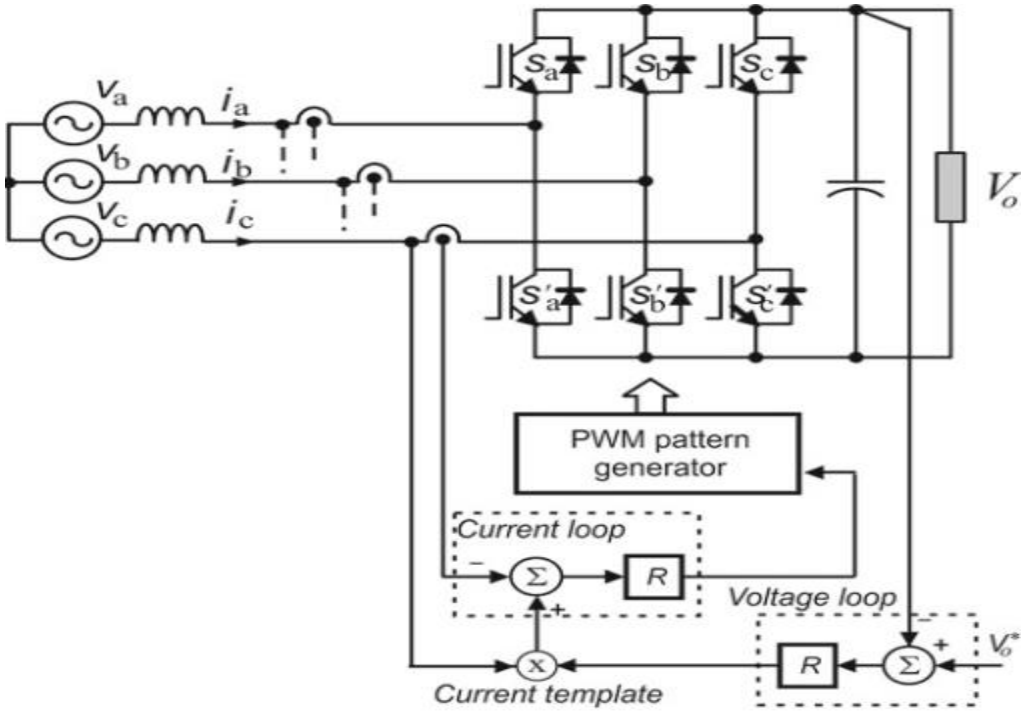

Fig. 1.51 Voltage current controlled PWM rectifier

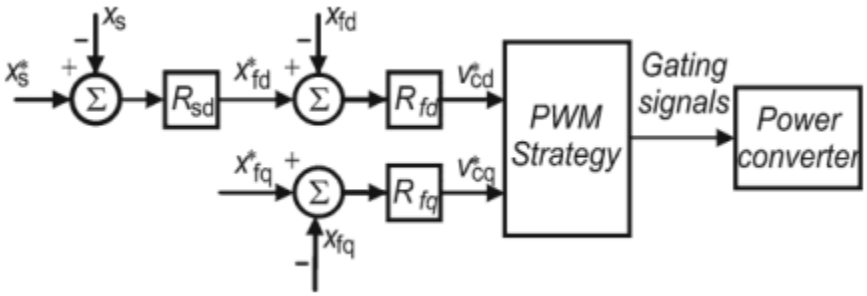

Fig. 1.52 Space-vector control scheme

Two controllers, typically PI, give the control values v_{mcd} and v_{mcq} that generate the PWM pattern which controls the VSR.The inverse transformation *dq/abc* allows for obtaining the gate drive pulses for the switches. An important point is that the current controller can be modified by other signals like the signal of balancing capacitor voltages in NPC multilevel converter.

1.1.9 Pulse Width Modulation

A PWM pattern is essential in the schemes shown in Figs. 1.46, 1.48, and 1.52. The following sections will present more advanced PWM strategies that are used in control of DC/DC and DC/AC converts. The PWM strategies will be applied to a three-phase PWM VSI and then used for a PWM CSR. It will also be indicated how these strategies can also be applied to three-phase PWM CSIs and PWM VSRs.

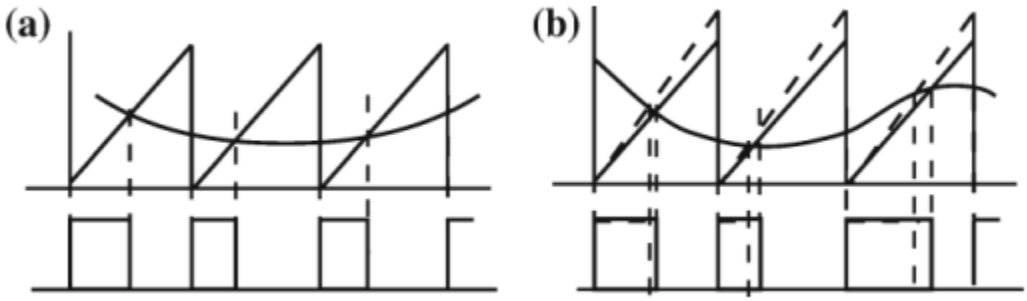

Fig. 1.53 Two principles of PWM modulators: a variation of the control voltage and saw-tooth carrier with constant slope, and b variation of the carrier amplitude

1.1.10 PWM Techniques for DC/DC Converters

The most popular DC PWM is the voltage-mode control. It is obtained by com- paring a saw-tooth (carrier) with a control voltage (modulating signal). The adjustment of the control voltage allows adjustment of the output pulse width and is shown in Fig. 1.53a. As the control voltage is increased or decreased, the *D* is increased or decreased, causing an increase or decrease in the converter output voltage. For this reason, the voltage-mode control is also called duty-cycle control, which is largely employed to control DC/DC power converters. The pulse-width control can also be obtained by varying the carrier amplitude as shown in Fig. 1.53b. For digital implementation, a digital comparator and the modulating signal are replaced by a sampled signal .

1.1.11 PWM Techniques for Two-Level Voltage Source *Converters*

PWM has been the subject of intensive research and is widely employed to control the output voltage of static power converters. A large variety of feed forward and feedback control schemes has been described in the literature, such as the Selective Harmonic Elimination PWM, but the most widely used methods of PWM are the sinusoidal pulse-width modulation (SPWM), the non-sinusoidal carrier PWM techniques, the space vector modulation (SVPWM), and the hybrid PWM (HPWM) .

The PWM techniques discussed for the VSI can be directly applied to the VSR or Boost Rectifier. Although the basic operation principle of VSR consists in keeping the load DC link voltage at a desired reference value, the PWM scheme for the VSR must provide an adjustable modulation index for the DC voltage control in addition to the reduction in the total harmonic distortion at the input current, mainly by controlling the input power factor.

1.1.11.1 Selective Harmonic Elimination PWM

Selective harmonic elimination (SHE) PWM can be explained from the output voltage waveform in Fig. 1.54, obtained by operating the circuit in Figs. 1.3 and 1.19, with 2Vi Vdc and four extra commutations per cycle in relation to the square wave. The choice of the values of the angles a1 and a2 allows to eliminate or reduce two selected harmonics in the squarewave form. The Fourier analysis of the waveform given in Fig. 1.19 allows for determining the amplitude of the fundamental and harmonic voltage content of the pole voltage waveform, that is,

$$V_{\mathrm{ao}(n,m)} = \frac{4}{\pi}\frac{V_{\mathrm{dc}}}{2}\left(\frac{1 - 2\cos n\alpha_1 + 2\cos n\alpha_2}{n}\right) \tag{1.15}$$

Specific harmonics will be eliminated when the numerator of Eq. (1.15) is set equal to zero for a given value of *n*. For example, the third and fifth harmonics are the largest present in the square-wave voltage, and because they are relatively close to the fundamental frequency they are also the most difficult to filter. Their elimination is obtained by solving two trigonometric equations issued from (1.15), assuming that $0\circ<a_1<90\circ$; $0\circ<a_2<90\circ$ and $a_1<a_2$; which results in

$$\alpha_1 = 23.62^\circ$$

$$\alpha_2 = 33.30^\circ$$

$$\alpha_1 = 16.25^\circ$$

$$\alpha_2 = 22.07^\circ$$

More harmonics can be eliminated by the introduction of additional notches.

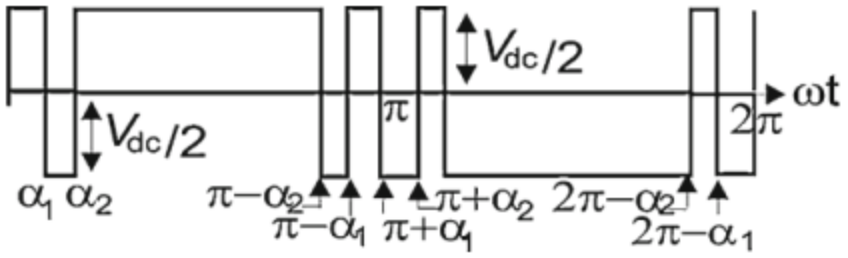

Fig. 1.54 Selective harmonic elimination PWM

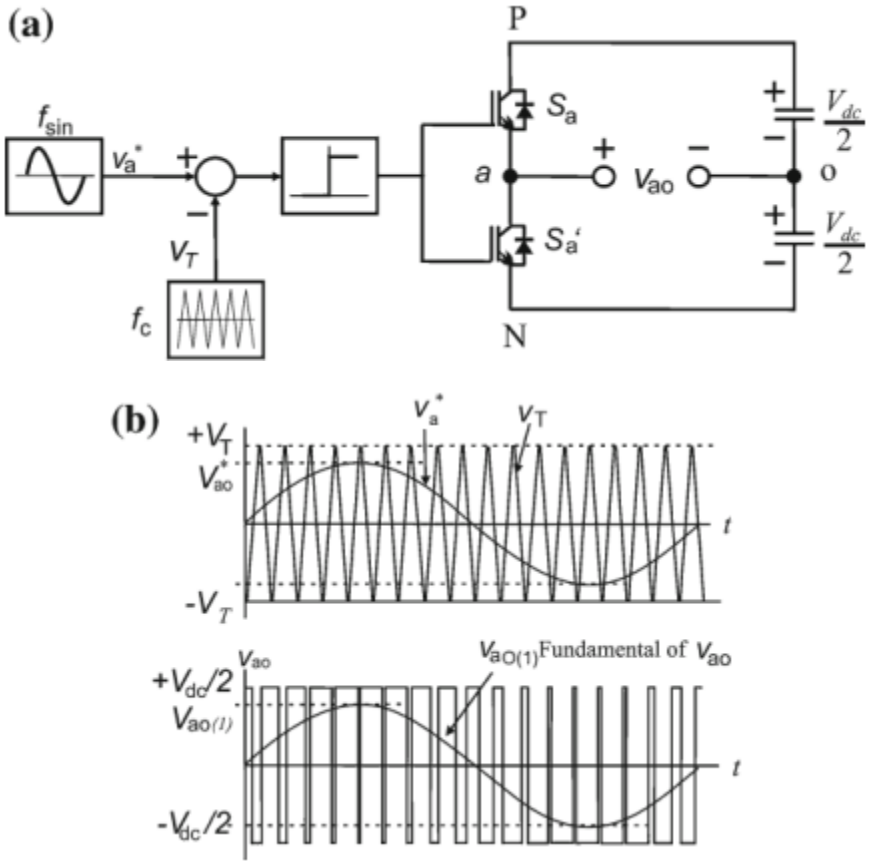

Fig. 1.55 Sinusoidal PWM a bipolar voltage switching for half-bridge inverter, b control signals (*upper*) and pole voltage (*lower*)

1.1.11.2 Carrier Modulation

In Sect. 1.3, a modulated pulse width is obtained by comparing a triangular wave at the carrier frequency with a sine wave signal at the modulating frequency. This technique is known as Sinusoidal PWM [1, 3, 5, 12). Its principle is shown in Fig. 1.55a, b, for a half-bridge inverter. When the modulating signal, v *a; is higher than the carrier signal, *vT*; the upper switch is turned on and the inverter leg assumes a switching state ‘‘P’’. The pole voltage is then equal to *V*dc=2: When the modulating signal is lower than the carrier signal, the lower switch is turned-on, and the inverter leg assumes a switching state ‘‘N’’. The pole voltage is then equal to *V*dc/2: The ratio between the amplitudes of the sine wave and the carrier signals is defined as amplitude modulation ratio *ma*; and that between the carrier frequency and the modulating frequency is defined as the frequency modulation ratio, *mf*: In order to

avoid the effects of sub-harmonics *mf* should be an odd integer. When *mf* is high enough, the amplitude of the fundamental frequency component of the pole voltage, *V*ao; in Fig. 1.55a is linear with the variation of *ma*; that is,

$$V_{Ao1m} = m_a \frac{V_{dc}}{2} \tag{1.20}$$

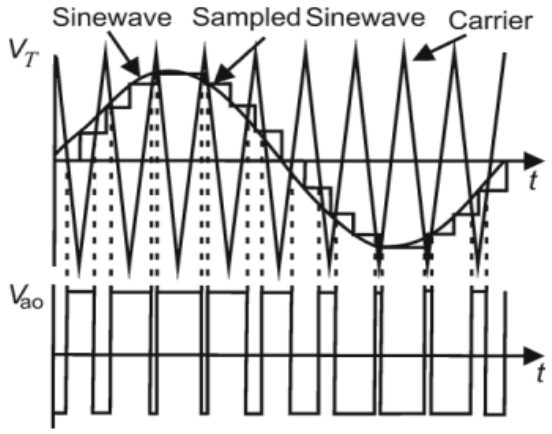

Fig. 1.56 Regular-sampled PWM

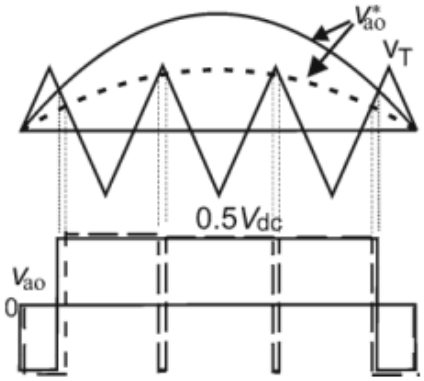

Fig. 1.57 Operation in over modulation region

Also, the harmonics of the output voltage waveform appear centered around harmonics m_f, $2m_f$ and so on, as sidebands.

The pulses are almost centered inside the switching interval; the use of high switching frequencies to improve this location can be avoided by sampling the signals as done for the regular sampled modulation (RSPWM) [13] shown in Fig. 1.56. Nevertheless, sinusoids will continue to be used in the examples that follow.

A value of $m_a>1$ causes over modulation with a reduction in the number of pulses in the pole voltage v_{ao1} waveform, as shown in Fig. 1.57, and loss of linearity. However, the addition of an adequate zero-sequence component, either continuous or discontinuous, to each of the pole voltage reference waveforms makes possible to increase in 15.5 % the fundamental of the output voltages [14]. Figure 1.58 shows an example of the third harmonic injection PWM (THIPWM), which is somewhat flattened on the top [15]. Injection of other zero-sequence components makes possible to generate different PWM strategies such as Symmetrical PWM and Discontinuous PWM [5, 14–20].

The above concept can be expressed in terms of the sinusoidal reference plus a zero-sequence signal v_h; that is,

$$v_a^{*'} = v_a^* + v_h \tag{1.21}$$

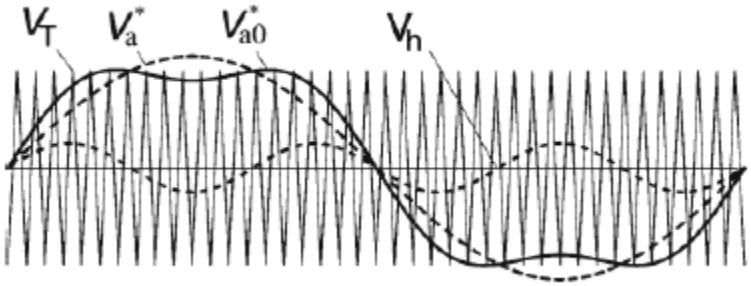

Fig. 1.58 Operation in over modulation region—non-sinusoidal PWM:sinusoidal reference, v_{ma}, modulating signal generated, $V_{ao}{}^m$; and zero-sequence signal v_h (middle) for the THIPWM strategy

From (1.21), the SPWM corresponds to V_h =0. For the three-phase inverter shown in Fig. 1.59a there are three modulating signals, one for each of the phases, and one carrier signal, as shown in Fig. 1.59b. This figure shows the pole voltage and the line–line voltage of the inverter.

In the following section, it will be shown how to build different PWM techniques for the three-phase VSI, using the concepts mentioned above. The extension of Eq. (1.21) to the three-phase case results in

$$v_j^{*'} = v_j^* + v_h \quad (j = a, b, c) \tag{1.22}$$

An important feature is that the injected zero-sequence signal V_h will not increase the LF harmonic distortion in the inverter output voltage.

The most used v_h signal can be easily determined for any of the Sectors from I to VI, which divide the fundamental period, as shown in Fig. 1.60, from [21].

$$v_h = \frac{v_M + v_m}{2} \tag{1.23}$$

That is, from the average value of V_M+Vm; where V_M and V_m are the maximum and the minimum values among the three sinusoidal reference voltages, V_a; V_b and Vc; respectively. In the switching interval considered, V_a and V_c have the maximum and minimum values, respectively, while V_b is at an intermediate value. Therefore, in the case, V_h corresponds to the intermediate values, V_{mid}; along the three references along the fundamental period (see the dashed line in Fig. 1.60), since V_a; V_b and V_c change position in the different sectors. The continuous line in Fig. 1.61 represents the new modulating signal for one phase.

As mentioned, many other continuous and discontinuous zero-sequence components can be employed in Eq. (1.22), resulting in different non-sinusoidal carrier-based PWM techniques, but their discussion is out of the scope of this

chapter. The combination of the conduction of the switches ‘‘P’’ (upper switches) and the switches ‘‘N’’ (lower switches) in legs a, b, and c of the inverter in Fig. 1.59a, allows for eight possible switch combinations, denoted by SCi (i = 0, 1…7). Six of these switch combinations, SC1 = PNN, SC2 = PPN, SC3 = NPN, SC4 = NPP, SC5 = NNP, and SC6 = PNP, apply voltage to the output (active switch combinations) while switch combinations SC0 = NNN and SC7 = PPP correspond to the short circuiting of the lower switches and of the upper switches, respectively.

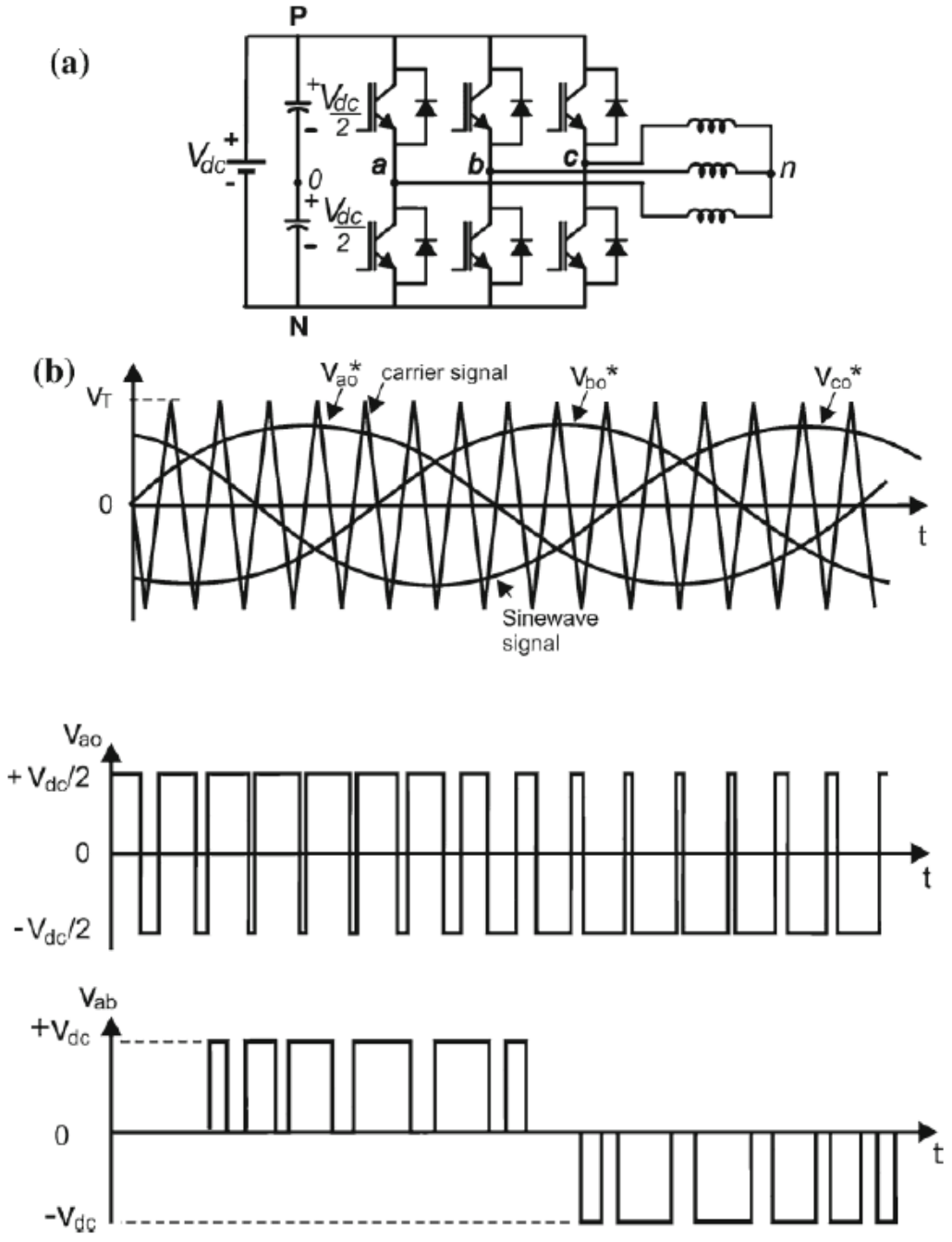

Fig. 1.59 Three-phase sinusoidal PWM: a inverter circuit, b principle, pole voltage, and inverter output voltage

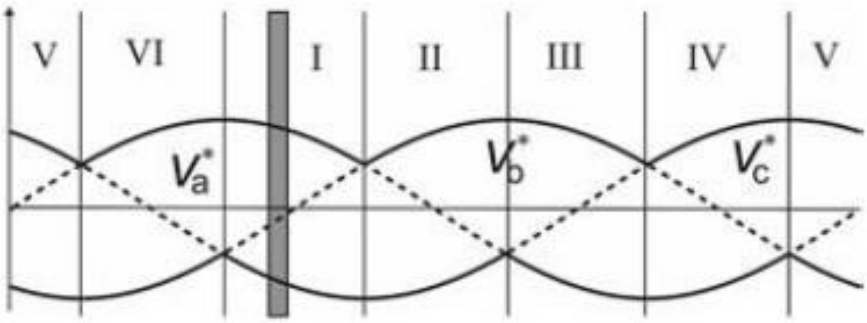

Fig. 1.60 Sectors inside one period

Figure 1.62 shows the representation of the modulated pulse waveforms inside a switching interval of Sector I. The intersection of modulating voltages (references) V_M V_a^m V_m V_b^m, and V_{mid} V_c^m with the triangle defines: (1) the pulse widths for each of the phase voltages, S_1;S_2 and S_3; (2) the distances between the switching instants for phases a, b, c, the delay of the first switching procedure t01; the distances of the switching instants, t_1 and t_2; and the remaining time of the

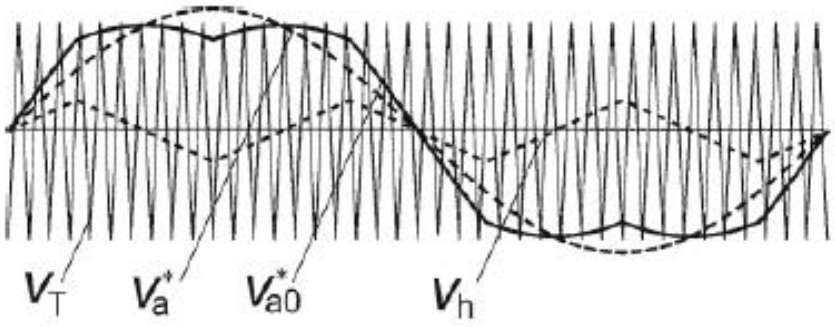

Fig. 1.61 Operation in over modulation region—non- sinusoidal PWM: V_a^m; modulating signal generated, V_{ao}^m; and zero-voltage signal V_h (middle) generated for Symmetric PWM

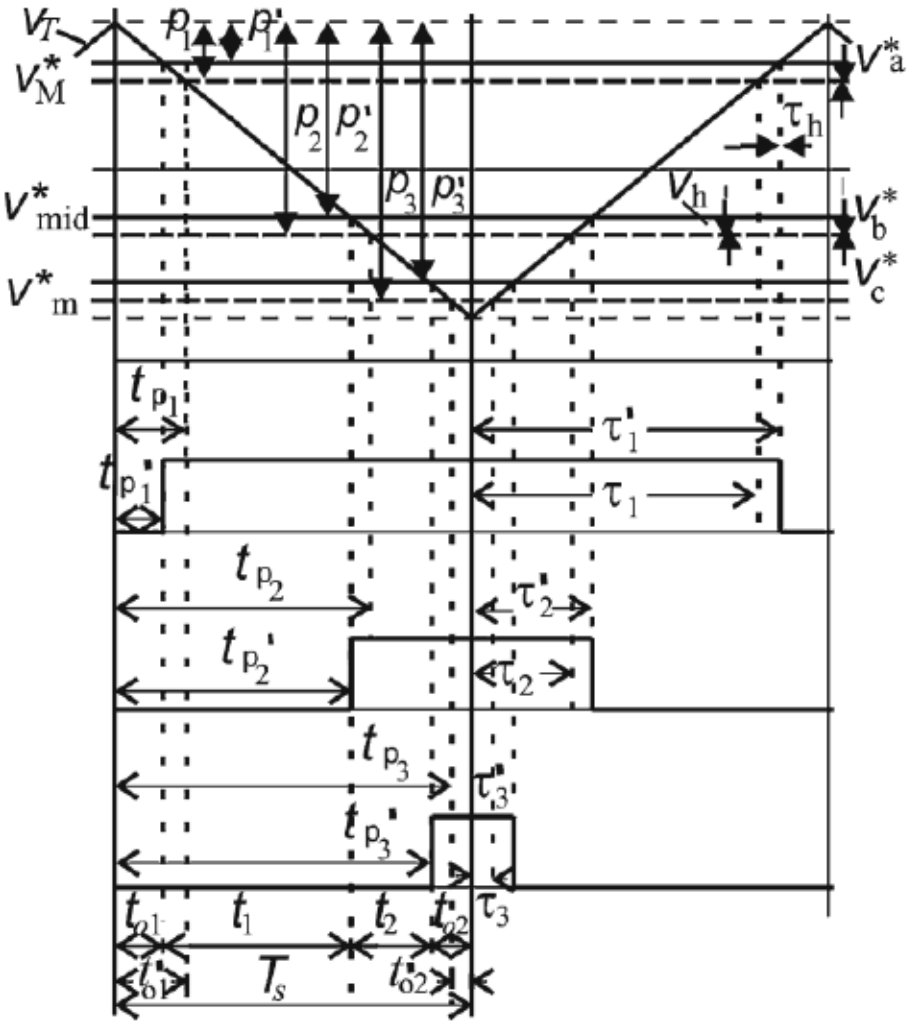

Fig. 1.62 Pole voltage pulse width inside a switching interval

sampling period t_{02}; and (3) the time intervals t_{p1}; t_{p2}; and t_{p3} (switching delays) before each leg changes in a given switching interval. When the zero-sequence component is added to the sinusoidal reference, the intervals t_1 and t_2 between the phase pulses remain the same. Instead, the pulse widths for each of the phase voltages, S_1; S_2; and s3; do change, and become S_{01}; S_{02}; and S_{03}: Note that, inside the switching interval, the intervals t_{01}; t_1; t_2, and t_{02} indicate the duration of the switch combinations NNN, ONN, PPN, and PPP, which occur in all switching periods inside Sector I. Note, also, that

$$t_z = t_{01} + t_{02} = T_s - (t_1 + t_2) \qquad 1.24$$

In Eq. (1.24), $t_z = t_{01} + t_{02}$ constitutes the total freewheeling interval. Note, finally, that t_{01} and t_{02} are equally distributed at the beginning and at the end of the switching interval. In reality, these zero interval constituents can assume different values provided that the condition in (1.24) is observed.

1.1.11.3 Space Vector Modulation

The space vector pulse-width modulation (SVPWM) technique does not consider each of the three-phases as a separate entity. The three-phase voltages are simultaneously performed within a two-dimensional reference frame (plane), the complex reference voltage vector being processed as a whole. Because of its flexibility of manipulation, the SVPWM technique became popular .

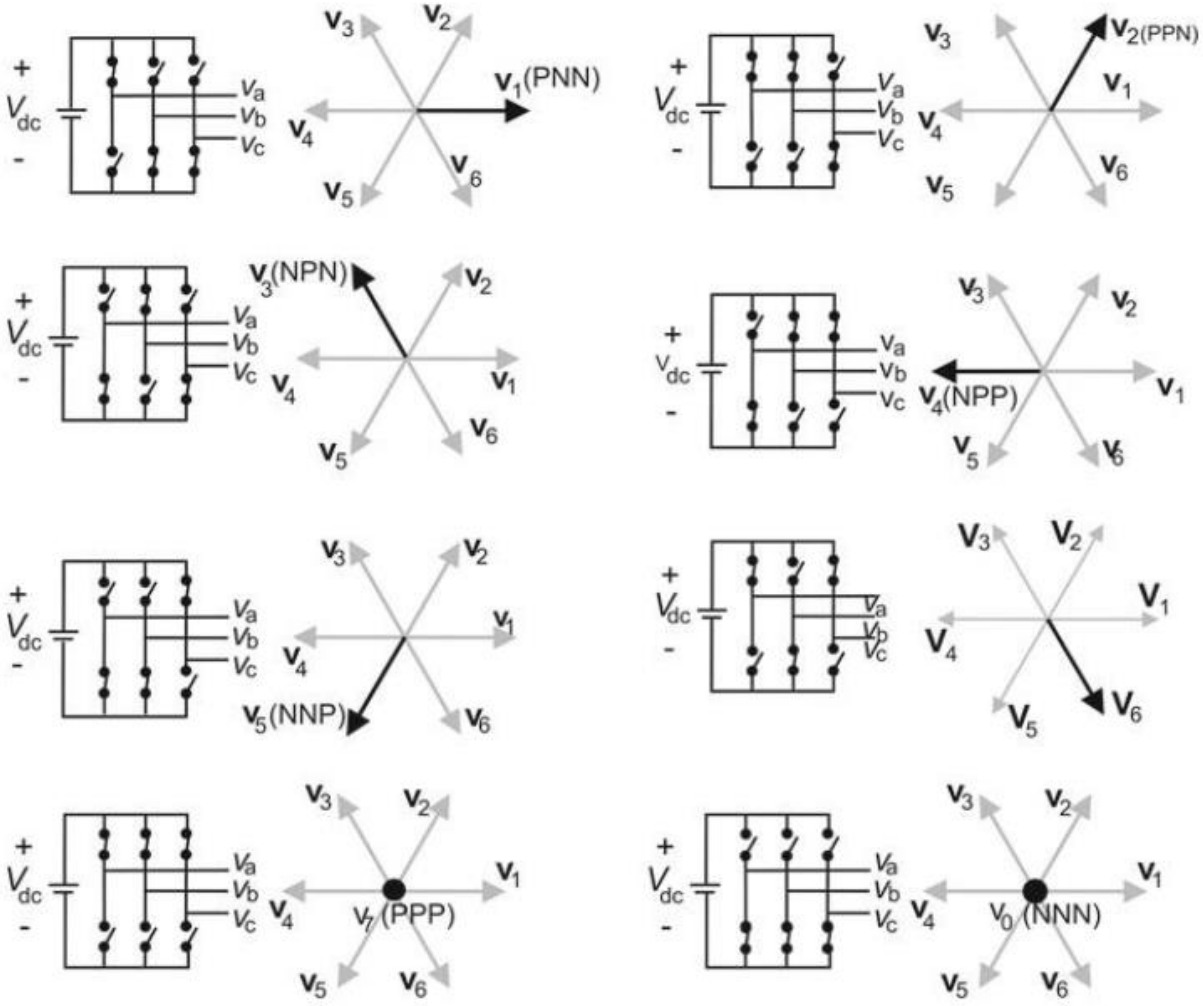

Fig. 1.63 Relation of the inverter switching configurations and the state vectors

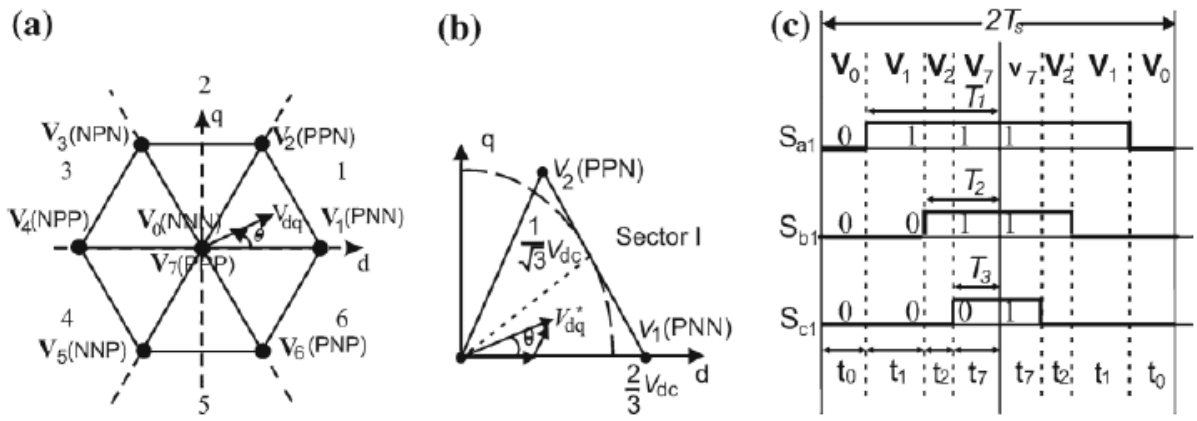

Fig. 1.64 a Space vector diagram and sector definition, b synthesis of the reference state vector in *Sector I* using switching vectors ~V_0; ~V_1; ~V_2; and ~V_7, and c switching pattern

1.1.12 PWM Techniques for Other Two-Level Converters

In the following section on the PWM techniques for the CSI and the CSR and AC/ AC converters will be introduced.

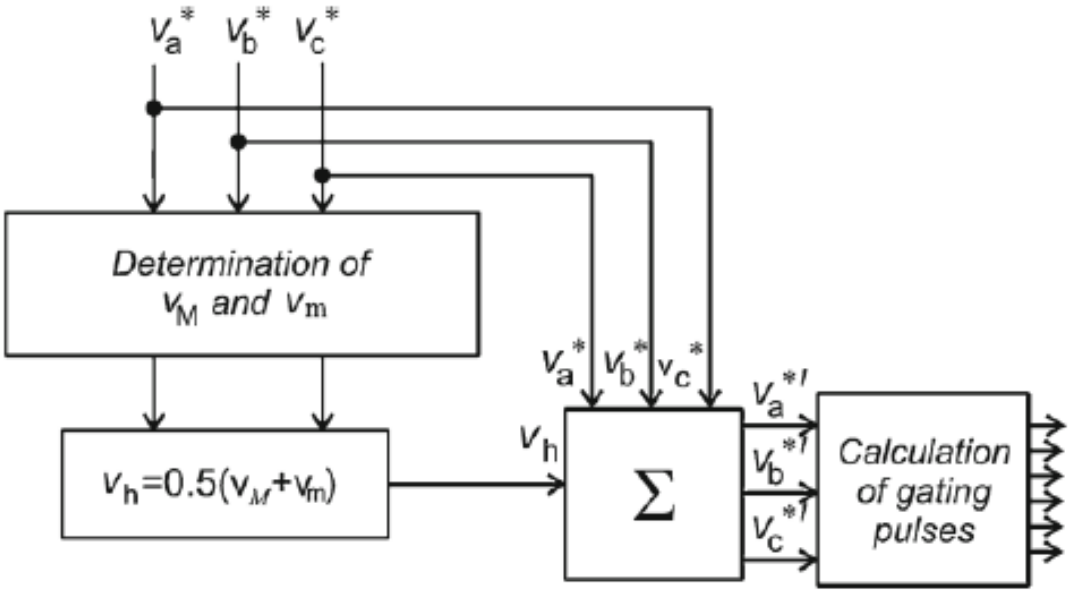

Fig. 1.65 Block diagram for calculation of the pulse width

A. Current Source Converters

The three-phase CSI is the dual of the voltage source three-phase inverter. Because of this the line-to-line output voltage waveform of a VSI is the line output current waveform of a CSI. Using this knowledge, the CSI can be controlled by the same PWM techniques used to control the VSI. However, there are two differences :

1. In CSI the current signals are used as references, instead of voltages as in VSI.

2. For VSI, the PWM pattern can be used to directly control the switching devices and in the CSI the phase switching states cannot be used directly to control the switching devices, since these are controlled by line switching states[16].

High power and its high quality as current source PWM has applications in AC drives, VAR generator, active filters, and superconductive magnetic energy storage (SMES) . But it is much less used than the VSR. The PWM techniques used for the CSI can be directly applied to the CSR. However, the PWM scheme for the CSR must provide an adjustable modulation index for the DC current control in addition to the reduction in the total harmonic distortion. CSR or Buck Rectifier

B. AC/AC Converters

PWM techniques for indirect and direct (matrix) AC/AC converters will be examined next. Due to the fact that the VSR can be modeled as a controllable DC voltage source, its natural load is a VSI. The connection of these two voltage source converters sharing a common capacitor DC link (as in Fig. 1.40) allows two-way energy flow and four-quadrant operation. This four-quadrant converter is presently applied to asynchronous drives, electric power generation using asynchronous, energy storage systems, like UPS and flywheel energy storage systems, and transmission and distribution systems multilevel converter-based (Universal Power Flow Controller, UPFC, High Voltage DC-Light, HVDC-Light, Dynamic Voltage Regulation, DVR) .

The major objective in matrix converters is to simultaneously control their input currents, managing inclusively the reactive power flowing between the grid and the load. This is also the major difficulty found in PWM schemes to control these converters. Many schemes have been proposed to solve this problem . This problem does not exist in indirect converters because of the independent control of the input currents (at the rectifier stage) an output voltage is independent from the control (in the inverter stage) due to the capacitor in DC link. The two-stage direct power converter (DPC) topology has a structure similar to the AC/DC/AC converter, but without the DC link capacitor. Based on this, dissociation between input currents and output voltages controls in the matrix converter was proposed. The space vector modulator implemented includes the adaptation of the DPC duty-cycles to the matrix converter topology.

The technique was also implemented using a generalized PWM strategy similar to those studied for two-level converter to control both input currents and output voltages.

1.1.13 PWM Techniques for Multilevel Converters

Multilevel inverters have emerged as the solution for working with higher voltage levels. They have been considered for an increasing number of applications due to not only their high power capability, but also lower output harmonics and lower commutation losses.

The three-level NPC inverter topology shown in Fig. 1.66a will be used as an example. This topology has 12 active switches (note that the number of switches increases with the number of level K). In each leg of the inverter, the switches can be positive (S_1 and S_2) or negative (S_3 and S_4), which in turn can be external (S_1 and S_4) or internal (S_2 and S_3), in phase a of inverter. Also, each inverter leg can assume three switching states, ‘‘P’’, ‘‘O’’, and ‘‘N’’, as shown from the equivalent circuit in Fig. 1.66b. Taking into account the three-phases, the inverter has a total of 27 possible combinations of switching states as indicated in the three-level space vector diagram in Fig. 1.67, obtained through the same procedure used for the two-level inverter. Such representation allows not only to establish the correlation between the state vectors and the switching configurations but, also, to visualize the division of the voltage vectors into four groups as a function of the vector amplitude: Large Vectors, when the three pole voltages assume only the states P and N; Medium Vectors, when the three pole voltages assume the states P, O, and N; Small Vectors, when the three pole voltages assume only the states P and O or O and N; Null Vectors: NNN, PPP, OOO. In SVPWM, in order to optimize the modulation, each sector is typically divided into four triangles (regions 1 to 4). The knowledge of the position of the reference vector inside a region of a certain sector allows for calculating the pulse widths of the gating pulses. One possibility is to consider the space vector diagram as formed of six small two-level hexagons, each of them centered in one vector of the small vectors

$\sim V_1$; $\sim V_2$; $\sim V_6$; as shown in Fig. 1.67. Using the adjacent state vectors of the small hexagon reproduces a partial reference vector. The reference voltage vector V_m is then obtained by subtracting the center vector of the corresponding small hexagon from the original reference vector (see vectors in triangle D of Sector I). This means that in that region the pole voltage modulates, for instance, between P and O levels. For a K-level inverter, its state phase-diagram is simplified to that of a K-1 level inverter and so on, till that of the two-level inverter.

Alternatives are the use of SHE modulation or the use a carrier-based PWM, such as the in-phase disposition (IPD) modulation[17] illustrated in Fig. 1.68a for the three-level inverter (K = 3). The number of carrier signals is K-1 = 2. For this reason, the modulating signal intersects two triangular waves, generating the pulse widths of each pole voltage.

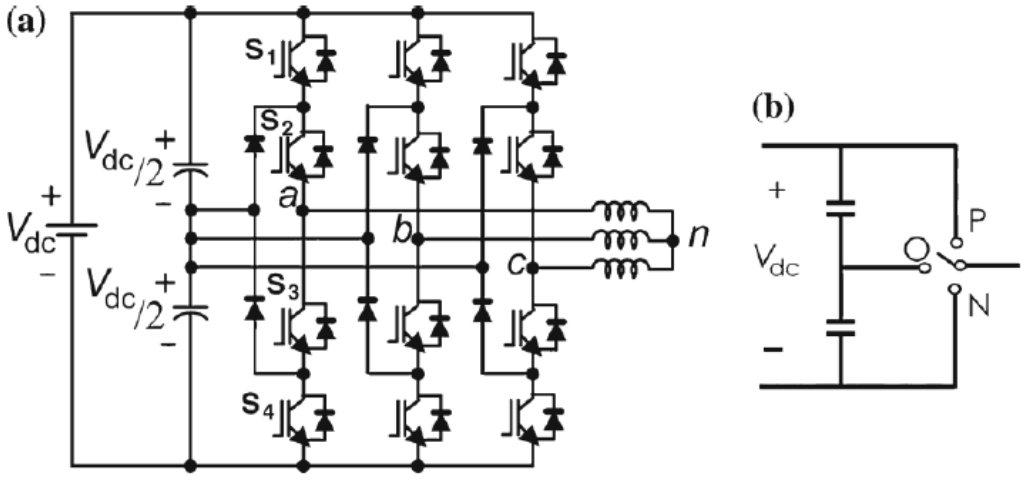

Fig. 1.66 a Three-level NPC inverter topology and b equivalent circuit

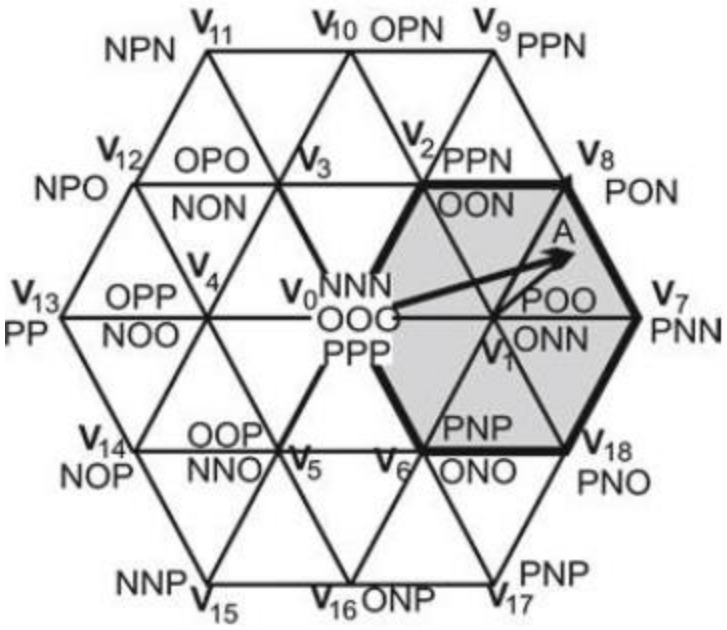

Fig. 1.67 Space vector diagram of a three-level converter

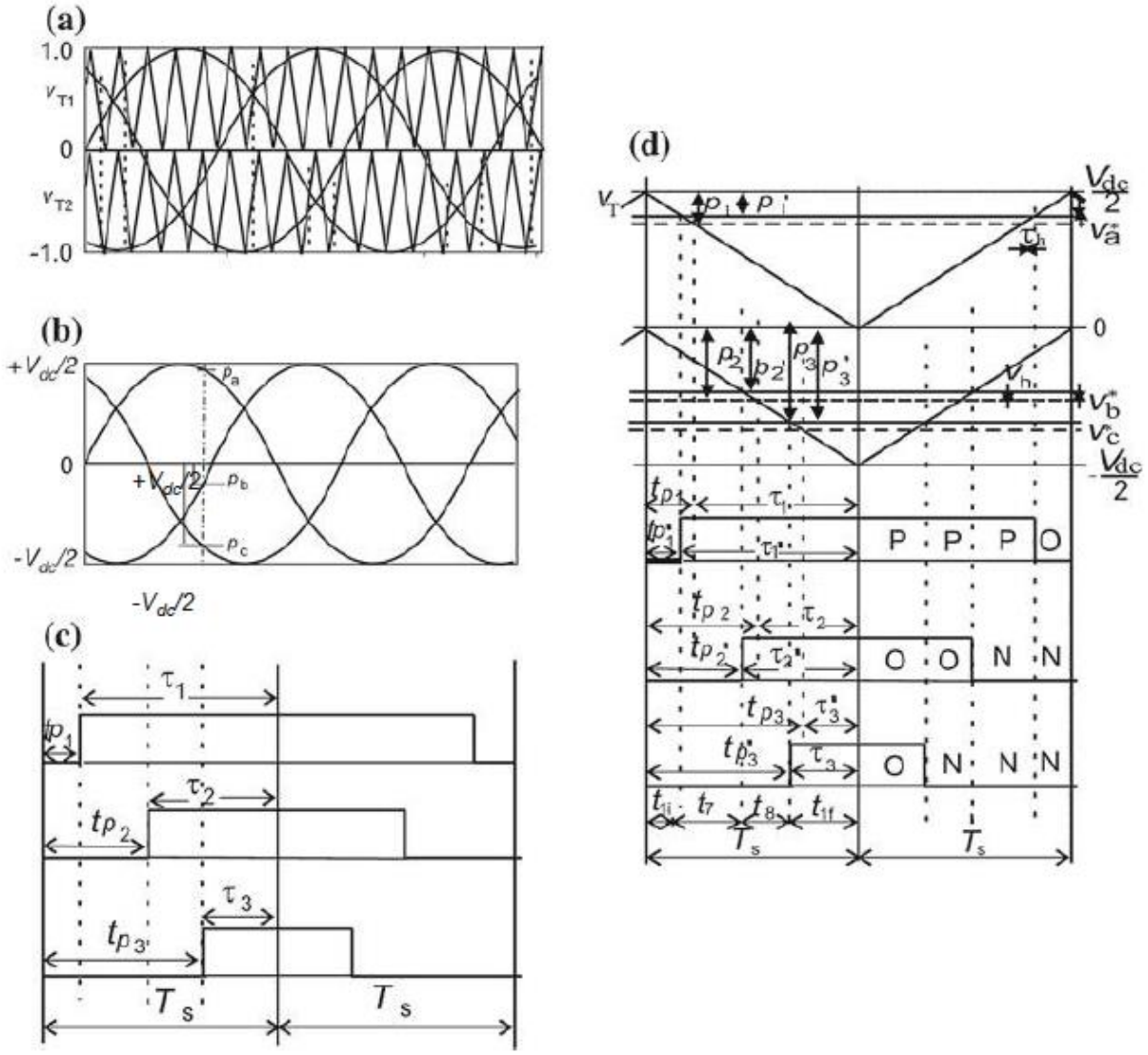

Fig. 1.68 Three-level inverter: a modulation principle (IPD), b definition of pi (i = 1, 2, 3), c the relation of pi with the pulse delays in the switching interval t_{pi}, and d the switching interval considering the addition of the zero-sequence signal, V_h

Chapter 2

Related Field Study

2.1 Buck Converter

The step-down dc-dc converter, commonly known as a buck converter, is shown in Fig. 2.1a. It consists of dc input voltage source V_s controlled switch S, diode D, filter inductor L, filter capacitor C, and load resistance R. Typical waveforms in the converter are shown in Fig. 2.1b under the assumption that the inductor current is always positive. The state of the converter in which the inductor current is never zero for any period of time is called the continuous conduction mode (CCM). It can be seen from the circuit that when the switch S is on state, the diode D is reverse-biased. When the switch S is off, the diode conducts to support an uninterrupted current in the inductor. The relationship among the input voltage, output voltage, and the switch duty ratio D can be derived, for instance, from the inductor voltage V_L waveform (Fig. 2.1b). According to Faraday's law, the inductor volt-second product over a period of steady-state operation is zero. For the buck converter

$$(V_s - V_o)DT = -V_o(1 - D)T \tag{2.1}$$

Hence, the dc voltage transfer function, defined as the ratio of the output voltage to the input voltage, is

$$M_v \equiv \frac{V_o}{V_s}=\text{D} \tag{2.2}$$

It can be seen from Eq. (2.2) that the output voltage is always smaller that the input voltage.

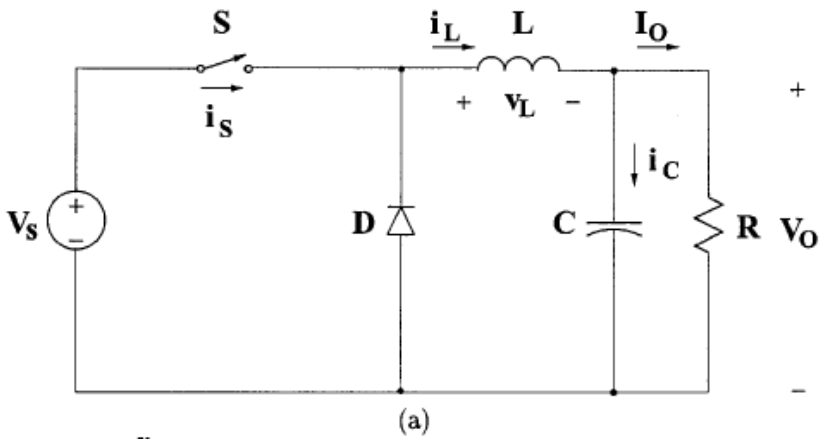

(a)

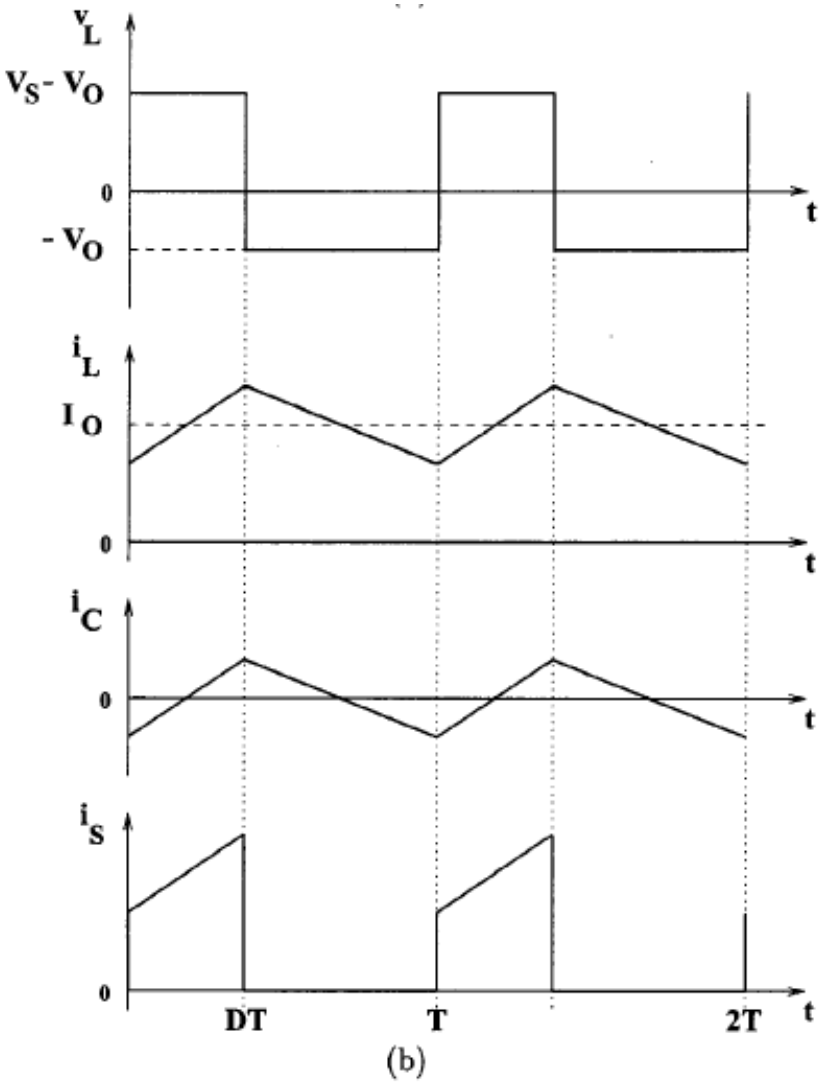

Fig. 2.1 Buck converter: (a) circuit diagram; (b) waveforms

The dc-dc converters can operate in two distinct modes with respect to the inductor current i_L. Figure 2.1 b depicts the CCM in which the inductor current is always greater than zero. When the average value of the output current is low (high R) and the switching frequency f is low, the converter may enter the discontinuous conduction mode (DCM). In the DCM, the inductor current is zero during a portion of the switching period. The CCM is preferred for high efficiency and good utilization of semiconductor switches and passive components. The DCM may be used in applications with special control requirements because the dynamic order of the converter is reduced (the energy stored in the inductor is zero at the beginning and at the end of each switching period). It is uncommon to mix these two operating modes because of different control algorithms. For the buck converter, the value of the filter inductance that determines the boundary between CCM and DCM is given by

$$L_b = \frac{(1-D)R}{2f} \tag{2.3}$$

For typical values of D=0.5, R=10 Ohm, and f=100 kHz, the boundary is L_b =25 mH. For L> L_b, the converter operates in the CCM.

The filter inductor current i_L in the CCM consists of a dc component IO with a superimposed triangular ac component. Almost all of this ac component flows through the filter capacitor as a current i_c . Current i_c causes a

small voltage ripple across the dc output voltage V_o. To limit the peak-to peak value of the ripple voltage below a certain value V_r , the filter capacitance C must be greater than

$$C_{min} = \frac{(1-D)V_o}{8V_r L f^2} \tag{2.4}$$

At D=0.5, V_r=V_o . 1%, L=25 mH, and f =100 kHz, the minimum capacitance is Cmin=25 mF.

Equations (2.3) and (2.4) are the key design equations for the buck converter. The input and output dc voltages (hence, the duty ratio D), and the range of load resistances R are usually determined by preliminary specifications. For the compactness and low conduction losses of a converter, it is desirable to use small passive components. The switching frequency is limited, however, by the type of semiconductor switches used and by switching losses. It should also be noted that values of L and C may be altered by the effects of parasitic components in the converter.

2.2 Boost Converter

Figure 2.2a depicts a step-up or a PWM boost converter. It consists of dc input voltage source VS, boost inductor L, controlled switch S, diode D, filter capacitor C, and load resistance R. The converter waveforms in the CCM are presented in Fig. 2.2b.

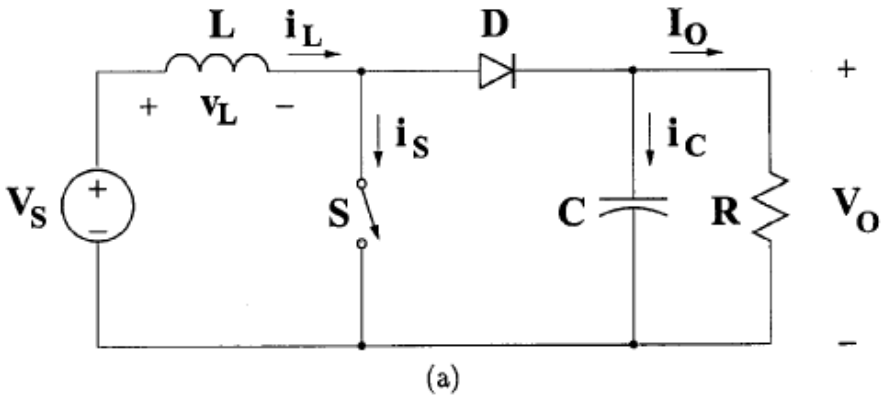

(a)

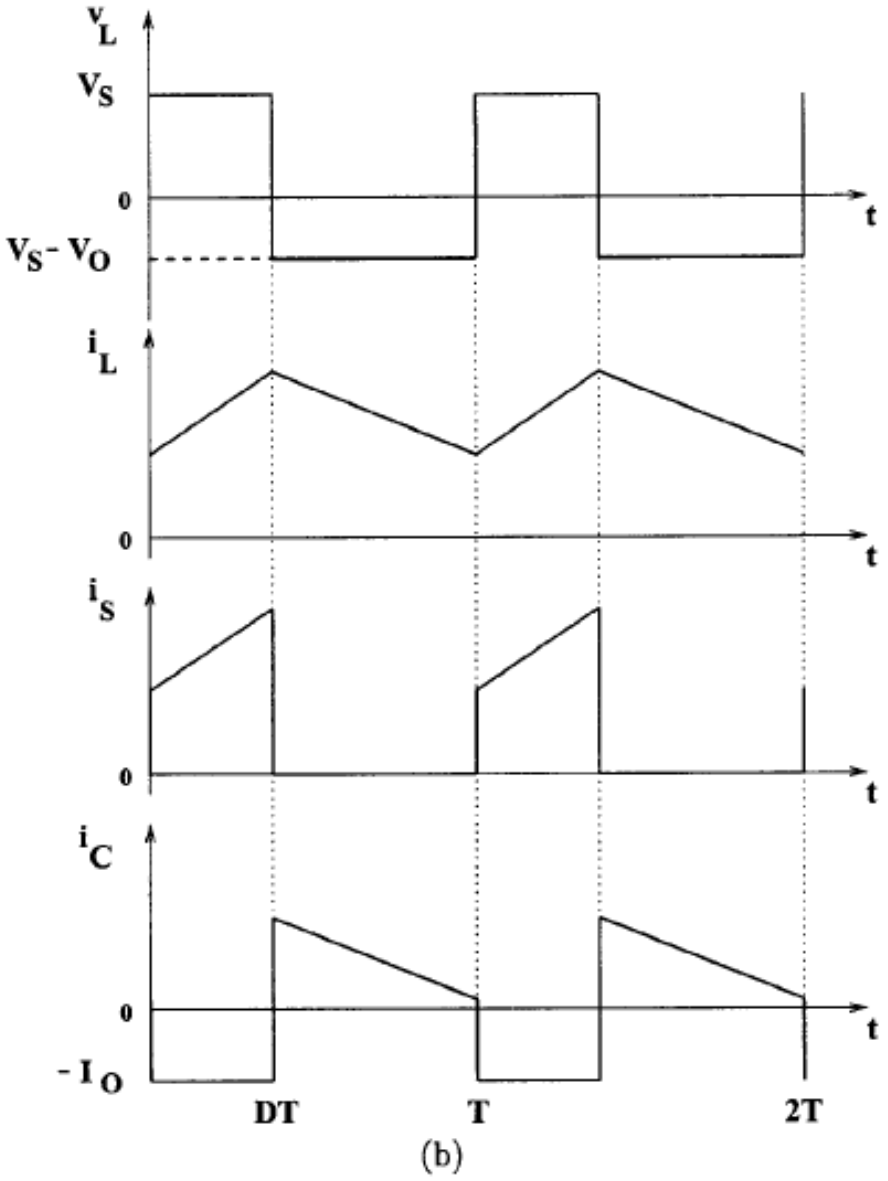

Fig. 2.2 Boost converter: (a) circuit diagram; (b) waveforms

When the switch S is in the on state, the current in the boost inductor increases linearly and the diode D is off at that time. When the switch S is turned off, the energy stored in the inductor is released through the diode to the output RC circuit. Using Faraday's law for the boost inductor

$$V_s DT = (V_o - V_s)(1 - D)T \tag{2.5}$$

from which the dc voltage transfer function turns out to be

$$M_v \equiv \frac{V_o}{V_s} = \frac{1}{1 - D} \tag{2.6}$$

As the name of the converter suggests, the output voltage is always greater than the input voltage. The boost converter operates in the CCM for L > $L_b$where

$$M_v = \frac{(1-D)^2 DR}{2f} \tag{2.7}$$

For D=0.5, R=10 Ohm, and f =100 kHz, the boundary value of the inductance is L_b=6.25 mH.

As shown in Fig. 2.2b, the current supplied to the output RC circuit is discontinuous. Thus, a larger filter capacitor is required in comparison to that in the buck-derived converters to limit the output voltage ripple. The filter capacitor must provide the output dc current to the load when the diode D is off. The minimum value of the filter capacitance that results in the voltage ripple V_o is given by

$$C_{min} = \frac{DV_o}{V_r Rf} \tag{2.8}$$

At D =0.5, V_r=V_o . 1%, R =10 Ohm, and f= 100 kHz, the minimum capacitance for the boost converter is Cmin =50 mF. The boost converter does not have a popular transformer (isolated) version.

2.3 Buck-Boost Converter

A non-isolated topology of the buck-boost converter is shown in Fig. 2.3a. The converter consists of dc input voltage source V_s, controlled switch S, inductor L, diode D, filter capacitor C, and load resistance R. With the switch on, the inductor current increases while the diode is maintained off. When the switch is turned off, the diode provides a path for the inductor current. Note the polarity of the diode that results in its current being drawn from the output. The buck-boost converter waveforms are depicted in Fig. 2.3b. The condition of a zero volt-second product for the inductor in steady state yields

$$V_s DT = -V_o(1-D)T \tag{2.9}$$

Hence, the dc voltage transfer function of the buck-boost converter is

$$M_v \equiv \frac{V_o}{V_s} = -\frac{D}{1-D} \tag{2.10}$$

The output voltage V_o is negative with respect to the ground. Its magnitude can be either greater or smaller (equal at D=0:5) than the input voltage as the name of the converter implies.

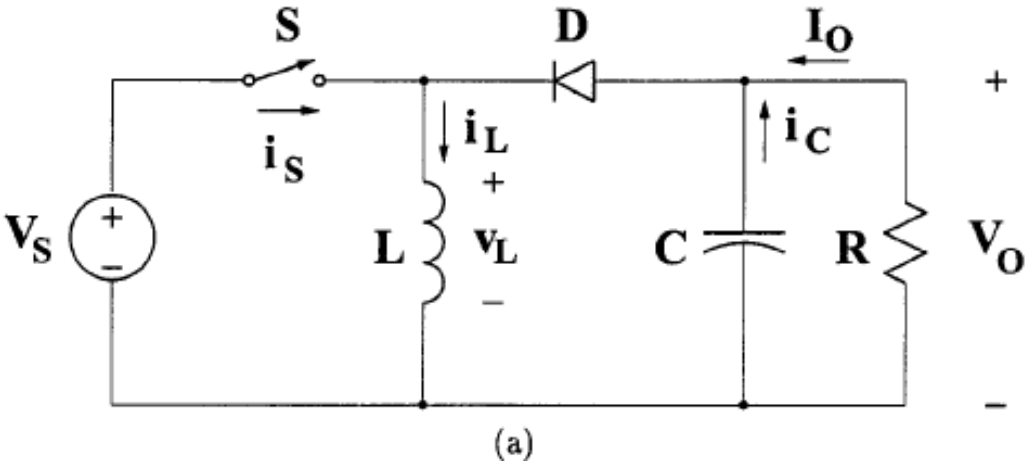

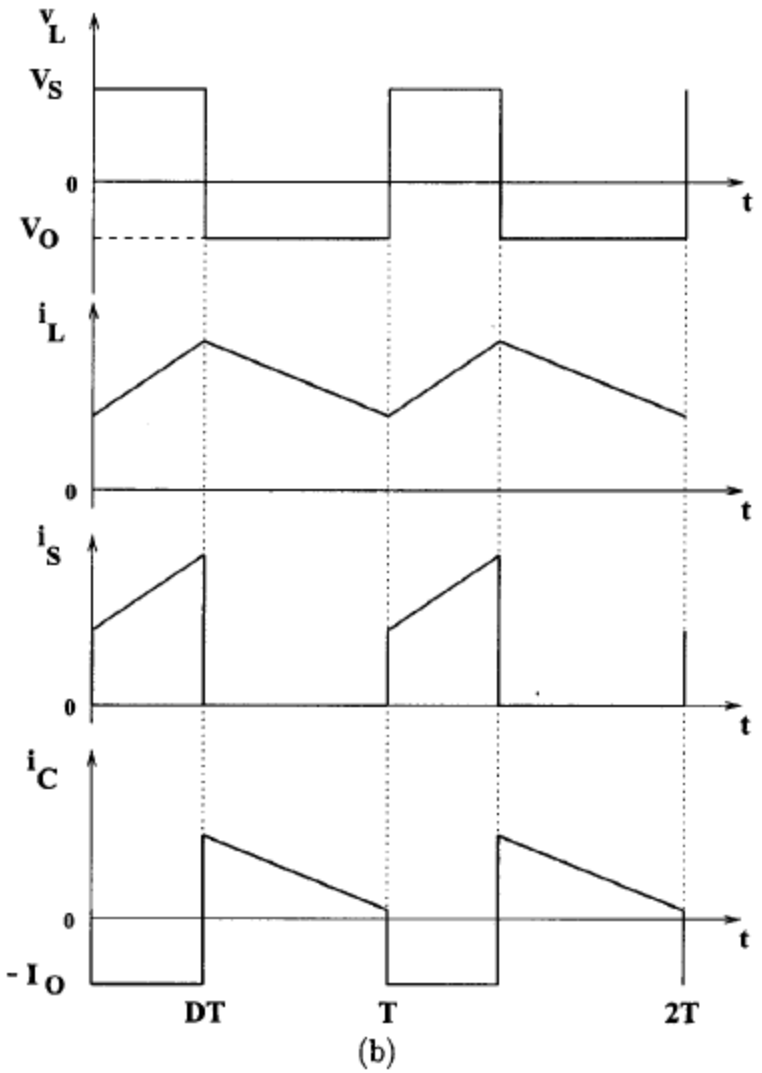

Fig. 2.3 Buck-boost converter: (a) circuit diagram; (b) waveforms.

The value of the inductor that determines the boundary between the CCM and DCM is

$$L_b = \frac{(1-D)^2 R}{2f} \tag{2.11}$$

The structure of the output part of the converter is similar to that of the boost converter (reversed polarities are the only difference).

2.4 Cük Converter

The circuit of the Cük converter is shown in Fig 2.4a. It consists of dc input voltage source VS, input inductor L_1, controllable switch S, energy transfer capacitor C_1, diode D, filter inductor L_2, filter capacitor C, and load resistance R. An important advantage of this topology is a continuous current at both the input and the output of the converter. Disadvantages of the Cük converter are a high number of reactive components and high current stresses on the switch, the diode, and the capacitor C_1. The main waveforms in the converter are presented in Fig. 2.4b. When the switch is on, the diode is off and the capacitor C_1 is discharged by the inductor L_2 current. With the switch in the off state, the diode conducts currents of the inductors L_1 and L_2, whereas capacitor C_1 is charged by the inductor L_1 current.

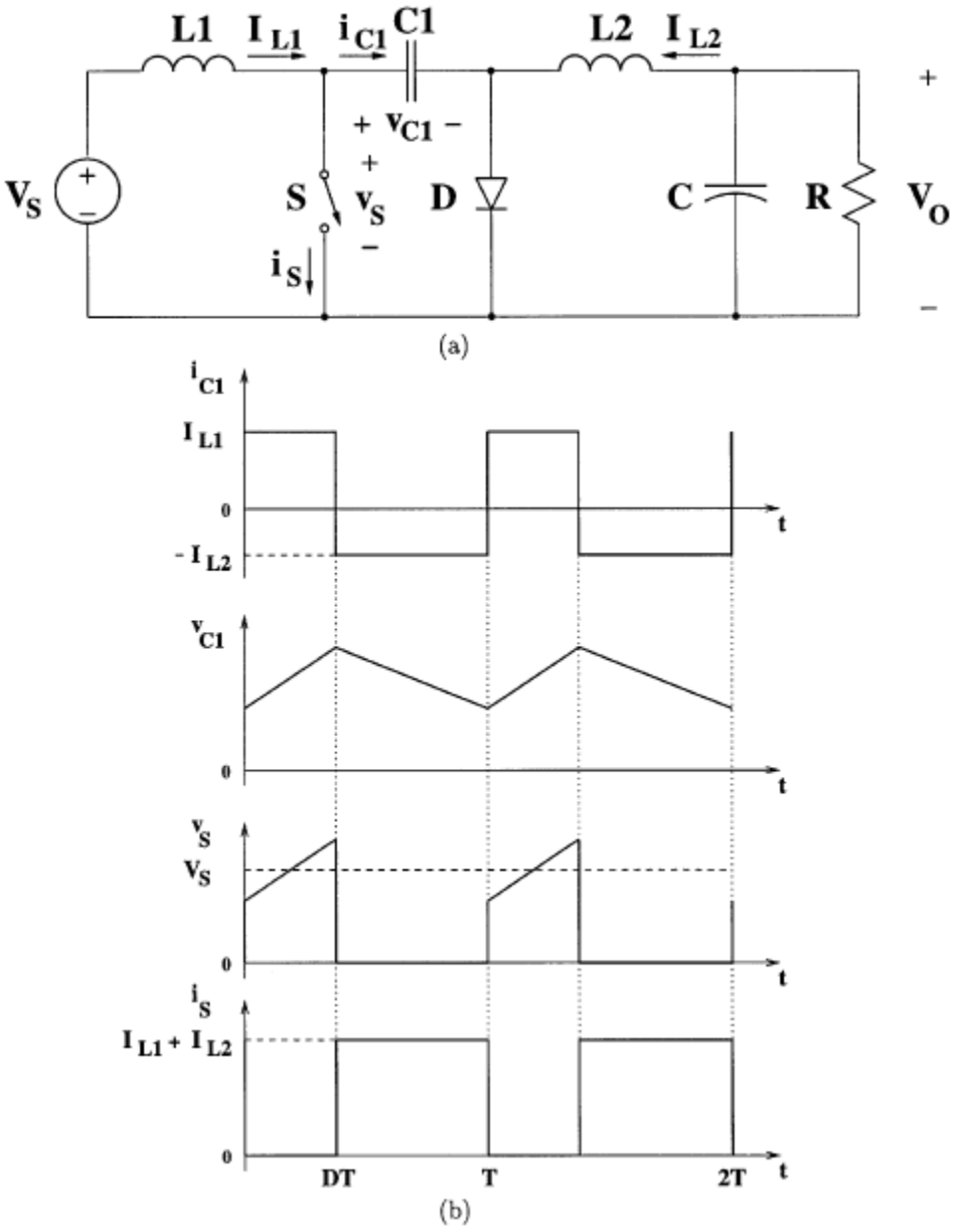

Fig. 2.4 Cük converter: (a) circuit diagram; (b) waveforms.

To obtain the dc voltage transfer function of the converter, we shall use the principle that the average current through a capacitor is zero for steady-state operation. Let us assume that inductors L_1 and L_2 are large enough that their ripple current can be neglected. Capacitor C_1 is in steady state if

$$I_{L2}\,DT=I_{L3}\,(1\text{-}D)T \tag{2.12}$$

For a lossless converter,

$$P_s=V_sI_{L1}=-V_oI_{L2}=P_o \tag{2.13}$$

Combining these two equations, the dc voltage transfer function of the Cük converter is

$$Mv \equiv \frac{Vo}{Vs} = -\frac{D}{1-D} \tag{2.14}$$

This voltage transfer function is the same as that for the buck-boost converter. The boundaries between the CCM and DCM are determined by

$$L_{b1} = \frac{(1-D)R}{2Df} \tag{2.15}$$

for L_1 and

$$L_{b2} = \frac{(1-D)R}{2Df} \tag{2.16}$$

for L_2. The output part of the Cük converter is similar to that of the buck converter. Hence, the expression for the filter capacitor C is

$$Cmin = \frac{(1-D)Vo}{8VrL_2f^2} \tag{2.17}$$

The peak-to-peak ripple voltage in the capacitor C1 can be estimated as

$$V_{r1} = \frac{DVo}{C_1r_f} \tag{2.18}$$

A transformer (isolated) version of the Cük converter can be obtained by splitting capacitor C1 and inserting a high frequency transformer between the split capacitors.

Advantage and disadvantage of Boost Converters

In recent year, high voltage gain dc-dc converters play more and more important role in many industry applications such as uninterrupted power supplies, power factor correctors, distributed photovoltaic (PV) generation systems and fuel cell energy conversion systems. In these applications, a classical boost converter is normally used, but the extremely high duty cycle will result in large conduction loss on the power devices and serious reverse recovery problems . Thus, the conventional boost converter would not be acceptable for realizing high step-up voltage gain along with high efficiency.

To achieve a high conversion ratio without operating at extremely high duty ratio, some converters based on transformers or coupled inductors or tapped inductors have been provided . However, the leakage inductance in the transformer, coupled inductor or tapped inductor will cause high voltage spikes in the switches and reduce system efficiency. In order to solve the voltage spike, snubber circuits, such as resistor---capacitor---diode snubber, non dissipative snubber and active clamp circuit, can be applied, but increase the complexity of converter structure.

Some non-isolated topologies have been proposed to achieve a high conversion ratio and avoid operating at extremely high-duty cycle. These converters include the switched-capacitor type, switched-inductor type , the voltage-doubler circuit, and the capacitor-diode voltage multiplier. All of them can obtain higher voltage gain than the conventional boost converter.

However, more switched capacitor or switched-inductor stages are needed for an extremely large conversion ratio, which result in higher cost and complex circuit. The voltage gain can be extended to satisfy the high-step-up requirements by employing the cascade structure. A cascaded boost converter with two stages was

proposed in. However, the cascade converter requires two sets of power devices and control circuits, which is complex and expensive.

Advantage and disadvantage of Cük Converter

By Cük converter, we can both step up or step down input voltage depending on duty cycle. Cük converter uses L-C type filter, so peak-peak ripple current of inductors are less as compared to the Buck-Boost converter. In Cük converter, when switch is closed then capacitor provides energy to the load as well as inductive filter. But when switch is open then energy stored in the filter inductor is fed back to the load. Where as in case of Buck-Boost converter, when switch is closed then source is disconnected from the load and when switch is open then energy stored in the inductor is fed back to the source.

For Cük converter efficiency is high at low duty cycle but with increase in duty cycle efficiency drops higher. On the other hand, THD at lower duty cycle of Cük converter is higher which is not desirable. By increasing duty cycle, THD (total harmonic distortion) can be reduced. Gain of Cük converter is too less relative to boost converter. Gain of Cük converter is about less than half of boost converter. Gain increased with increasing with duty cycle but it is less increase compared to boost converter.

For high step up operation, Cük converters are needed to be operated higher than 0.9 duty cycle and for better step down operation it has to be operated lower than 0.1 duty cycle. However, these extreme duty cycles reduce the efficiency and deteriorates the transient response of the system [59]. Moreover, such an extreme duty cycle requires very expensive and super-fast comparators within the control circuit.

We can take the advantage of both boost converter and Cük converter by cascading connection. For this cascading connection, a very popular method can be used known as CPSM (common part sharing method).

2.5 Common Part Sharing Method (CPSM)

In common part sharing method (CPSM) as name suggest common part of two circuits are kept common and then rest of the part of those circuits are joined to this common part. A novel topology of Cascaded Boost-Cûk (CBC) converter has been proposed which combines the Boost converter with an isolated Cûk converter as a series output module in order to obtain high step-up ratio and to overcome the drawbacks faced when using conventional circuits. Similar works has been done in cascading Boost-SEPIC converters using common parts sharing method[13]. A common part
sharing method as shown in Fig.1, has been used to amplify the output voltage while avoiding bridge rectification.. CPSM can be used for cascading boost and Cük converters.

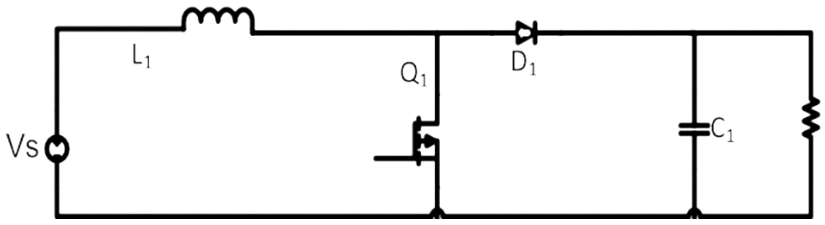

Fig. 2.5 Conventional Boost Circuit

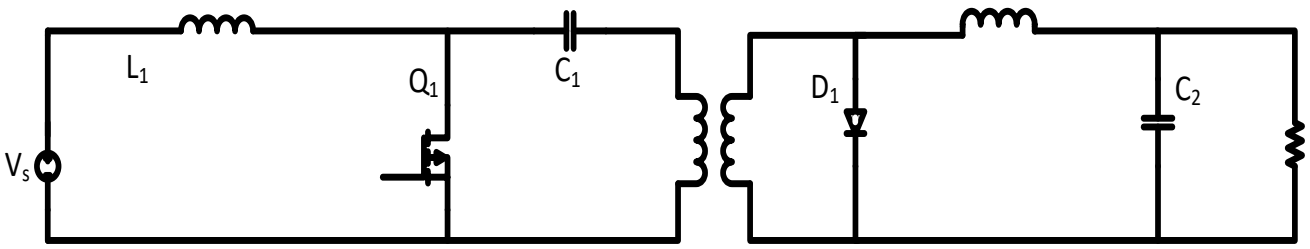

Fig. 2.6 Conventional Cük Circuit

Voltage source, inductor and MOSFET (switch) is common in fig. 2.5 and fig. 2.6. So this three element of boost converter and Cük converter can be kept common and rest of the element of boost circuit and Cük circuit can be connected.

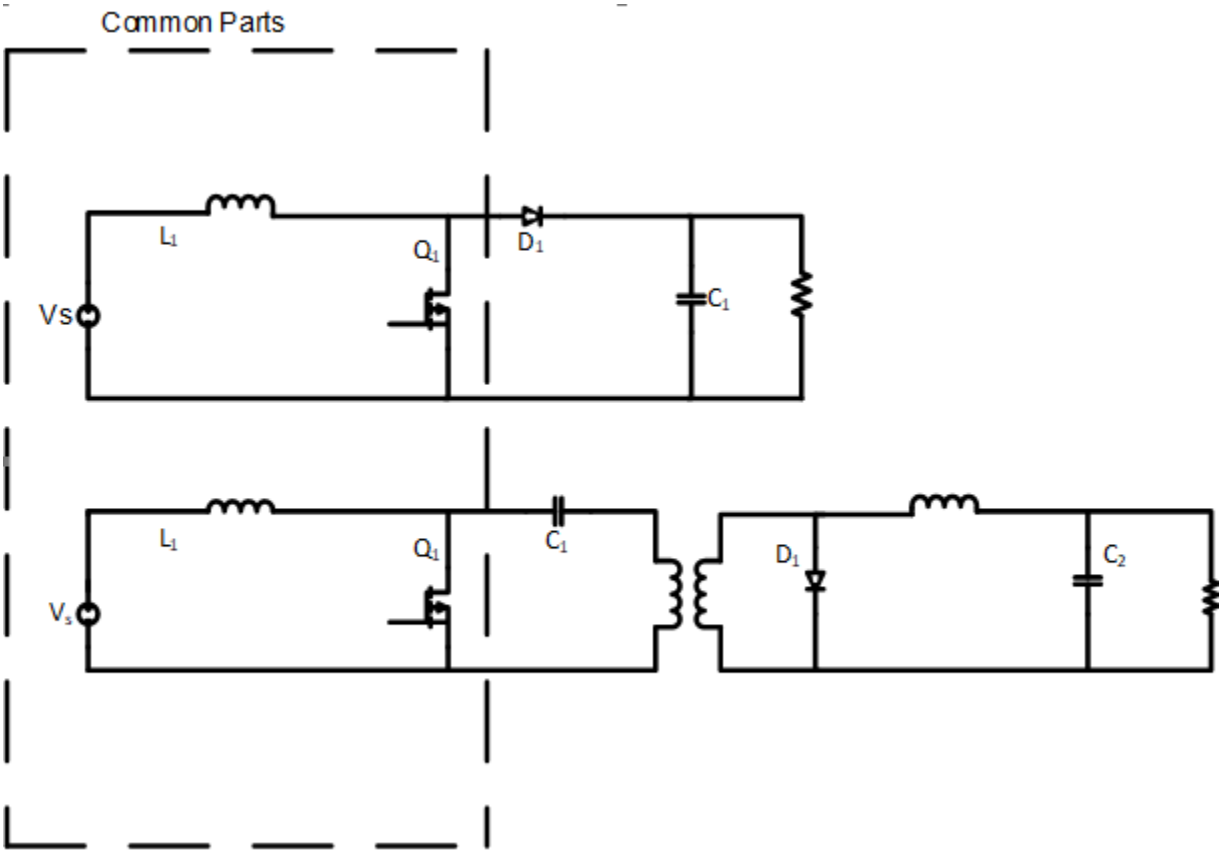

Fig 2.7 Common Parts in Boost and Cük Converter

Chapter 3

Proposed Circuit

3.1 Principle of Operation

3.1.1 Introduction to new topology

In this topology, Boost and Cûk converters topologies are cascaded using CPSM method described earlier. Bridge rectifier has been discarded since two different paths have been introduced for two half cycles. Switching loss remains almost same (or less in some cases) despite using more components in the proposed topology as compared to the basic Boost and Cûk converters. Hence, the basic operation of both the above mentioned circuits are combined. However, this proposed topology is expected to have higher efficiency since effort reduces hysteresis and excess energy loss may occur due to magnetization of the components in case of the rectifiers containing bridge topology.

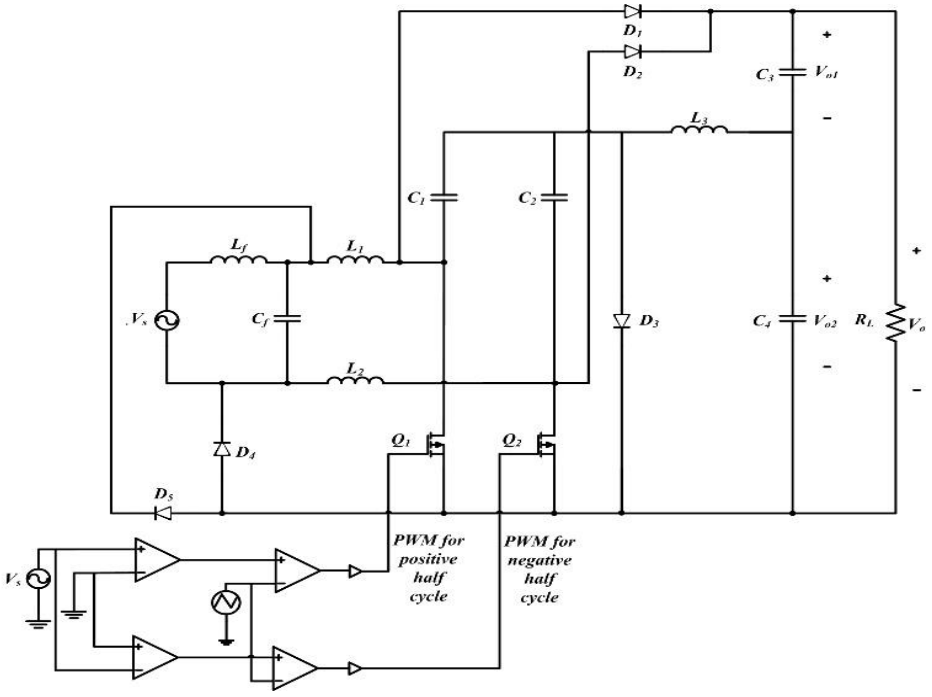

Fig. 3.1 Proposed Cascaded Boost-Cûk (CBC) converter.

The proposed circuit shown in Fig. 5 is a Cascaded Boost-Cûk (CBC) converter which has been used to get an output voltage greater than the voltage of the source. The circuit consists of four inductors (L_1, L_2, L_3 and L_f), five capacitors (C_1, C_2, C_3, C_4 and C_f), two switches (Q_1 and Q_2), five diodes (D_1, D_2, D_3, D_4 and D_5) and a resistor (R_L) which acts as the load for the circuit.

A sub-circuit has been proposed, under the proposed topology, which provides the gating signal to the switches (Q_1 and Q_2) The circuit can operate as an AC-DC converter on both positive and negative half cycles of the input signal.

As discussion of the operation of this circuit can be divided into two parts

I. Gate driving circuit
II. Cascaded Boost-Cûk (CBC) topology

3.1.2 Gate driving circuit

During the positive half cycle, the switch Q_1 performs continuous on and off operation while the switch Q_2 remains off. Conversely during the negative half cycle the, switch Q_2 performs continuous on and off operation while the switch Q_1 remains off.

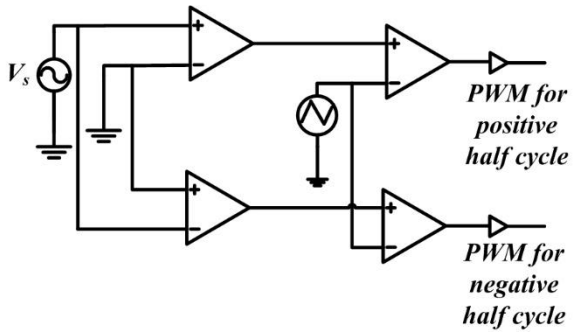

Fig. 3.2 Gate driving circuit of the proposed CBC converter.

Here we have used four operational amplifiers in two stages. In 1st stage one op-amp is working in inverting and other working in non-inverting mode. Both taking input from the voltage generation source which typically works in 50Hz in our country. The objective of using these two op-ams is two pass positive and negative half cycle simultaneously so that the converter can work both in positive half cycle and negative half cycle of the source. As the 1st stage passes both half cycles separately to the 2nd stage there are two inverting op-amp, in input to which there is a triangular pulse generator with a frequency of 50KHz. So, it is converting the both pulse to a strain of pulses which are given to the input of the MOSFET gates, which are used as switches for the operating main circuit. Fig 3.3 illustrates the working principle of the gate driving circuit and shows the theoretical output of different stages of the gate driving circuit.

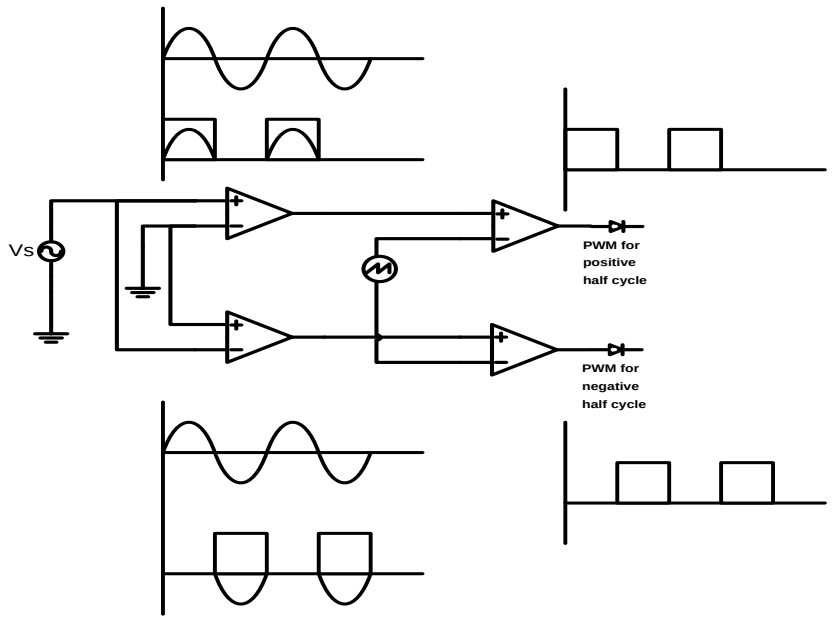

Fig. 3.3 Output of different stages of Gate driving circuit

3.1.2 Cascaded Boost-Cûk (CBC) topology

The basic principle of the circuit consists of two states:

- During the positive half cycle, the switch Q_1 performs continuous on and off operation while the switch Q_2 remains off. When Q_1 is ON it causes an increase in the inductor current L_3. When Q_1 is OFF the only path offered to the inductor current is through the flyback diode (D_1), the capacitor (C_4) and the load (R_L). This leads to the transfer of energy accumulated during the On-state into the capacitor.
- During the negative half cycle, the switch Q_2 performs continuous on and off operation while the switch Q_1 remains off. When Q_2 is ON it causes an increase in the inductor current L_3. When Q_2 is OFF the only path offered to the inductor current is through the flyback diode (D_2), the capacitors (C_3, C_4) and the load (R_L). This leads to the transfer of energy accumulated during the On-state into the capacitors.

The capacitor C_1 has alternate connections to the input and output via the commutation of the transistor and diode and is used for the transfer of energy. For short instances of time it can be considered that an inductor is a current source as it maintains a constant current. The conversion becomes needed due to the fact that if it were connected directly to the voltage source, the current would be limited by the parasitic resistance, leading to high energy losses.

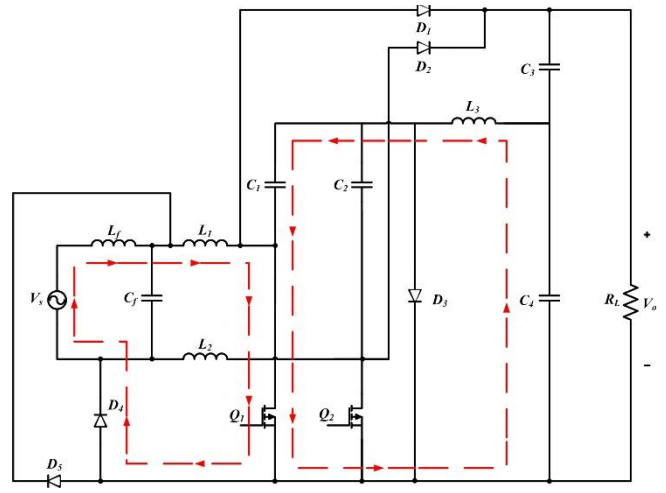
D1
D2
C3
L3
C1
C2
Lf
L1
Vs
Cf
D3
C4
RL
Vo
L2
D4
Q1
Q2
D5

(a)

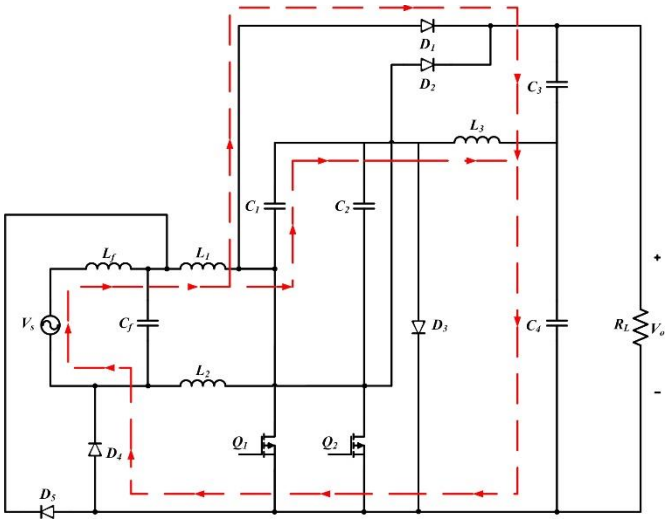
D1
D2
C3
L3
C1
C2
Lf
L1
Vs
Cf
D3
C4
RL
Vo
L2
D4
Q1
Q2
D5

(b)

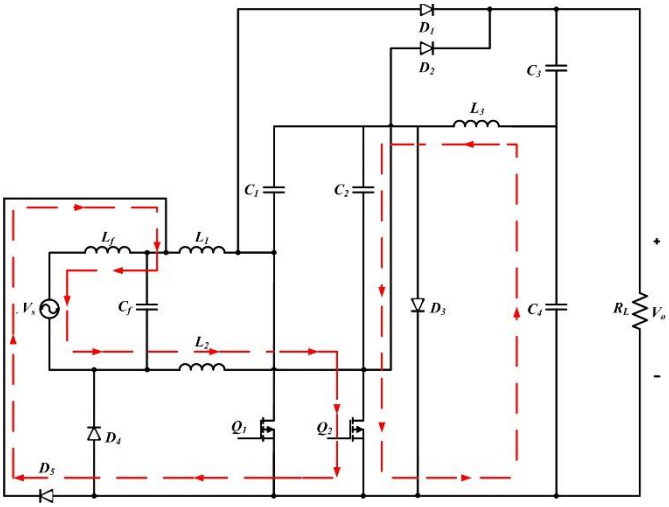
D1
D2
C3
L3
C1
C2
Lf
L1
Vs
Cf
D3
C4
RL
Vo
L2
D4
Q1
Q2
D5

(c)

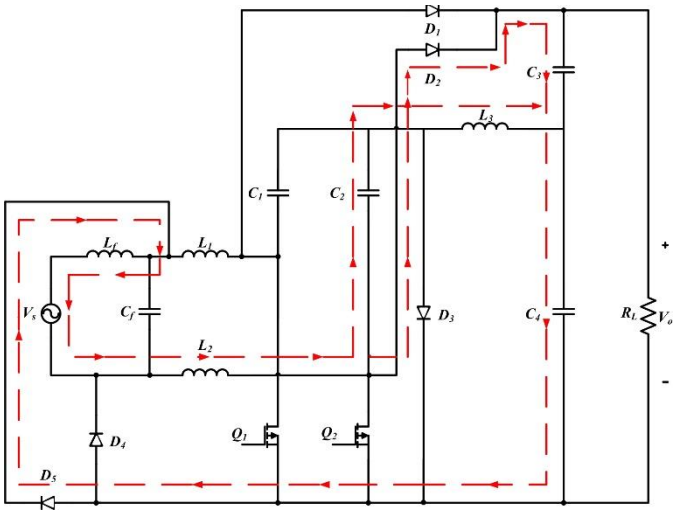

(d)

Fig. 3.4 Operation principle of CBC converter. (a) Mode 1: During positive half cycle, switch Q_1 is on and Q_2 is off, (b) Mode 2: During positive half cycle ,switch Q_1 is off and Q_2 is off, (c) Mode 3: During negative half cycle, switch Q_1 is off and Q_2 is on and (d) Mode 4: During negative half cycle switch Q_1 is off and Q_2 is off

Fig 3.4 shows the current paths for both positive and negative half cycle. Both charging and discharging path for both the half cycle is shown in the figures mentioned above.

3.2 Voltage Gain Analysis

3.2.1 Steady State Analysis

Cascaded Boost-Cûk (CBC) converter has been proposed which combines the Boost converter with an isolated Cûk converter as a series output module in order to obtain high step-up ratio and to overcome the drawbacks faced when using conventional circuits.

The voltage gain of the conventional Boost converter is given by equation (1),

$$\frac{V_i}{L}DT = \Delta i_L = -\frac{Vi - < V_o >}{L}(1-D)T \tag{3.1}$$

$$V_iD = (-V_i + < V_o >)(1-D)$$

$$V_iD = -V_i + < V_o > + V_iD + < V_o > D$$

$$0 = -V_i + < V_o > (1-D)$$

$$\frac{< V_o >}{< V_i >} = \frac{1}{1-D} \tag{3.2}$$

The voltage gain of the conventional Cûk converter is given by equation (2),

Average voltage across capacitor Cs over one full switching cycle T can be written as,

$V_s - V_{LS} - V_{CS} - V_{LO} - V_O = 0$

$V_s - V_{CS} - V_O = 0$

$V_{CS} = V_s - V_O$

At steady state, Average voltage across inductors over one full switching cycle is zero. Hence

$V_{LS} = V_{LO} = 0$ Now,

$V_{LS(ON)} = V_S DT$

$V_{LS(OFF)} = (V_s - V_{CS})(1-D)T$

So, average voltage across L_s for one full switching cycle

$$\overline{V_{LS}} = \frac{V_{LS(ON)} + V_{LS(OFF)}}{T}$$

$$\overline{V_{LS}} = \frac{V_S DT + (V_s - V_{CS})(1-D)T}{T}$$

$$\overline{V_{LS}} = V_S D + (V_s - V_s + V_O)(1-D)$$

$$\overline{V_{LS}} = V_S D + V_O(1-D)$$

$$\overline{V_{LS}} = D(V_S - V_O) + V_O$$

$$\frac{V_{02}}{V_s} = \frac{D}{1-D} \qquad (2)$$

The proposed converter has the output voltage equivalent to the summation of the Boost and CUK converter. The summation of output voltage from Boost and Cûk converters will be the output voltage of the proposed circuit. equations are shown below are for steady state operation, where the parameters have been considered similar to continuous conduction mode.

Overall voltage gain for CBC converter,

$$V_o = V_{o_1} + V_{o_2} \qquad (3.3)$$

$$V_o = \frac{1}{1-D}V_s + \frac{D}{1-D}V_s$$

$$V_o = (\frac{1}{1-D} + \frac{D}{1-D})V_s$$

$$V_o = \left(\frac{1+D}{1-D}\right)V_s$$

$$V_o = GV_s \qquad (3.4)$$

The overall voltage gain for proposed converter,

$$G = \frac{1+D}{1-D}$$

it is observed, from the derivation above, that the output voltage is $\frac{1+D}{1-D}$ times the input voltage. This implies a high gain has been achieved.

3.3 Approach to model a new converter

To obtain even better performance, closed loop implementation of the proposed converter can be conducted to attain better power factor by employing suitable power factor correction techniques.

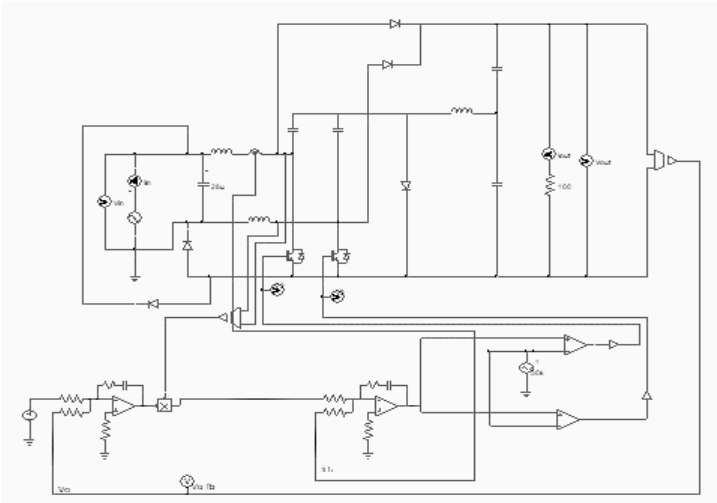

Fig-3.5 Power factor correction circuit with inner/outer loops (op. amp) implemented with proposed circuit

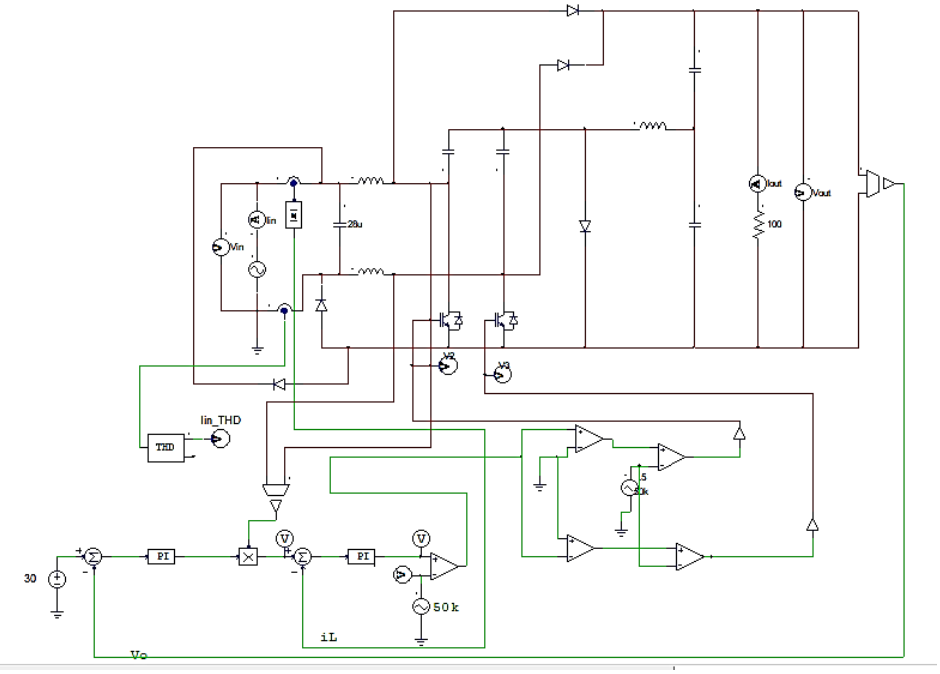

Fig-3.6 Power factor correction circuit with inner/outer loops (op. amp) implemented with proposed circuit

The basic idea of approach is here that we are giving a reference voltage and trying to build a linear relation between the reference voltage and output voltage. Also to improve the PF and THD of the output of the circuit. The reason behind choosing closed loop implementation is that, they are more accurate than open loop system due to

their complex construction. They are equally accurate and are not disturbed in the presence of non-linarites. Since they are composed of a feedback mechanism, so they clear out the errors between input and output signals, and hence remain unaffected to the external noise sources.

Chapter 4

Simulation and Results

4.1 Assumptions

Following assumptions were made to simplify the theoretical analysis.
• All the components are assumed to be ideal.
• For the simplification of analysis, |Vin| was considered as a purely rectified sinusoidal source.
• Larger value of output capacitor C_0 was considered to refer V_0 as a pure dc voltage.
• The converters have been simulated using PSPICE for the following data specifications:

The parameters of the proposed circuit used for simulation is given in Table 1. The proposed IBC topology has been compared with conventional single phase AC-DC diode-bridge Boost rectifier conversion circuit.

Table 4.1. Specification of design parameter of IBC converter.

Parameter	Value
Input voltage(V_s)	220 (AC)
Input frequency(f_{in})	50 Hz
Switching device	MOSFET
Switching frequency (f_{sw})	50 kHz
Inductor (L_1-L_3)	0.1 mH
EMI Filter Inducor(L_f)	10 mH
EMI Filter Capacitor (C_f)	1 uF
Capacitor (C_1-C_4)	1 pF
Output Capacitor	220 uF
Load	100 Ω

4.2 Comparative Analysis

4.2.1 Cascaded Boost-Cûk (CBC) converter

4.2.1.1 Input Power Factor Comparison

Our proposed topology has higher power factor compared to both the conventional boost (except some cases) converter and the conventional Cûk as illustrated in Fig. 4.1. The input inductor L_m followed by the switched capacitor network form an input L-C type filter for each half cycle of operation. This L-C input filter improves the input power factor of the system

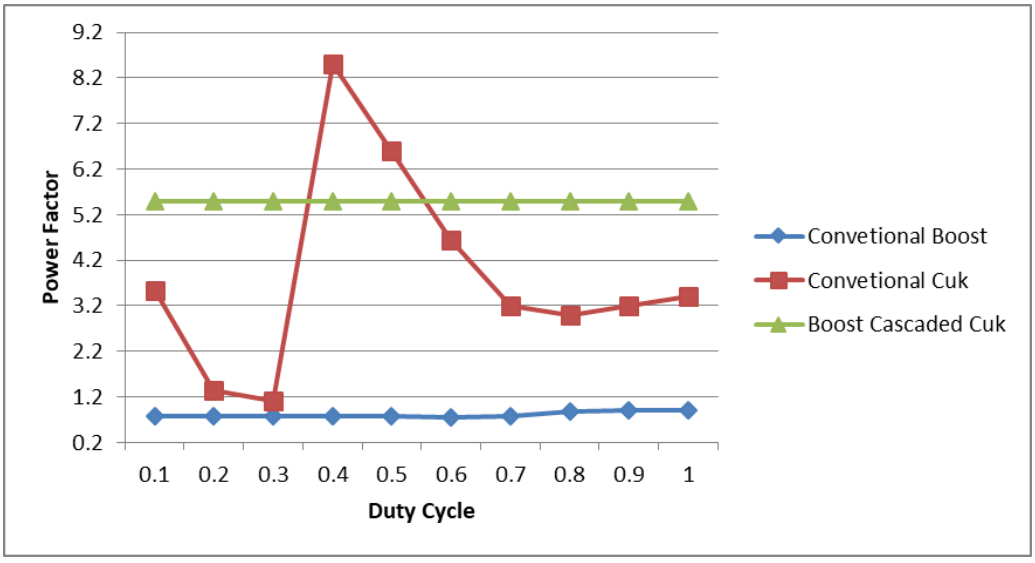

Fig. 4.1: Input PF Comparison of Conventional Boost, Conventional Cûk and proposed Converters

Duty Cycle	Conventional Boost (PF)	Conventional Cûk (PF)	Boost Cascaded Cûk (PF)
10%	0.77721317	0.0918016	0.8021
20%	0.78344182	0.67018407	0.80215322
30%	0.78673832	0.72379134	0.8021411
40%	0.78527905	0.78068589	0.80214321
50%	0.77595969	0.82780347	0.80214532
60%	0.75349556	0.8480536	0.80214836
70%	0.76994954	0.77142082	0.80215033
80%	0.87164489	0.56519159	0.80215213
90%	0.89854247	0.29596365	0.80215374
100%	0.89579024	0.0000133	0.80214181

Table. 4.2: Input PF Comparison of Conventional Boost, Conventional Cûk and proposed Converters

4.2.1.2 Efficiency Comparison

Our proposed topology has greater efficiency compared to both the conventional boost converter and the conventional Cûk as illustrated in Fig. 4.2. The most efficient configuration is the double stage bridgeless switched capacitor network based buck-boost converter which has been proposed in this paper since there are separate paths introduced for each half cycle of operation. As two separate paths are used for two half cycles of operation, there are less reduction of hysteresis and loss of energy due to magnetization. Mathematically it is proved that our topology has greater efficiency compared to both the conventional as well as the single stage switched capacitor network based buck-boost converter.

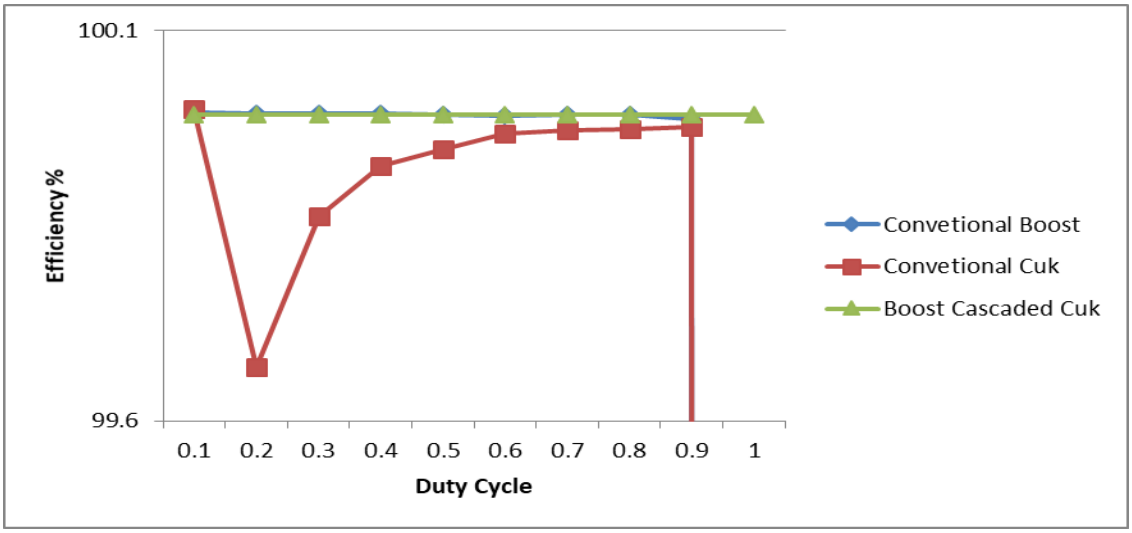

Fig. 4.2: Efficiency Comparison of Conventional Boost, Conventional Cûk and proposed Converters

Duty Cycle	Conventional Boost (% efficiency)	Conventional Cûk (% efficiency)	Boost Cascaded Cûk (% efficiency)
10%	99.9947	100	99.992
20%	99.9945	99.669	99.992
30%	99.99374	99.86251	99.99286
40%	99.99326	99.9268	99.9921
50%	99.99304	99.94831	99.992
60%	99.99156	99.9682	99.9921
70%	99.99271	99.9723	99.992
80%	99.99175	99.974355	99.992
90%	99.98665	99.97626	99.9921
100%	0	0	99.9921

Table. 4.3: Efficiency Comparison of Conventional Boost, Conventional Cûk and proposed Converters

4.2.1.3 THD of Input Current Comparison

Our proposed topology has less total harmonic distortion (THD) of input current (in few cases) compared to the conventional boost converter and the conventional Cûk as illustrated in Fig. 4.3. An input inductor followed by a switched capacitor network is introduced which formed an L-C input filter for each half cycle of operation. This L-C input filter reduces the input current ripple resulting in lower total harmonic distortion with respect to both the conventional boost converter and the conventional Cûk

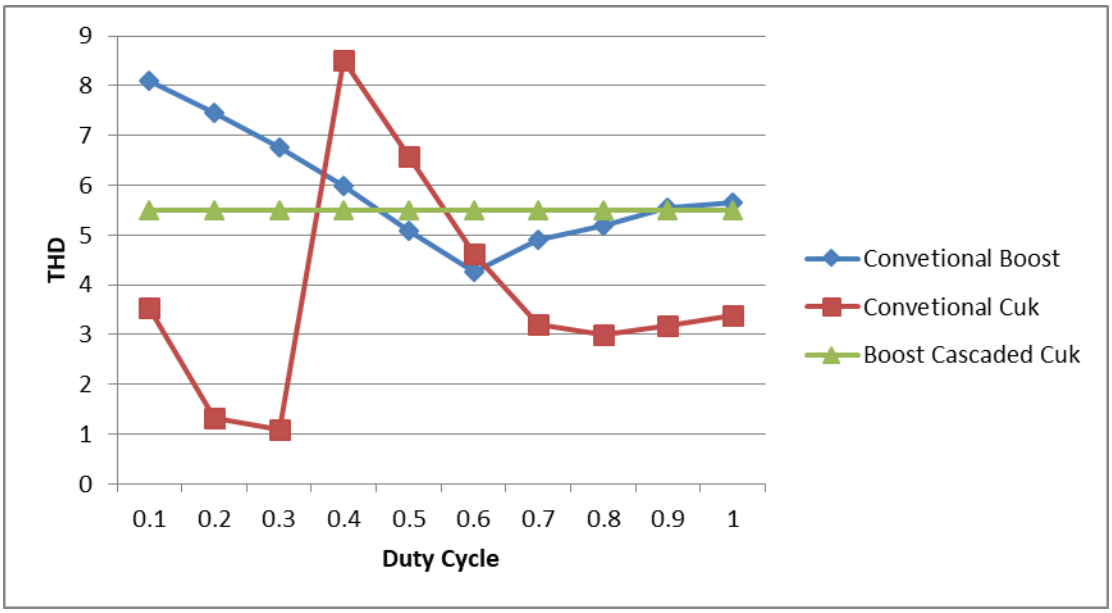

Fig. 4.3: THD of input current Comparison of Conventional Boost, Conventional Cûk and proposed Converters

Duty Cycle	Conventional Boost (THD)	Conventional Cûk (THD)	Boost Cascaded Cûk (THD)
10%	8.09871188	3.543305	5.494
20%	7.4640649	1.333027	5.4948
30%	6.76985	1.1028636	5.4947843
40%	5.989999	8.5064482	5.494766
50%	5.0842734	6.5914337	5.4947444
60%	4.2648772	4.6329022	5.4947341
70%	4.9153657	3.1924004	5.4947259
80%	5.193705	3.0051847	5.4947217
90%	5.5395732	3.1902734	5.4947064
100%	5.6470707	3.3971	5.494636

Table. 4.4: THD of input current Comparison of Conventional Boost, Conventional Cûk and proposed Converters

4.2.1.4 DC level Output Voltage Comparison

Our proposed topology has higher DC output voltage (in few cases) compared to the conventional boost converter and the conventional Cûk as illustrated in Fig. 4.4. As it gives constant output voltage throughout all the duty cycle it increases efficiency for all the duty cycles. Which makes it more useful for high step up application.

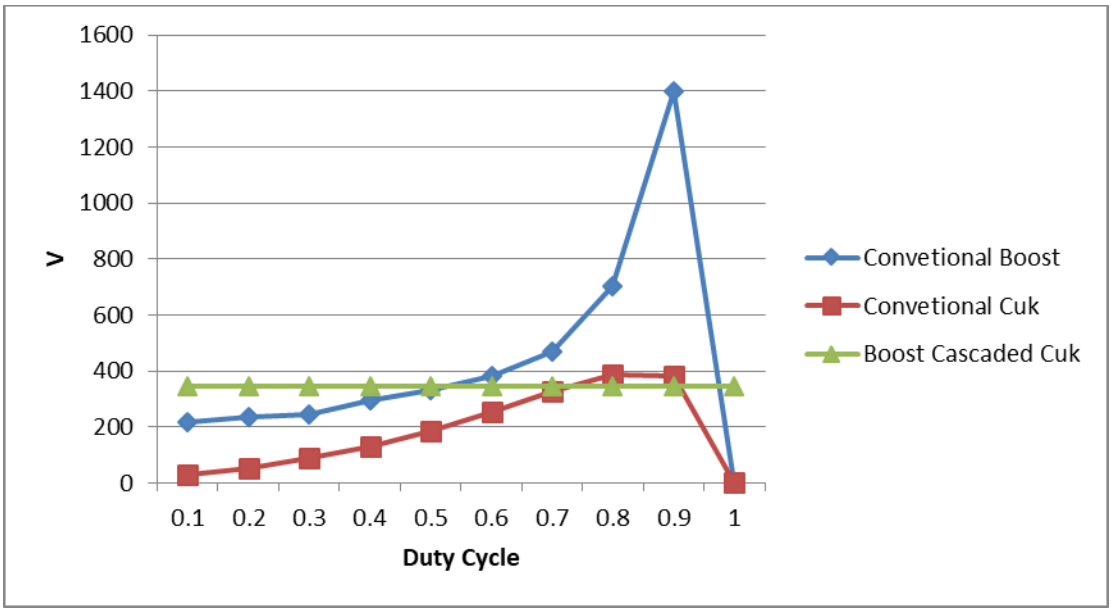

Fig. 4.4: DC output voltage Comparison of Conventional Boost, Conventional Cûk and proposed Converters

Duty Cycle	Conventional Boost (V_{rms})	Conventional Cûk (V_{rms})	Boost Cascaded Cûk (V_{rms})
10%	215.72499	27.93701	346.469
20%	236.9503	52.50313	346.469
30%	246.59998	86.874707	346.46712
40%	294.12969	129.36532	346.46756
50%	333.62981	185.13639	346.46794
60%	384.08452	255.71933	346.46855
70%	467.1629	329.16774	346.46892
80%	700.35777	384.38347	346.46927
90%	1400.4994	380.69423	346.46958
100%	0.1195038	0	346.46729

Table. 4.5: DC output voltage Comparison of Conventional Boost, Conventional Cûk and proposed Converters

Chapter 5

Applications

5.1 Application in renewable energy sources

Due to the rising need of renewable energy the importance of the development of more efficient circuits that transform energy has also risen. The multi-pulse AC-DC converters used in wind turbines often prove to be insufficient in the elimination of harmonics. This leads to additional active power filters, which operate at high switching frequencies, being used and the cost of the system being increased.

But since the proposed converter already gives a superior performance regarding harmonics elimination, we can integrate its use in renewable energy sources. Under ideal conditions the proposed single-phase CBC topology maintains a steady efficiency of 99.9%, THD of about 54.94%, power factor of about 0.80, leading and proper voltage regulation for all duty cycles in the basic state. If a feedback is implemented with the circuit we get even reduced THD. After implementing a feedback circuit, we get a steady efficiency of 96.3%, THD of about 30.02%, power factor of about 0.86, leading and proper voltage regulation for all duty cycles.

Typically renewable energy sources gives out a DC supply. Which is converted to uncontrolled AC supply by the use of an inverter. Which in turn gets converted to controlled AC. This is done since to get the supply as controlled AC. But since a lot of appliances use DC supply, again AC-DC conversion has to be done. This is where the proposed converter can be implemented. Since the supply goes through several steps of conversion, it is only natural that there will be an increased percentage of THD. So it is very significant that during AC to DC conversion the amount of THD is kept minimal.

The proposed circuit fits into the system of renewable energy sources right between the controlled AC stage and the supply for appliances that use DC. It has been shown in the block diagram given in fig-4.1.

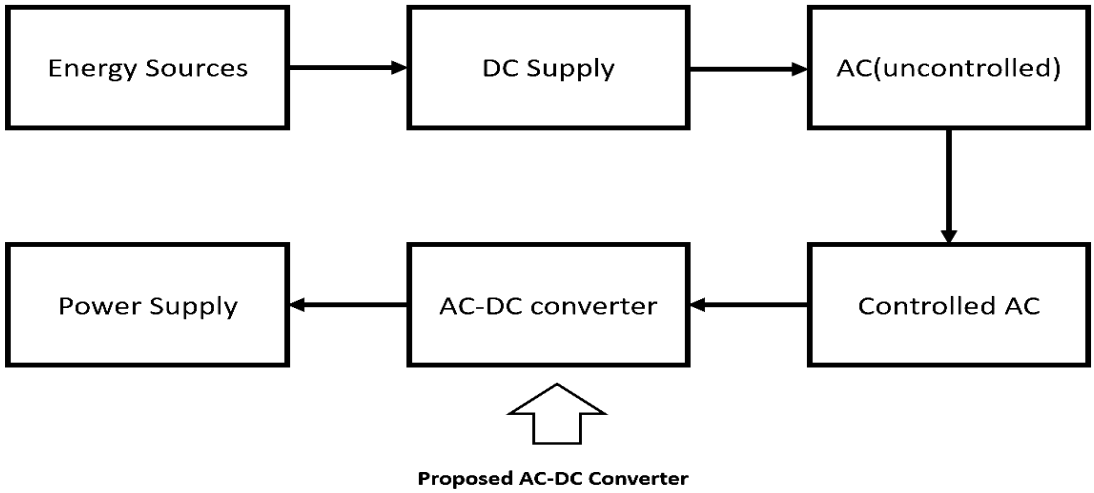

Fig-5.1 Block diagram of a typical renewable energy source with the proposed converter

5.2 Application in wind turbines

Simply stated, a wind turbine works the opposite of a fan. Instead of using electricity to make wind, like a fan, wind turbines use wind to make electricity. The wind turns the blades, which spins a shaft, which is connected to a generator via gear and coupling system. The generator gets mechanical energy input and converts it into electricity. The output from the generator is a uncontrolled AC. Which is then converted into controlled AC. The next step is to get the supply usable for DC appliances, so here AC to DC conversion is done. Since the supply goes through several steps of conversion, it is only natural that there will be an increased percentage of THD. So it is very significant that during AC to DC conversion the amount of THD is kept minimal.

The multi-pulse AC-DC converter systems are one of the methods used in the elimination of current and voltage harmonics; the uncontrolled rectifier-based converters are not enough to eliminate harmonics itself. In addition to this, converter requires active power filters that are operated at high switching frequencies in order to eliminate harmonic contents that have not been eliminated by uncontrolled rectifiers in high power applications. An active power filter such as this will increase the cost of the system.

This is where our proposed circuit comes in. The proposed converter already gives a superior performance regarding harmonics elimination, we can integrate its use in renewable energy sources. Under ideal conditions the proposed single-phase CBC topology maintains a steady efficiency of 99.9%, THD of about 54.94%, power factor of about 0.80, leading and proper voltage regulation for all duty cycles in the basic state. If a feedback is implemented with the circuit we get even reduced THD. After implementing a feedback circuit, we get a steady efficiency of 96.3%, THD of about 30.02%, power factor of about 0.86, leading and proper voltage regulation for all duty cycles.

So by implementing the proposed converter into wind turbine systems the necessity for additional active filters is eliminated. A block diagram of a typical wind turbine system integrated with the proposed converter is shown in fig-4.2.

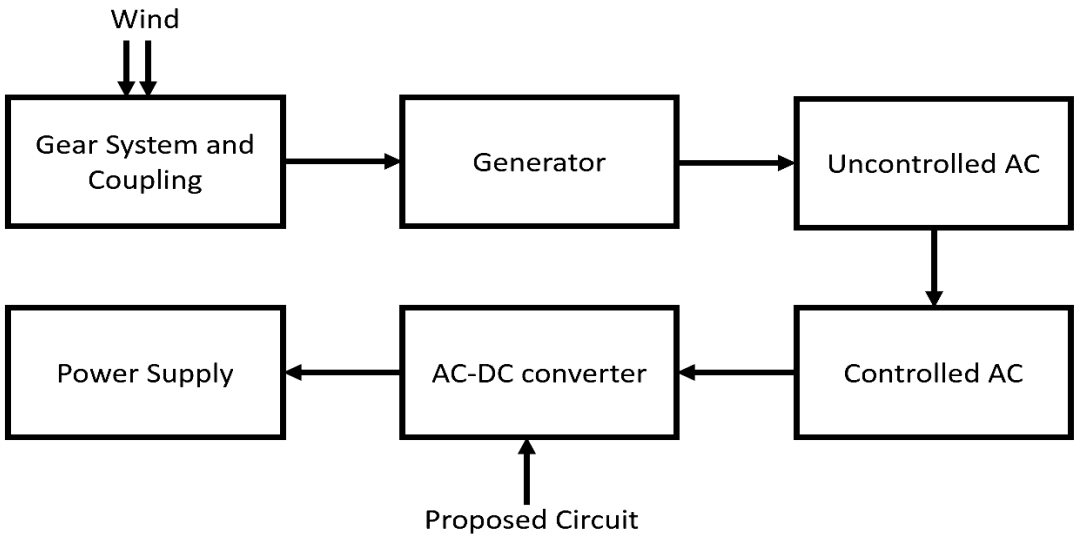

Fig-5.2 Block diagram of a typical wind turbine system with the proposed converter

Chapter 6

Conclusion

Using the common part sharing method (CPSM), we have designed a novel topology of Cascaded Boost-Cûk converter where an isolated Cûk converter and a Boost converter has been combined. The proposed circuit can have applications for high voltage operations with improved efficiency. The proposed circuit achieves high step-up ratio with the help of the added step-up ability of the isolated Cûk converter. Simultaneously, it also maintains the continuous input current characteristics of conventional Boost converters. Moreover, a significant improvement in performance parameters like efficiency (99.992%) and a leading Power Factor (0.802) is exhibited by the proposed CBC converter. The proposed converter has been implemented in closed loop so that, an even better power factor can be attained by the employment of suitable power factor correction techniques.

Results of implementation in a closed feedback loop have shown significant improvement in power factor and THD. Further improvements need to be made upon the proposed circuit and its closed loop implementation to obtain better results and eventual commercial usability. The circuit also requires practical implementation for a better understanding of it and even further improvement can be made through this.

Further study of the proposed circuit may help us design a suitable controller so that THD and PF can further be improved. The controller can also help reduce the ripple in the output voltage and current. The improvement of the proposed circuit has to be made so that it can have commercial feasibility. Development of an experimental prototype of the circuit with its controller so that optimum performance can be achieved is a future objective to be completed.

Chapter 7

Published Papers

Single-Phase AC-DC Cascaded Boost-Cûk (CBC) Converter for High Step-Up Applications using Common Part Sharing Method (CPSM)

4th International Conference on Electrical Engineering and Information & Communication Technology (iCEEiCT 2018), MIST, 2018

Chapter 8

Reference

1. Kabalci, Ersan & Irmak, Erdal & Colak, Ilhami. (2011). Design of an AC-DC-AC converter for wind turbines. International Journal of Energy Research. 35. 169 - 175. 10.1002/er.1770.
2. Kazem HA, Alboloshi AA, Al-Jabri A, Alsaidi KH., "Simple and advanced models for calculating singlephase diode rectifier line-side harmonics.", Proceedings of World Academy of Science, Engineering and Technology 2005; 9:179–183.
3. Po-Tai Cheng, S. Bhattacharya and D. M. Divan, "Application of dominant harmonic active filter system with 12 pulse nonlinear loads," in IEEE Transactions on Power Delivery, vol. 14, no. 2, pp. 642-647, April 1999.
4. J. P. Arias-Angulo, J. C. Rosas-Caro, E. Haro-Sandoval, A. Valderrabano-Gonzalez, J. C. Mayo-Maldonado and J. E. Valdez-Resendiz, "Input current ripple cancelation by interleaving boost and Cuk DC-DC converter," 2018 International Conference on Electronics, Communications and Computers (CONIELECOMP), Cholula, 2018, pp. 133-138.
5. B. W. Williams, "DC-to-DC Converters With Continuous Input and Output Power," in IEEE Transactions on Power Electronics, vol. 28, no. 5, pp. 2307-2316, May 2013.
6. J. Yang and H. Do, "Bridgeless SEPIC Converter With a Ripple-Free Input Current," in IEEE Transactions on Power Electronics, vol. 28, no. 7, pp. 3388-3394, July 2013.
7. J. P. R. Balestero, F. L. Tofoli, R. C. Fernandes, G. V. Torrico-Bascope and F. J. Mendes de Seixas, "Power Factor Correction Boost Converter Based on the Three-State Switching Cell," in IEEE Transactions on Industrial Electronics, vol. 59, no. 3, pp. 1565-1577, March 2012.
8. L. Huber, Y. Jang and M. M. Jovanovic, "Performance Evaluation of Bridgeless PFC Boost Rectifiers," in IEEE Transactions on Power Electronics, vol. 23, no. 3, pp. 1381-1390, May 2008.
9. M. A. M. Oninda, G. Sarowar and M. M. H. Galib, "Single-phase switched capacitor AC-DC step down converters for improved power quality," 2017 IEEE Region 10 Humanitarian Technology Conference (R10-HTC), Dhaka, 2017, pp. 520-523.
10. MEENADEVI, R & PREMALATHA, L. (2017). A Novel bridgeless SEPIC Converter for Power Factor Correction. Energy Procedia. 117. 991-998. 10.1016/j.egypro.2017.05.220.
11. B. Singh, S. Singh, A. Chandra and K. Al-Haddad, "Comprehensive Study of Single-Phase AC-DC Power Factor Corrected Converters With High-Frequency Isolation," in IEEE Transactions on Industrial Informatics, vol. 7, no. 4, pp. 540-556, Nov. 2011.
12. Sarowar, Golam & Hoque, Md. Ashraful. (2015). High Efficiency Single Phase Switched Capacitor AC to DC Step Down Converter. Procedia - Social and Behavioral Sciences. 195. 2527-2536. 10.1016/j.sbspro.2015.06.437.
13. Bazlur Rashid, Mohammad & Oninda, Mohammad & Faisal, Fahim & Nishat, Mirza & Sarowar, Golam & Hoque, Md. Ashraful. (2018). A Novel Topology of Single-Phase AC-DC Integrated Boost-SEPIC (IBS) Converter Using Common Part Sharing Method (CPSM) for High Step-Up Applications. Journal of Power and Energy Engineering. 06. 38-47. 10.4236/jpee.2018.66003.
14. Kassakian J, Schlecht M, Verghese G (1991) Principles of power electronics. Addison- Wesley, Reading
15. Batarseh I (2004) Power electronic circuits. Wiley, New York
16. Holmes D, Lipo T (2003) Pulse width modulation for power converters. IEEE/Wiley- Interscience, New York
17. Wu B (2006) High-power converters and AC drives. Wiley, New York
18. J. White, and W. Muldoon, "Two-Inductor Boost and Buck Converters", Proc. IEEE Power Electronics Specialists Conference, PESC1987, pp. 387-392.
19. W.-Y. Choi, J.-M. Kwon, and B.-H. Kwon, "Bridgeless dual-boost rectifier with reduced diode reverse-recovery problems for power-factor correction," IET Power Electron., vol. 1, no. 2, pp. 194–202, Jun. 2008.
20. M. Bilgili, A. Ozbek, B. Sahin, and A. Kahraman, "An overview of renewable electric power capacity and progress in new technologies in the world," Renewable and Sustainable Energy Reviews, vol. 49, pp. 323–334, 2015.

21. Alves A, da Silva E, Lima A, Jacobina C (1998) Pulse width modulator for voltage-type inverters with either constant or pulsed DC link. In: Proceedings of IEEE IAS'98, pp 229–1236
22. Seixas P (1988) Commande numérique d'une machine synchrone autopilotée. D.Sc. Thesis, L'Institut Nationale Polytechnique de Toulouse, INPT, Toulouse
23. Holmes D (1996) The significance of zero space vector placement for carrier-based PWM schemes. IEEE Trans Ind App 32:1122–1129
24. Grotstollen H (1993) Line voltage modulation: a new possibility of PWM for three phase inverters. In: Proceedings of the IEEE IAS'93, pp 567–574
25. Jacobina C, Lima A, da Silva E, Alves R, Seixas P (2001) Digital scalar pulse-width modulation: a simple approach to introduce non-sinusoidal modulating waveforms. IEEE Trans Power Electron 16:351–359
26. Oliveira A, da Silva E, Jacobina C (2004) A hybrid PWM strategy for multilevel voltage source inverters. In: Proceedings of the IEEE PESC'2004, pp 4220–4225
27. Van der Broeck H, Skudelny H, Stanke G (1988) Analysis and realization of a pulse width modulator based on voltage space vector. IEEE Trans Ind Appl 24:142–150
28. Jacobina C, Lima A, da Silva E (1977) PWM space vector based on digital scalar modulation. In: Proceedings of the IEEE PESC, pp 100–105
29. Zhou K, Wang D (2002) Relationship between space-vector modulation and three-phase carrier-based PWM: a comprehensive analysis. IEEE Trans Ind Appl 49:186–196
30. Ledwich G (2001) Current source inverter modulation. IEEE Trans Power Electron 6:618–623
31. Dahono P, Kataoka T, Sato Y (1997) Dual Relationships between voltage-source and currentsource three-phase inverters and its applications. In: Proceedings of the PEDS, pp 559–565
32. J. Wei, P. Xu, H. Wu, F. C. Jee, K. Yao, and M. Ye, "Comparison of three topology candidates for 12V VRM," in Proc. IEEE Appl. Power Electron. Conf. (APEC), 2001, pp. 245–251.
33. Boris Axelrod, Yefim Berkovich, Adrian Ioinovici, "Switched-Capacitor/Switched-Inductor Structures for Getting Transformerless Hybrid DC–DC PWM Converters"
34. Bing Lu, Ron Brown, Macro Soldnao, "Bridgeless PFC implementation using one cycle control technique," APEC, 2005, no. 2, pp. 812-817
35. Klumpner C, Blaabjerg F (2005) Modulation method for a multiple drive system based on a two-stage direct power conversion topology with reduced input current ripple. IEEE Trans Power Electron 20:922–929